Advances in
Robotic Brachytherapy

Yan Yu, Ph.D., MBA
Professor and Vice Chair, Director of Medical Physics

Department of Radiation Oncology, Thomas Jefferson University
Philadelphia, PA, 19107, U.S.A

May 14, 2013 AAPM CAMPS

Jefferson™
Kimmel Cancer Center
NCI-designated

Learning Objectives

1. Introduce the latest development in brachytherapy robotics.
2. Describe supporting laboratory investigations and clinical studies.
3. Outline future research directions

Jefferson™ Kimmel Cancer Center NCI-designated

Conventional Prostate Seed Implant Brachytherapy

Pubic Arch

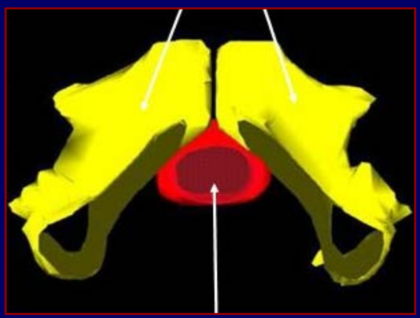

Prostate

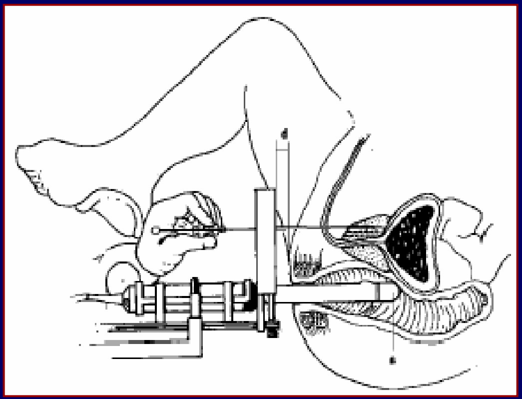

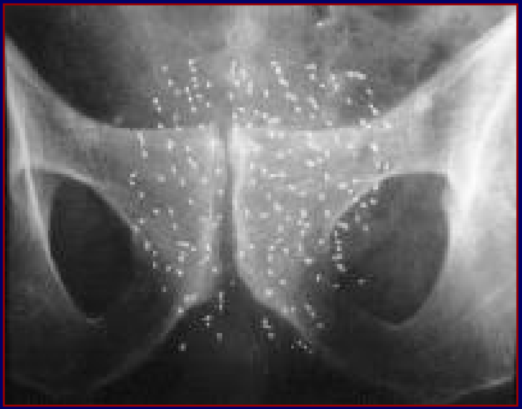

Fixed template

Needle angulation

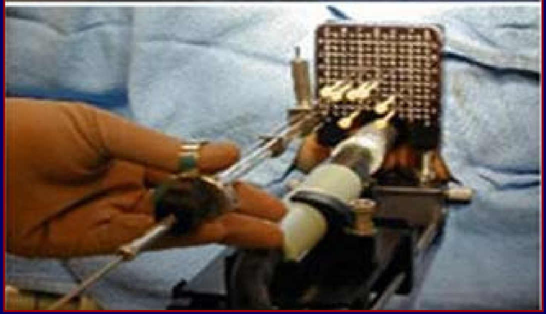

Fatigue & exposure

- Fixed template – limited maneuverability
- PAI – needle angulation difficult
- Consistency, accuracy, efficiency – techniques & human factors

Jefferson™ Kimmel Cancer Center NCI-designated

What is a "ROBOT"?

"A robot is a reprogrammable multi-functional manipulator designed to move materials, parts, tools, or specialized devices, through variable programmed motions for performance of a variety of tasks."

Jefferson™ Kimmel Cancer Center NCI-designated

ROBOTs

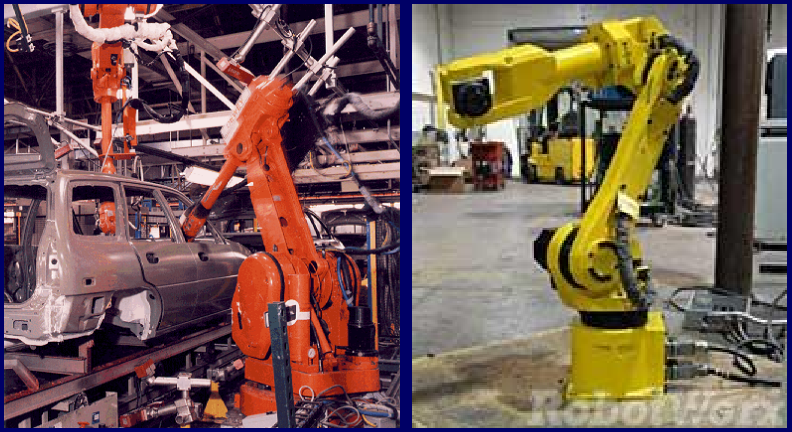

Industrial robots

Medical robots

Jefferson™
Kimmel Cancer Center
NCI-designated

Robotic IGBT System

IGBT: Image-Guided BrachyTherapy

Objectives:

- Increase accuracy and consistency of needle placement and seed delivery
- Increase avoidance of critical structures (urethra, pubic bone, rectum, etc.)
- Detect tissue heterogeneities and deformation via force sensing and imaging feedback
- Update dosimetry after each needle is implanted
- Reduce tediousness and assist clinicians
- Reduce trauma and edema
- Reduce radiation exposure
- Reduce learning curve
- Reduce OR time

The EUCLIDIAN Robotic System for IGBT

- EUCLIDIAN design & development
  - Positioning Module (3DOF cart, 6DOF platform)
  - Surgery Module (2DOF US driver, 3DOF gantry, 2DOF needle driver)
    - Robot workspace
    - In vivo force-torque & motion data collection
    - Needle bucking expt.
    - Force-reduction expt.
    - Reduction of tissue deformation expt.
    - Reduction of needle bending expt.
    - Improved prostate stabilization expt.
    - Friction reduction – needle coating expt.
    - Extended Kalman Filter for needle steering simulation & expt.
- EUCLIDIAN architecture
- EUCLIDIAN software
- Dosimetric planning
- Robotic IGBT procedures
- EUCLIDIAN performance

Jefferson™ Kimmel Cancer Center NCI-designated

Functional Requirements:

- Provision for reverting to conventional manual brachytherapy method at any time
- Quick and easy disengagement in case of emergency
- Improved of prostate immobilization
- Provision for periodic quality assurance
- Provision for reviewing and approving the motion plan and seed delivery
- Ability to modulate needle velocity by automatic feedback control
- Provision for needle tracking and seed detection
- Updating implant plan at any desired time
- Steering of the needle by automatic feedback control
- Visual/haptic force feedback during needle insertion
- Teach mode to simulate force/velocity patterns of expert practitioners
- Ease of operation and safety for the patient and OR environment

Jefferson™ Kimmel Cancer Center NCI-designated

Workspace in the OR

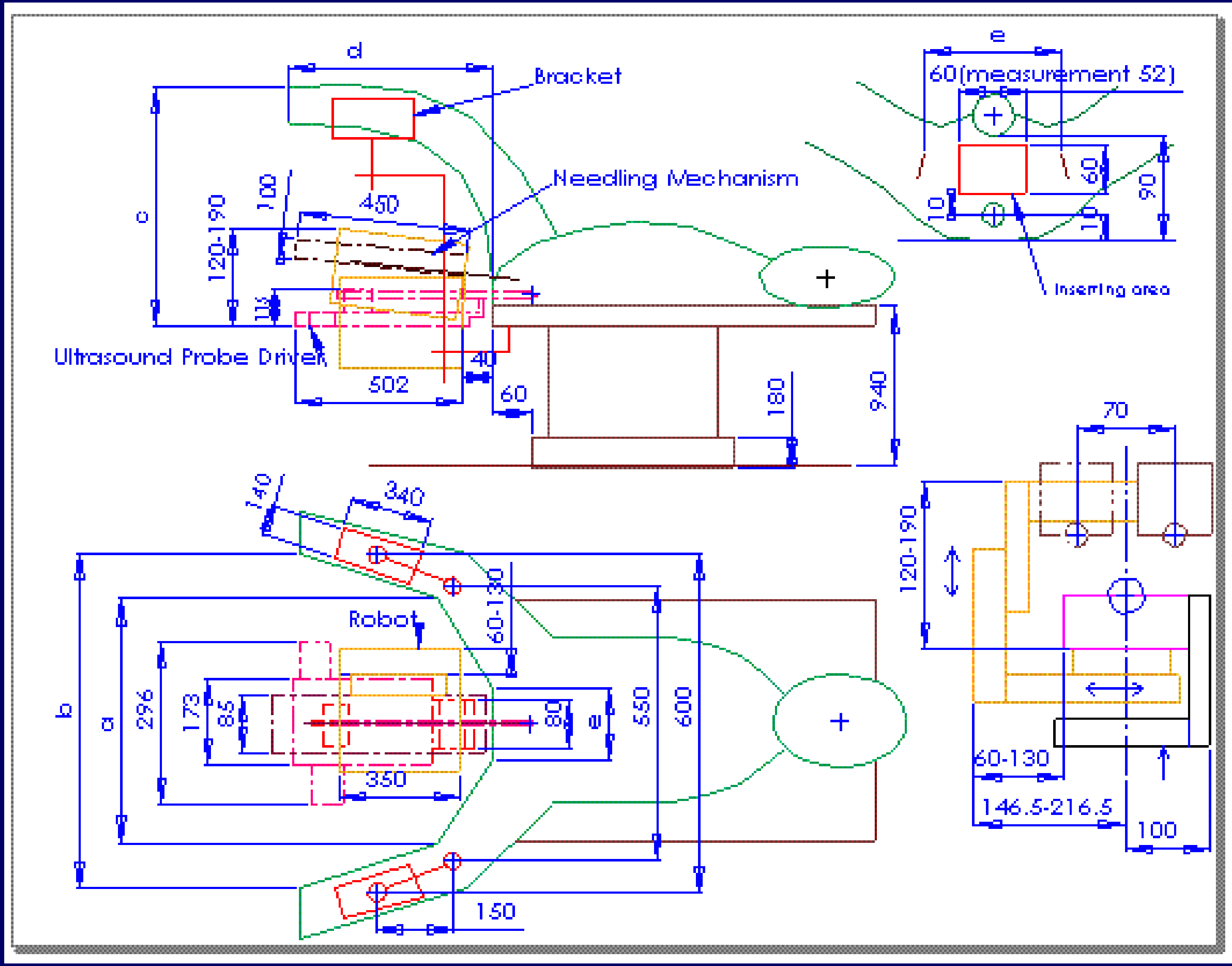

Jefferson™ Kimmel Cancer Center
NCI-designated

In Vivo Force Measurements

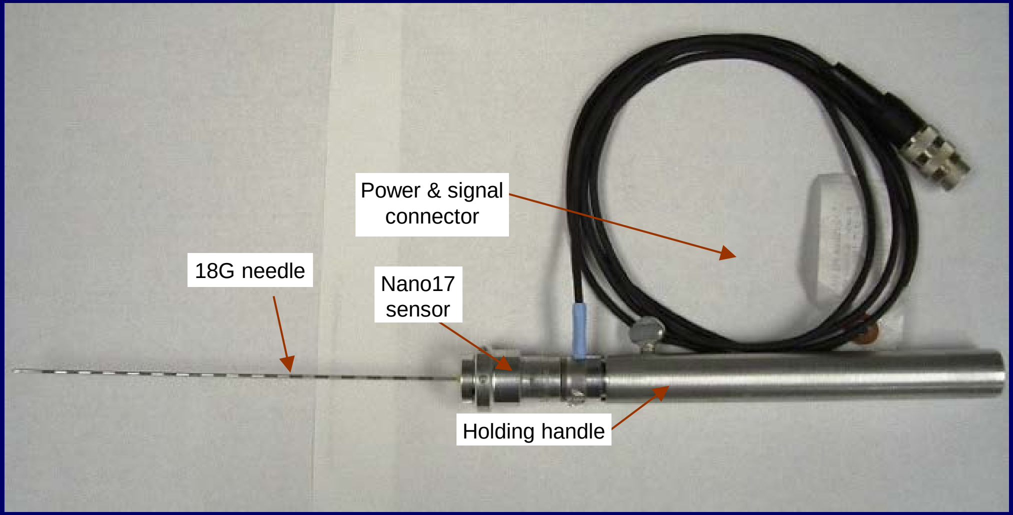

Hand-held adapter

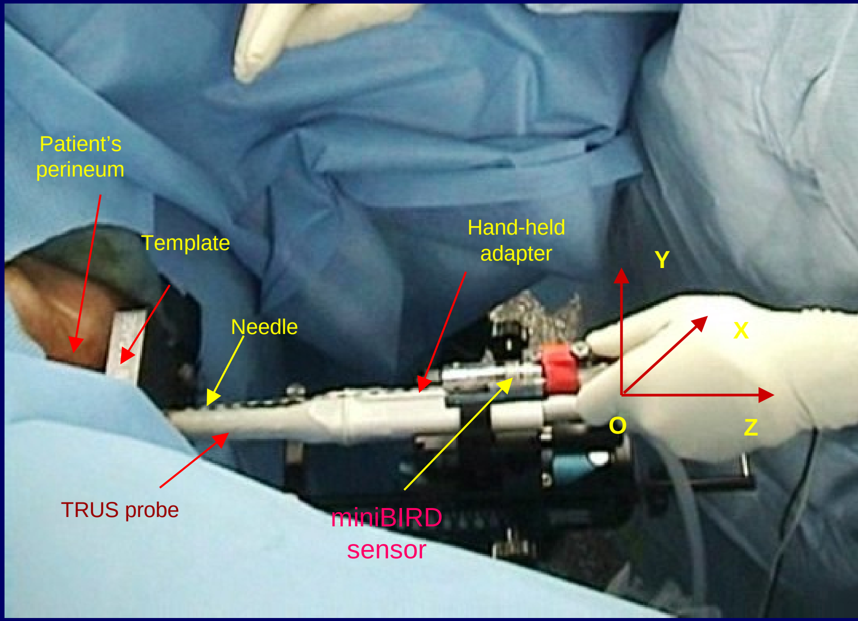

Force/torque and position data collection during actual brachytherapy procedure in the OR

Jefferson™ Kimmel Cancer Center NCI-designated

Patient #1, 17G Needle

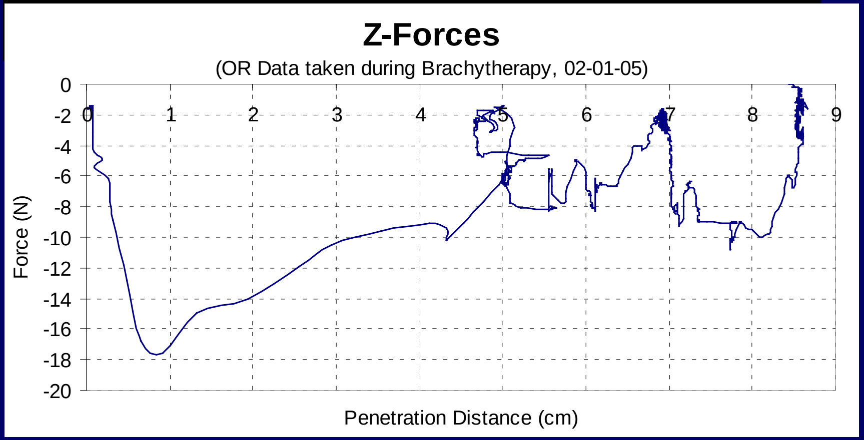

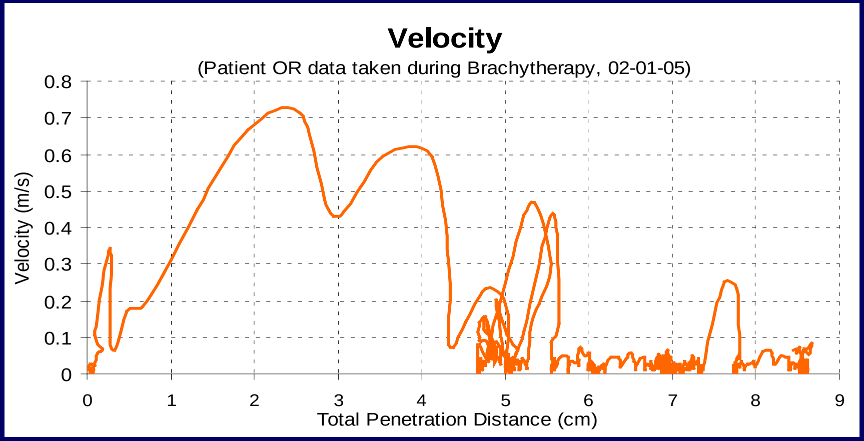

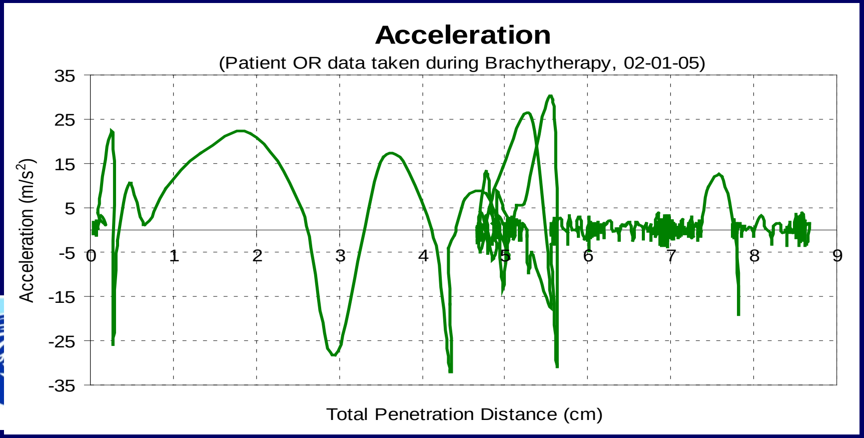

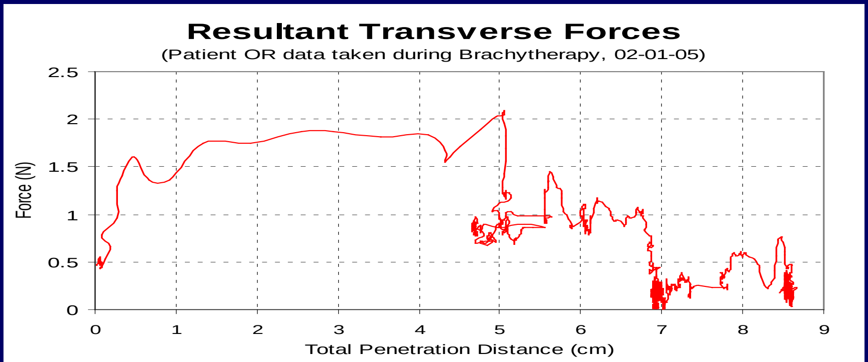

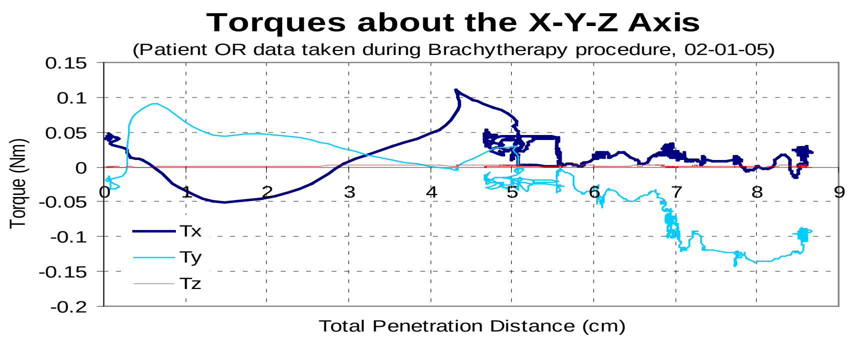

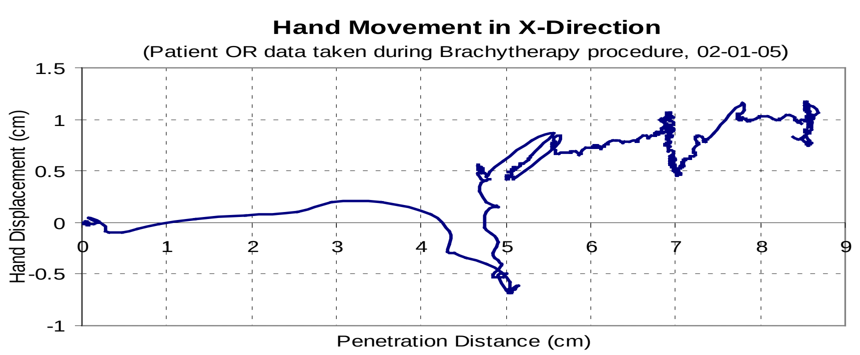

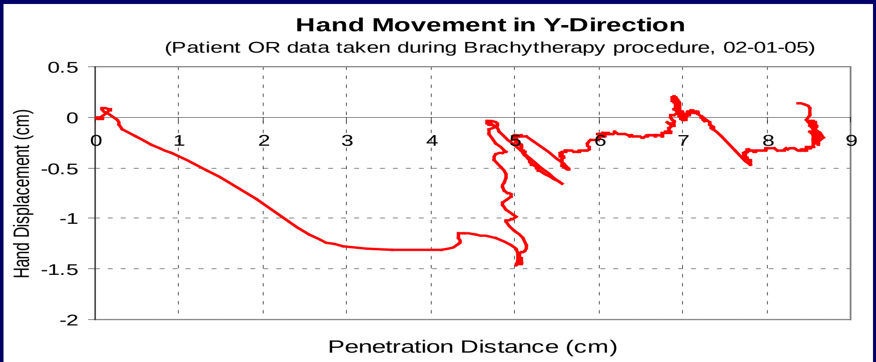

Prostate Deformation

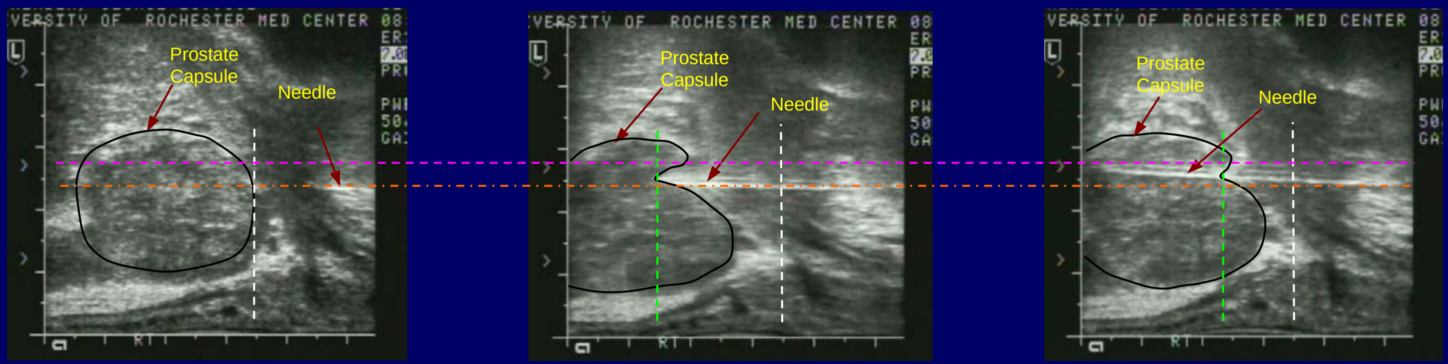

(a) *Prior to capsule puncture* (b) *During capsule puncture* (c) *After full insertion*

Video

Jefferson™ Kimmel Cancer Center
NCI-designated

Force & Target Deflection

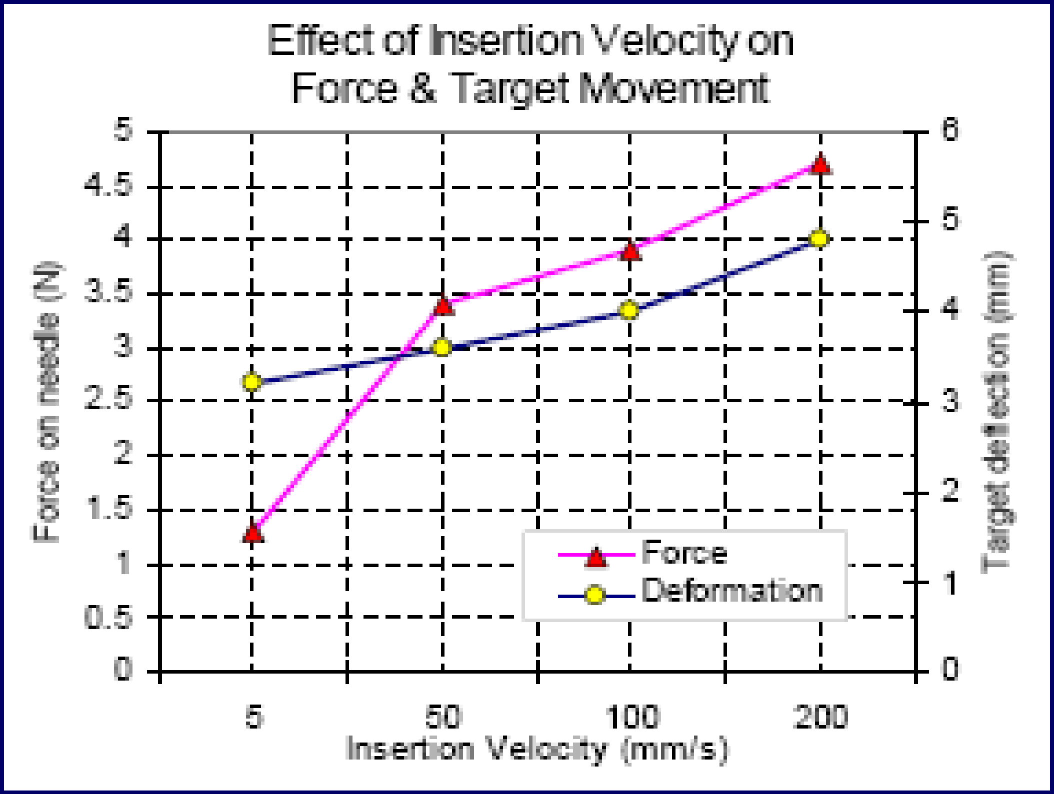

Jefferson™ Kimmel Cancer Center NCI-designated

Rotational Velocity Modulation

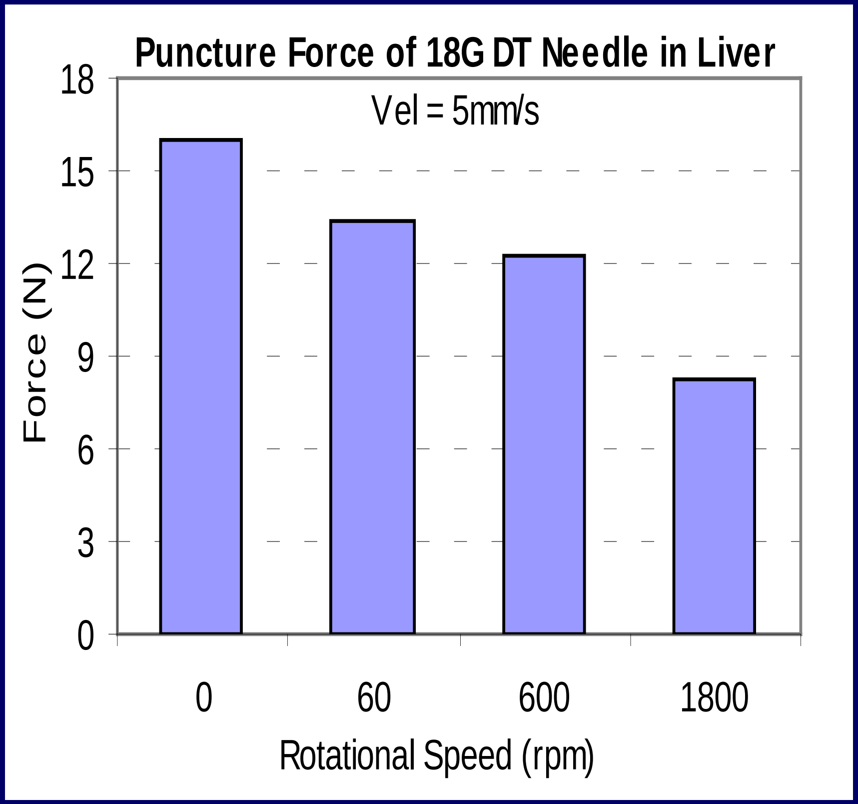

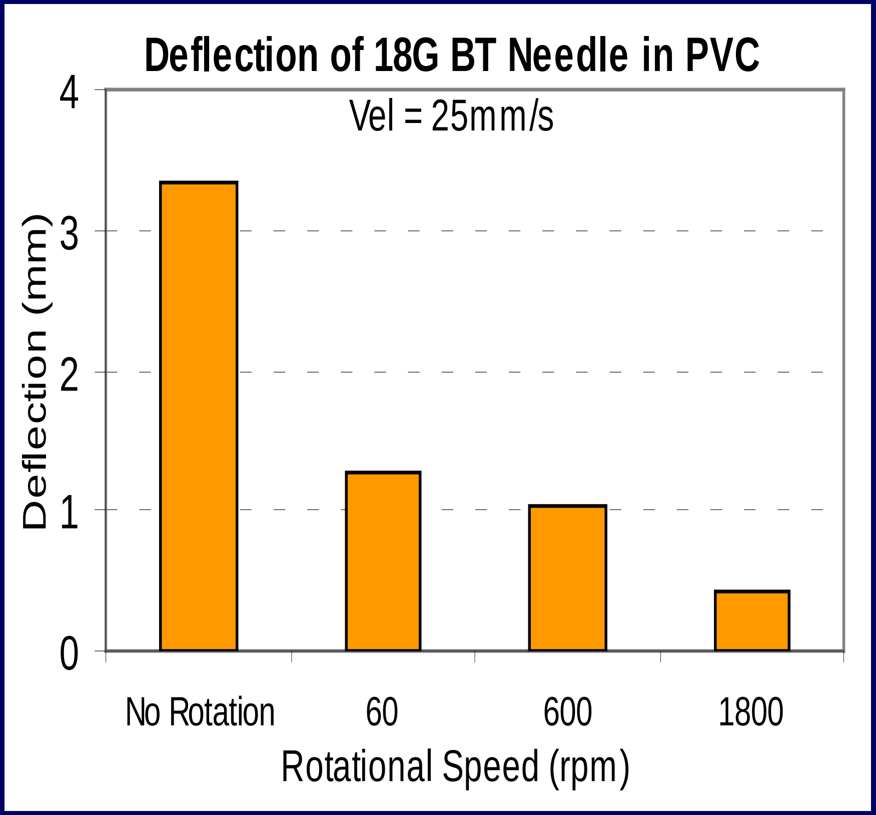

Jefferson™
Kimmel Cancer Center
NCI-designated

Robot Components for Brachytherapy

Hardware:

- Linkage/ mechanism
- Motors/ actuators
- Encoders/ sensors
- TRUS (CT, MR)
- Image acquisition board
- Industrial computer
- Power supply, amplifier

Software:

- Patient information handling
- Image acquisition
- Delineation of anatomic structures
- Dosimetric planning
- Needle tracking, seed detection
- Motion control and coordination
- 2D-3D visualization
- Position, velocity, force feedback

EUCLIDIAN OVERVIEW

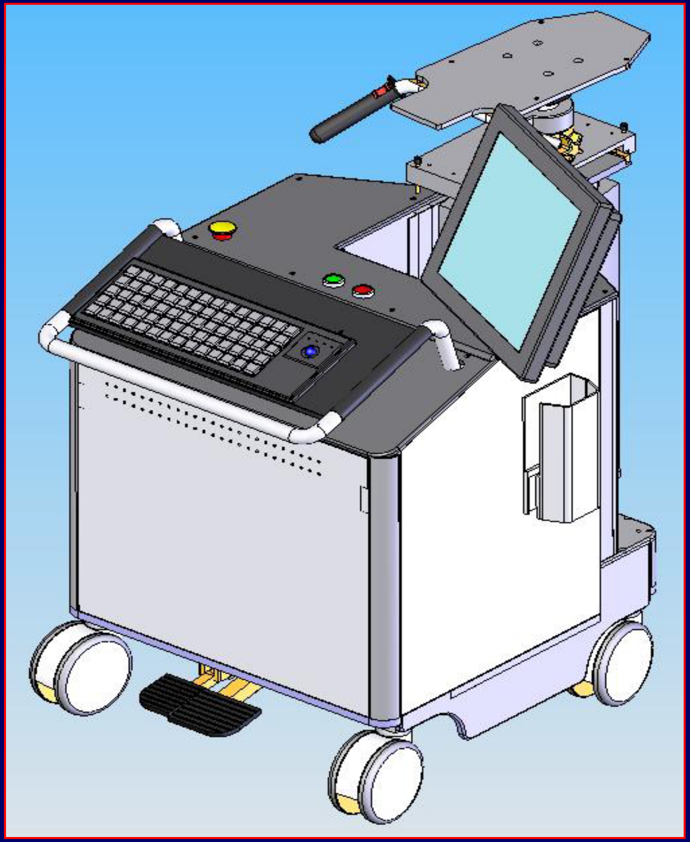

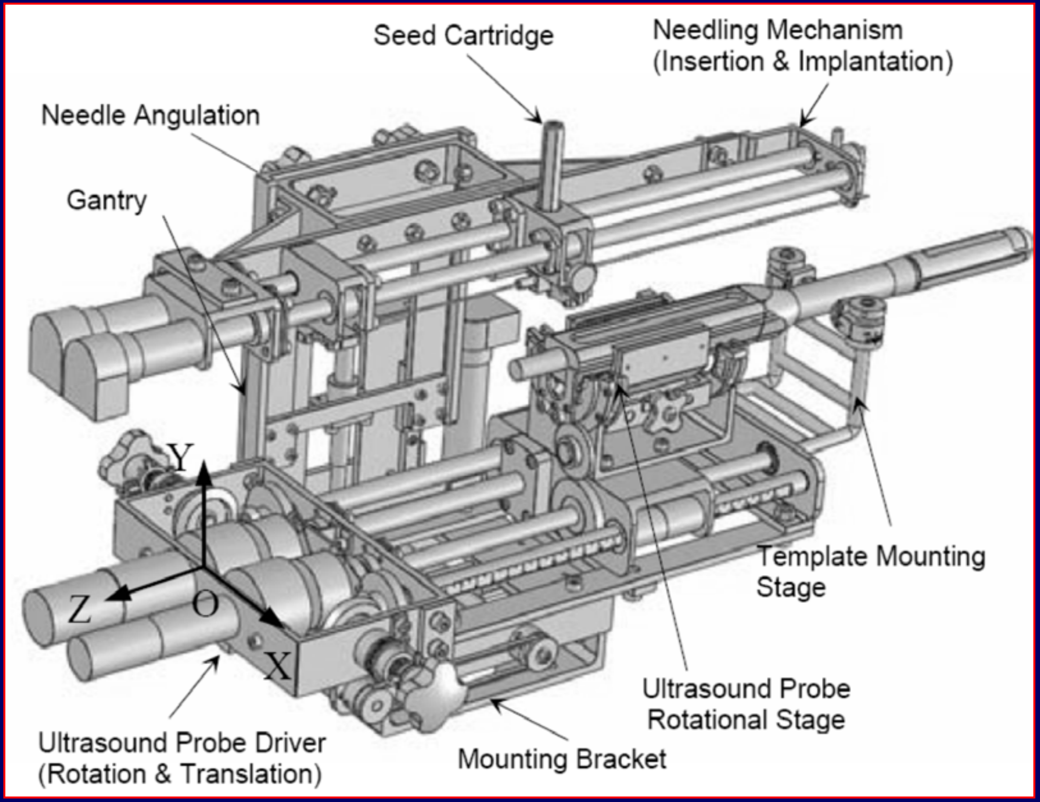

Jefferson™ Kimmel Cancer Center
NCI-designated

7 DOF Surgery Module

6DOF Supporting Platform

3 DOF Cart

Surgery Module

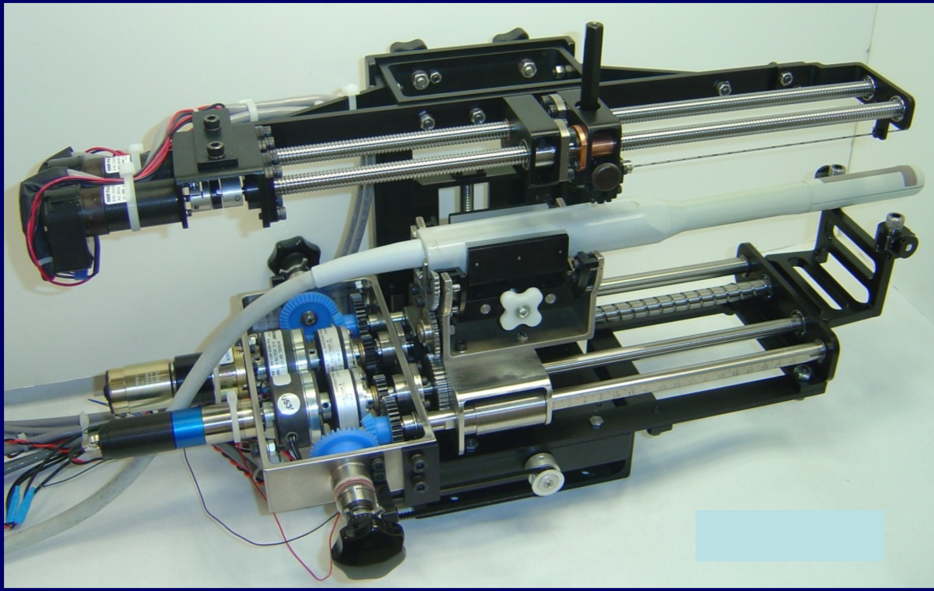

Jefferson™
Kimmel Cancer Center
NCI-designated

EUCLIDIAN in OR Setup

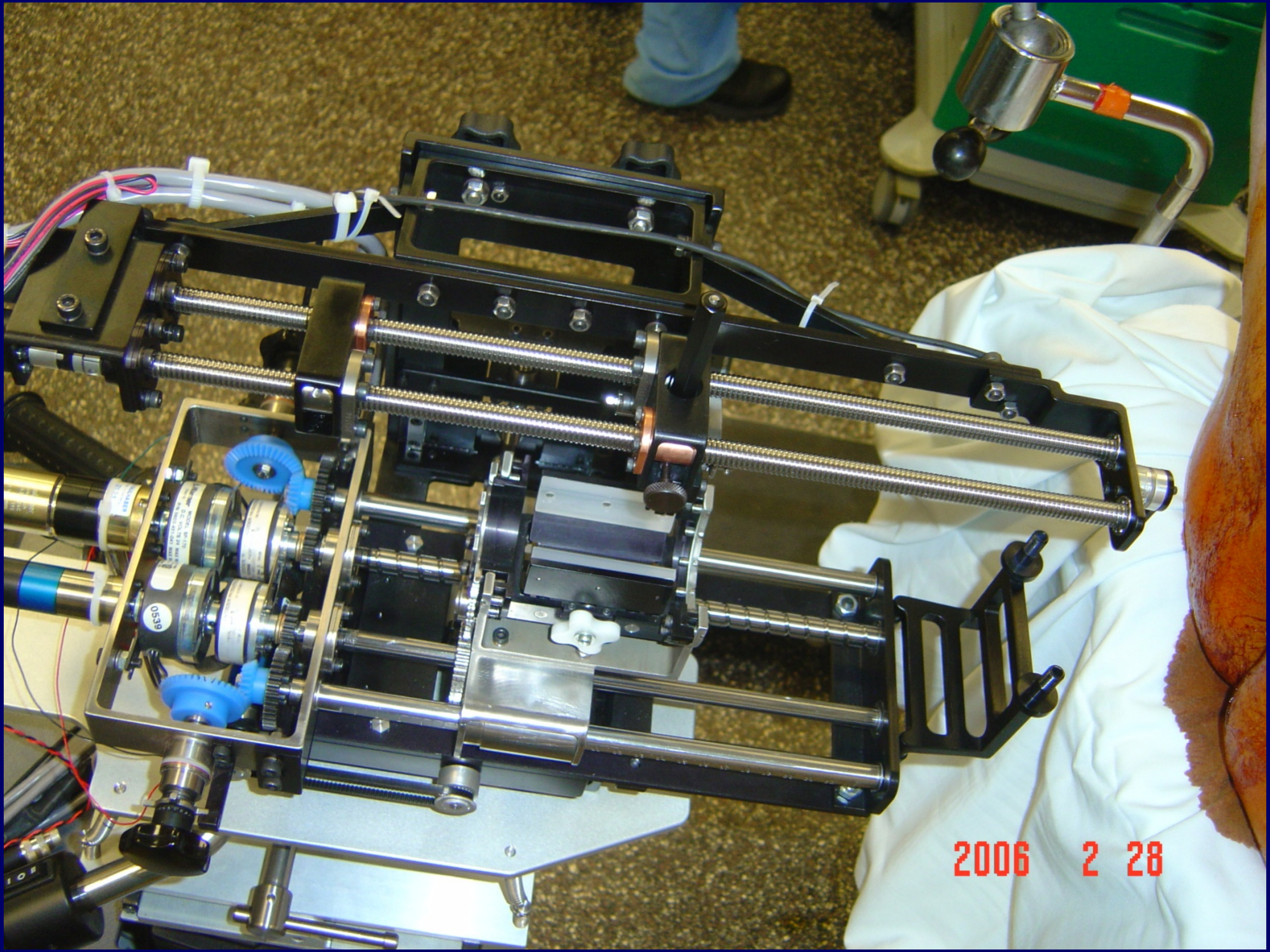

Jefferson™
Kimmel Cancer Center
NCI-designated

EUCLIDIAN - US Probe Driver

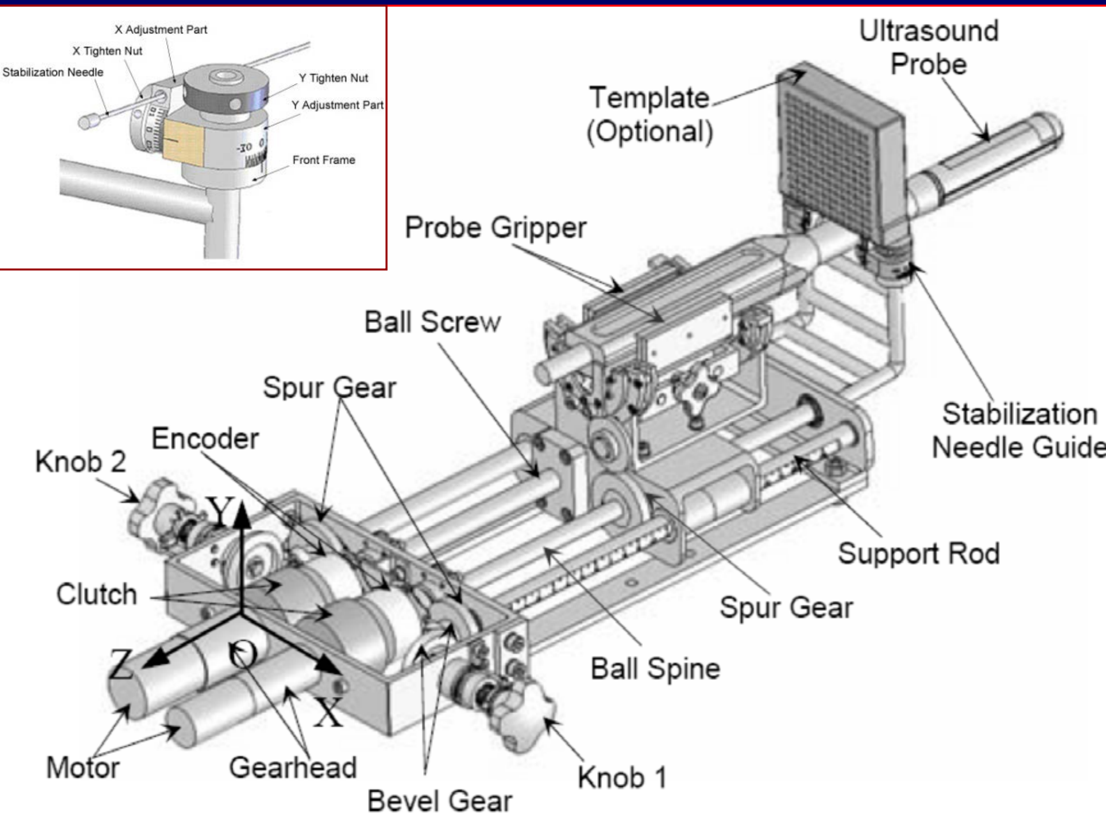

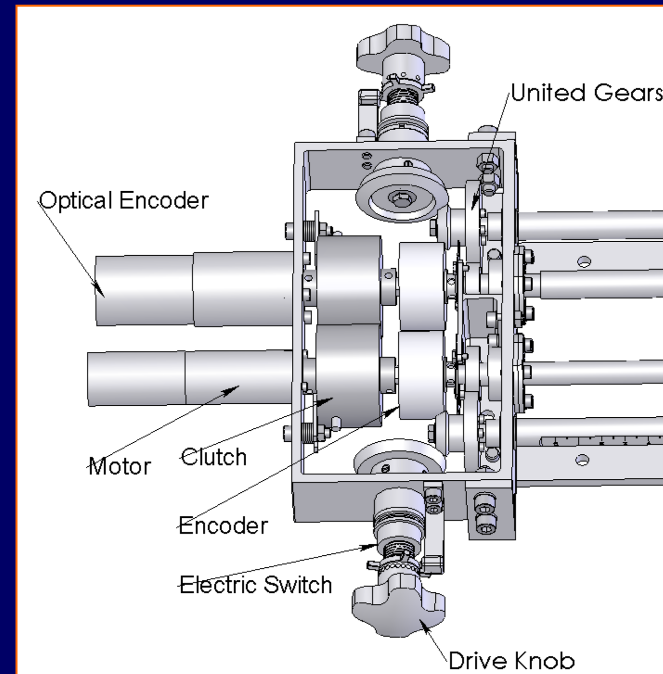

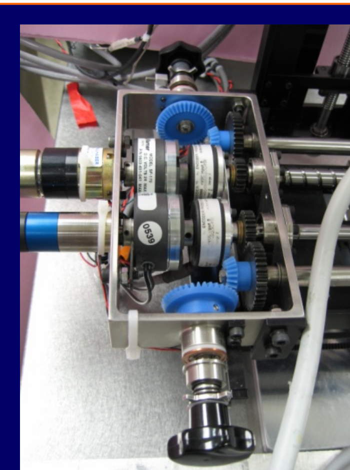

- Decoupled translation & rotation
- Motorized as well as manual
- Improved stabilization
- Provision for conventional method

Jefferson™
Kimmel Cancer Center
NCI-designated

EUCLIDIAN – Needle Insertion & Seed Delivery

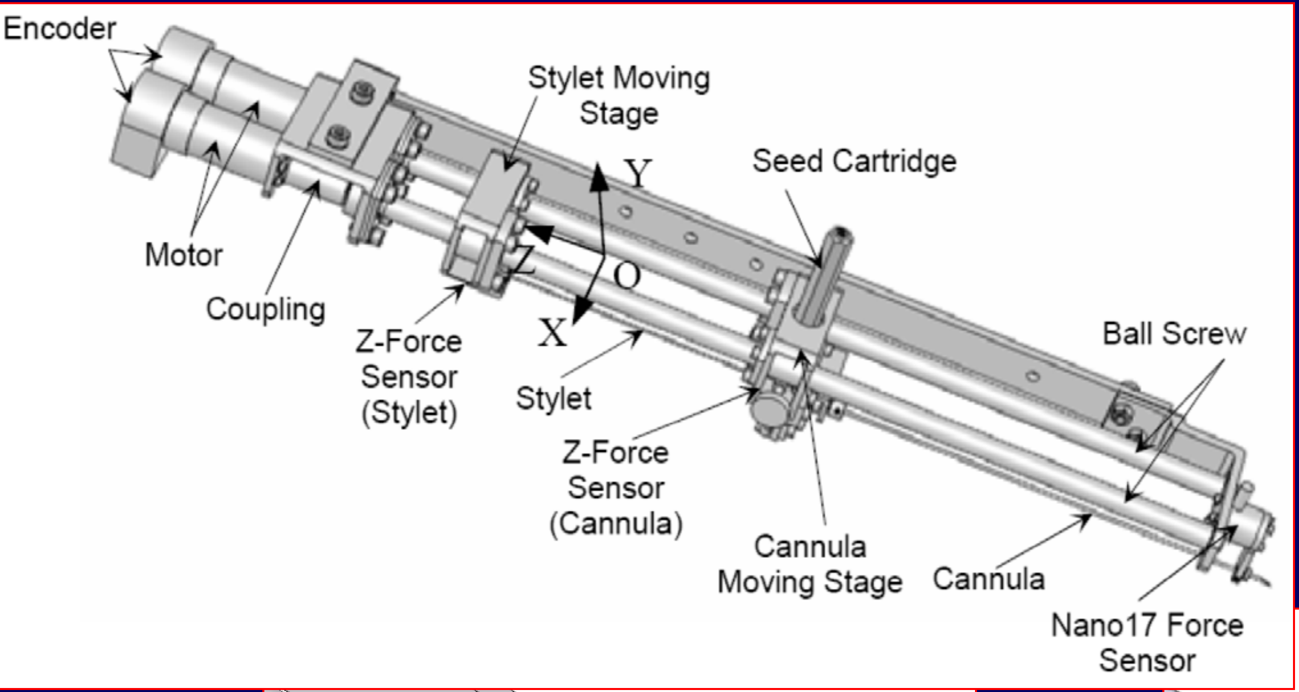

- 3 motorized motion
- Optical encoders
- Positive drive
- Cannula rotation
- 3 Force sensors
- Sterilizable seed passage

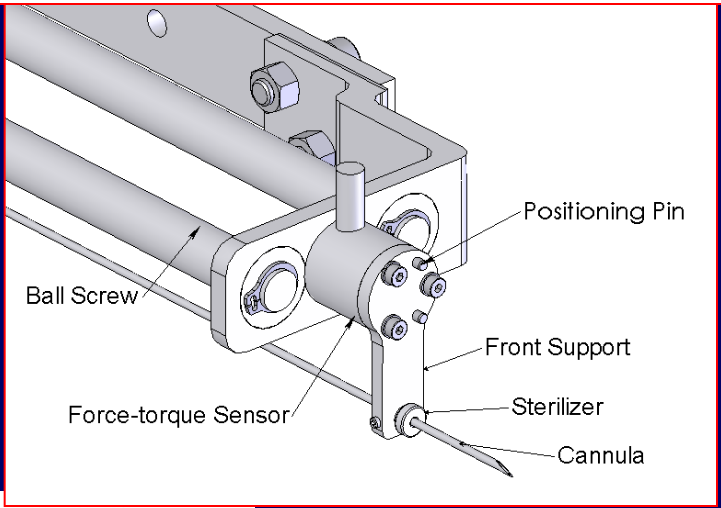

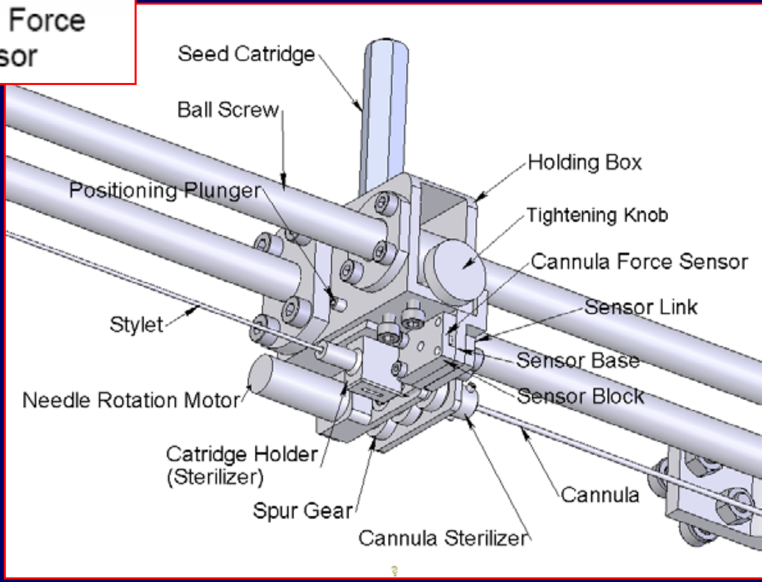

Jefferson™
Kimmel Cancer Center
NCI-designated

EUCLIDIAN – Gantry Robot

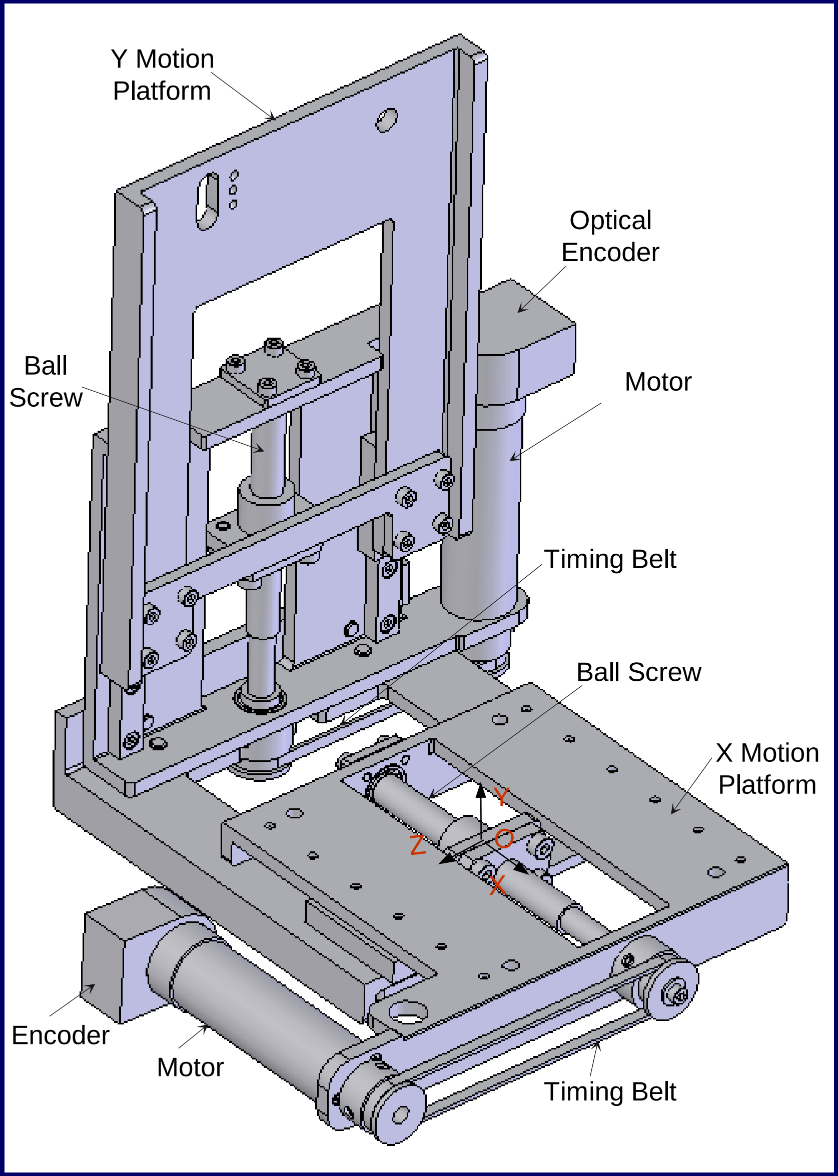

- Motorized x & y motion
- Angulation – up & down
- Optical encoders
- Positive drive – timing belt

Jefferson™
Kimmel Cancer Center
NCI-designated

EUCLIDIAN Software

Tasks:

1. Patient record handling
2. Image acquisition
3. Model building (prostate, urethra, pubic bone, rectum)
4. Dose distribution planning
5. 3D visualization
6. Real-time monitoring
7. Loop back to #2, 3 or 4 if requested by user

Jefferson™ Kimmel Cancer Center
NCI-designated

EUCLIDIAN Software

- Tasks:
  - Patient record handling
  - Image acquisition
  - Model building (prostate, urethra, pubic bone, rectum)
  - Dose distribution planning
  - 3D visualization
  - Real-time monitoring

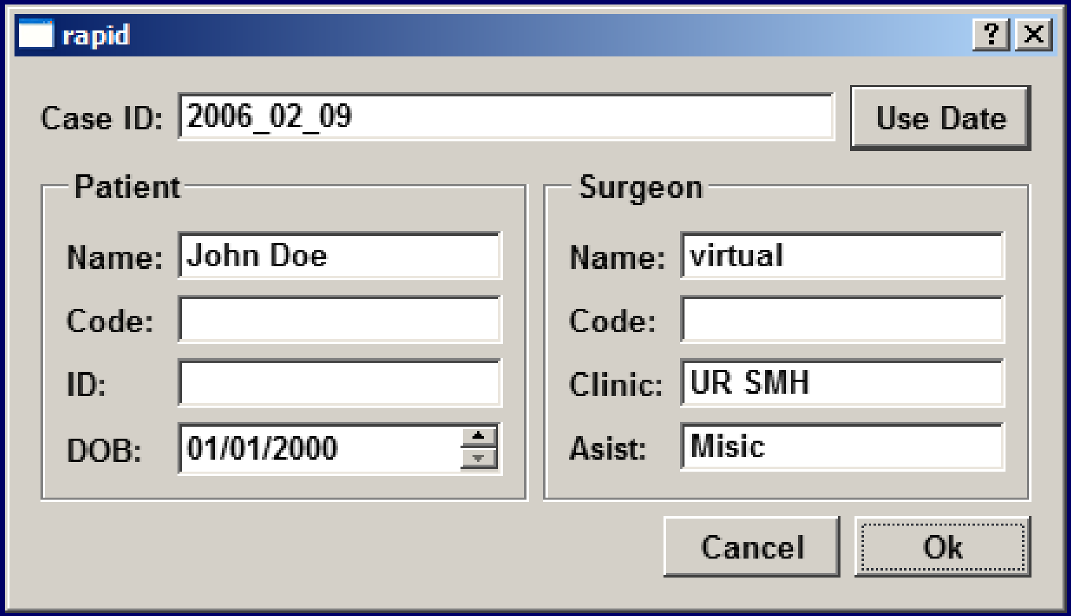

Jefferson Kimmel Cancer Center NCI-designated

EUCLIDIAN Software

- Tasks:
  - Patient record handling
  - Image acquisition
  - Model building (prostate, urethra, pubic bone, rectum)
  - Dose distribution planning
  - 3D visualization
  - Real-time monitoring

- Transverse, para-sagittal, and coronal views of the compounded volume
- Seamless spline interpolation
- Depends on surgeon experience

Jefferson™ Kimmel Cancer Center NCI-designated

EUCLIDIAN Software

- Tasks:
  - Patient record handling
  - Image acquisition
  - Model building (prostate, urethra, pubic bone, rectum)
  - Dose distribution planning
  - 3D visualization
  - Real-time monitoring

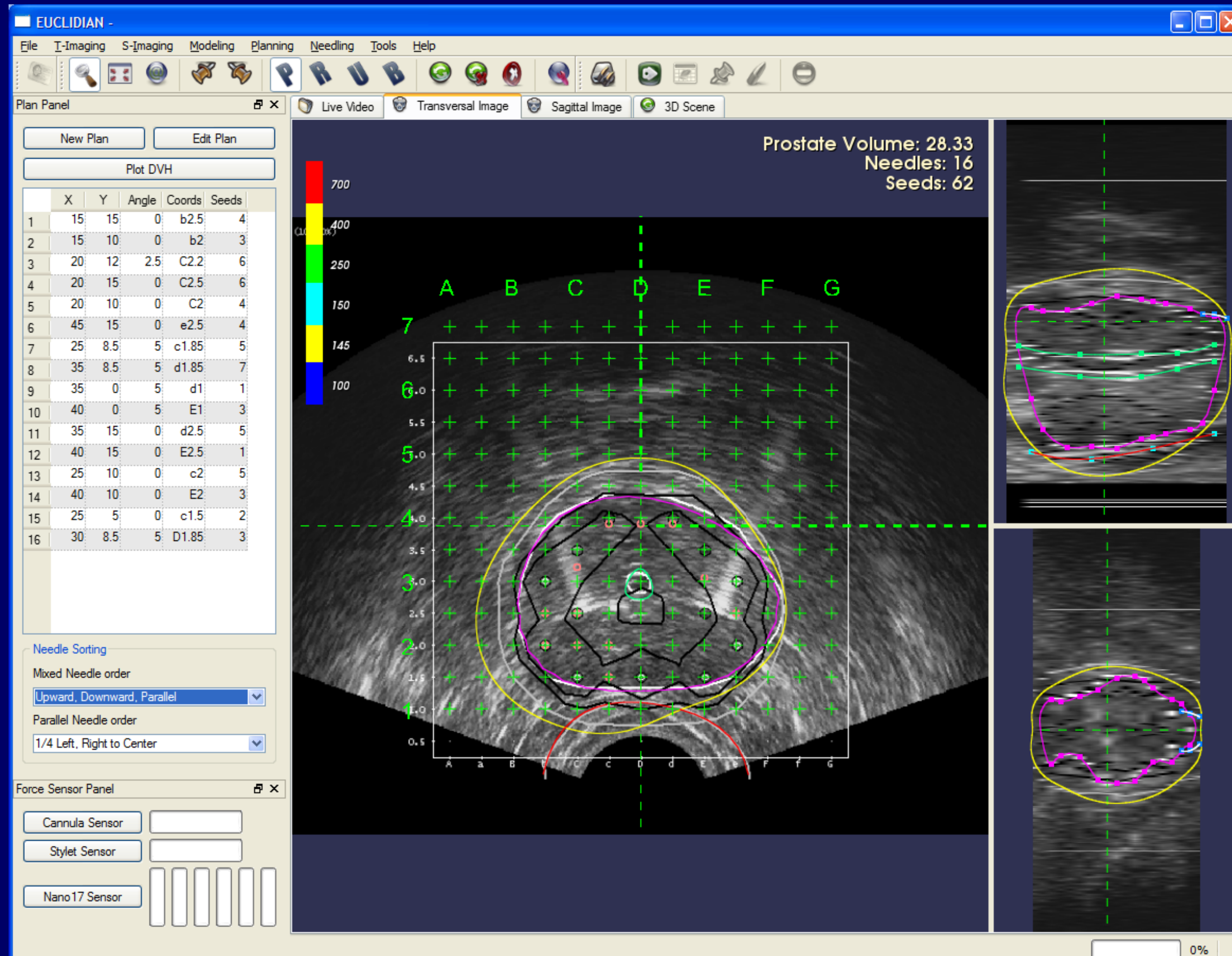

Jefferson™ Kimmel Cancer Center
NCI-designated

EUCLIDIAN Software

- Tasks:
  - Patient record handling
  - Image acquisition
  - Model building (prostate, urethra, pubic bone, rectum)
  - Dose distribution planning
  - 3D visualization
  - Real-time monitoring

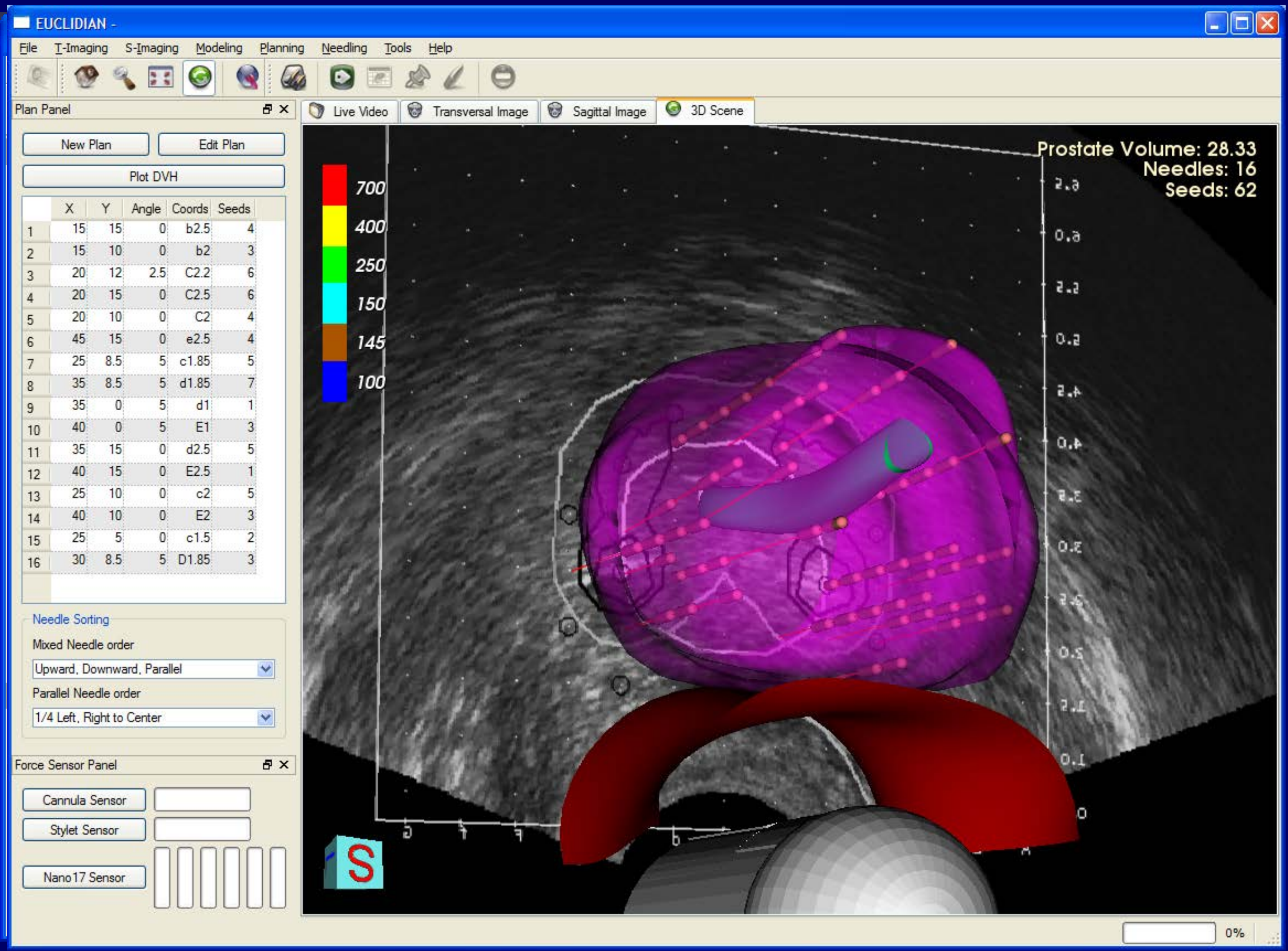

Jefferson™ Kimmel Cancer Center
NCI-designated

EUCLIDIAN Software

- Tasks:
  - Patient record handling
  - Image acquisition
  - Model building (prostate, urethra, pubic bone, rectum)
  - Dose distribution planning
  - 3D visualization
  - Real-time monitoring

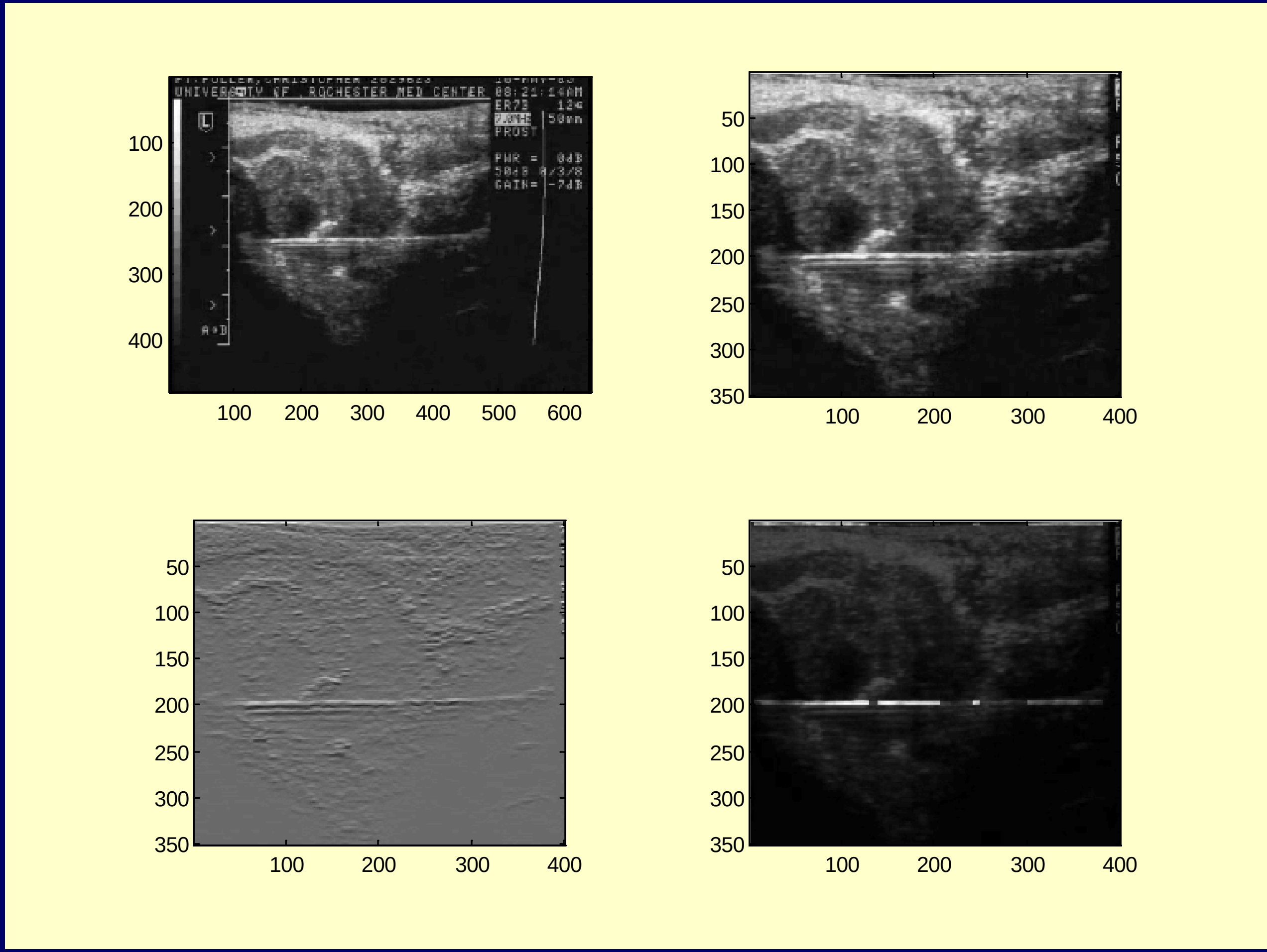

Jefferson™
Kimmel Cancer Center
NCI-designated

Kinematic calibration

Kinematic calibration determines

1)**System resolution** - the smallest incremental movement that the robot can physically perform
2)**Repeatability** - a measure of the ability of the robot to move back to the same position and orientation
3)**Accuracy** - the robot's ability to precisely move to a desired position in 3D space.

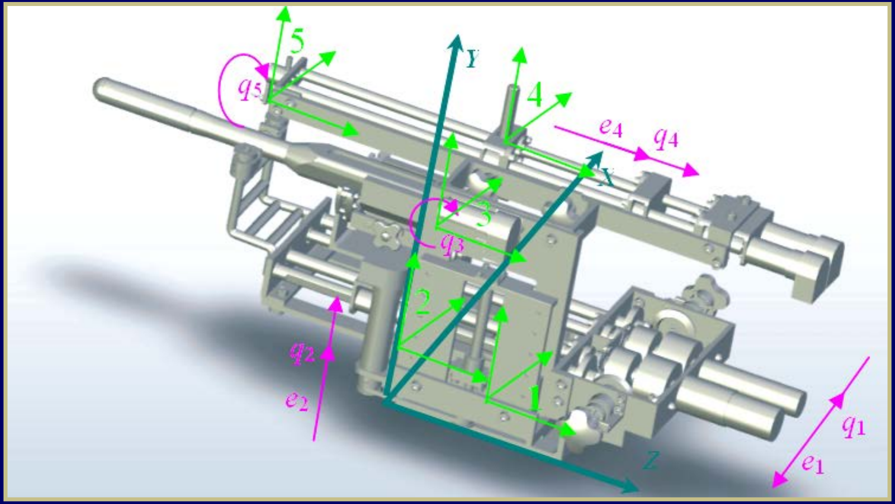

Generalized coordinates for Needling module

Kinematic calibration - procedure

1) DH model and table definition for robotic system,
2) Matrix transformation,
3) Definition of composite matrices
4) Direct kinematics solution,
5) Inverse kinematics solution,
6) Definition of robot initial position,
7) Calculation of position error and
8) Error correction method

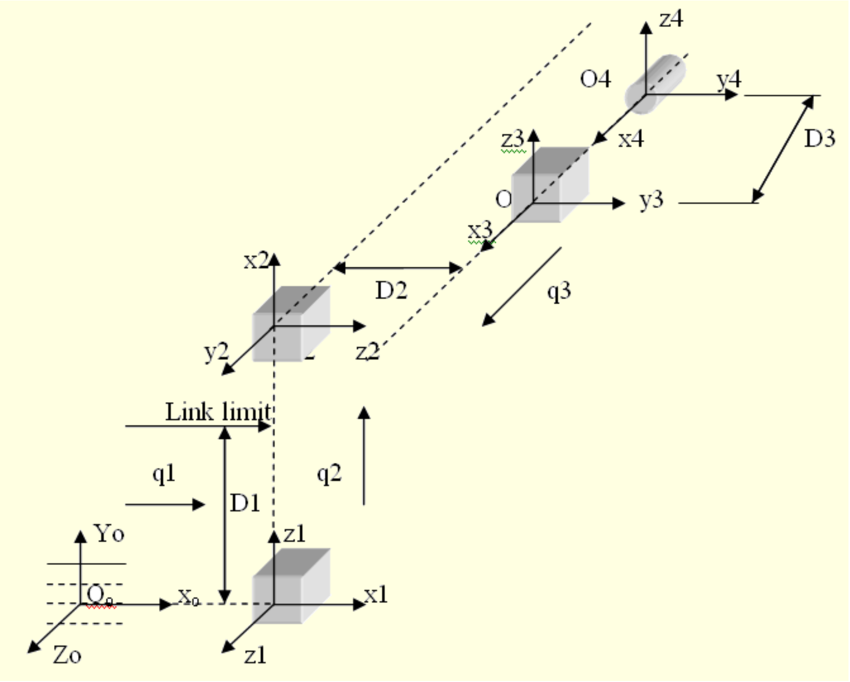

Kinematic DH calibration model

$$A = A_1 A_2 A_3 A_4 = \begin{bmatrix} 0 & \cos q_4 & -\sin q_4 & D_2 + q_1 + \delta_1 + \delta_4 \\ 0 & \sin q_4 & \cos q_4 & D_1 + q_2 + \delta_2 \\ 1 & 0 & 0 & D_3 + q_3 + \delta_3 + \delta_5 \\ 0 & 0 & 0 & 1 \end{bmatrix}$$

Real transformation matrix

$$\varepsilon = \sqrt{(p_{xid} - p_x)^2 + (p_{zid} - p_z)^2 + (p_{zid} - p_z)^2}$$

Position error

Jefferson™ Kimmel Cancer Center NCI-designated

Imaging calibration

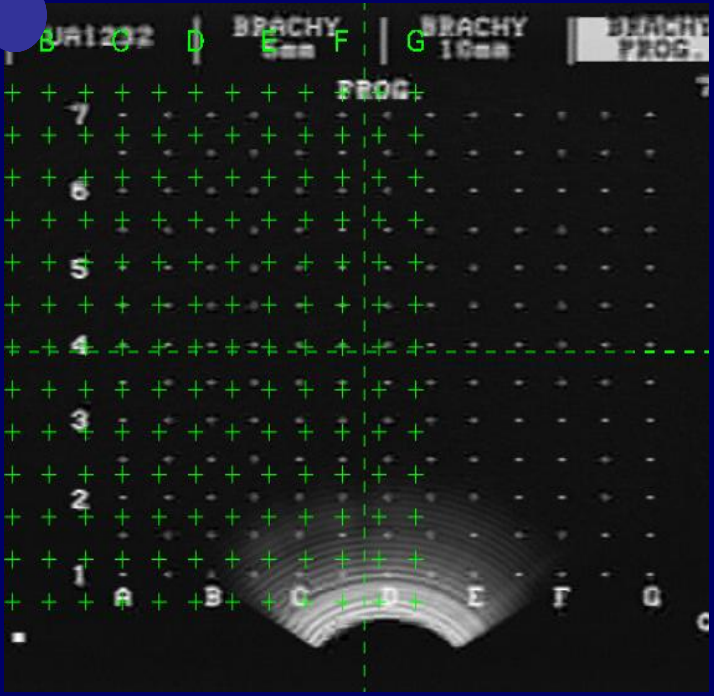

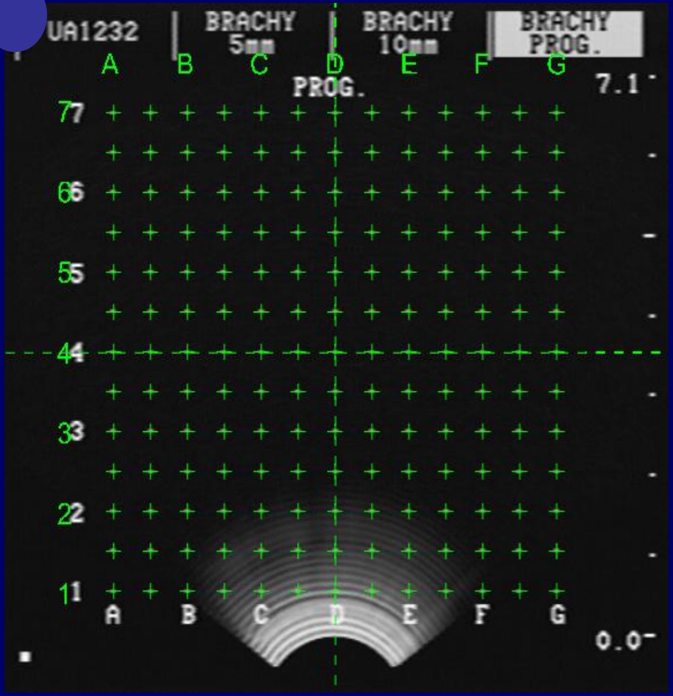

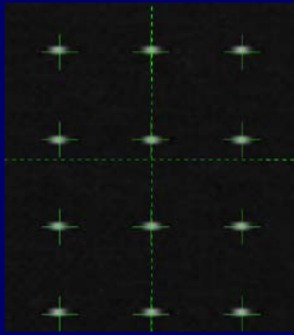

Imaging Calibration I – before image calibration

Imaging Calibration II – after image calibration

Jefferson™ Kimmel Cancer Center NCI-designated

Mutual (overall) calibration

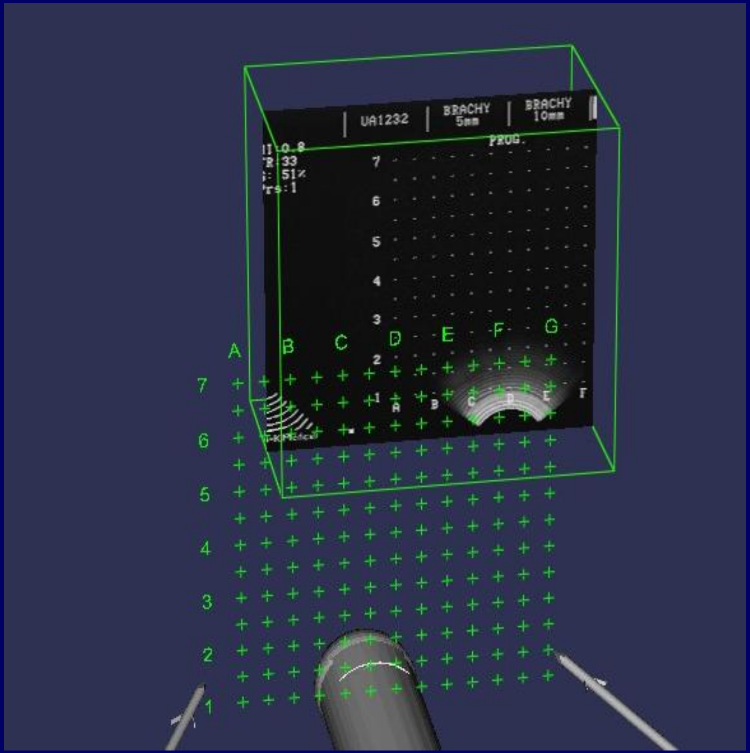

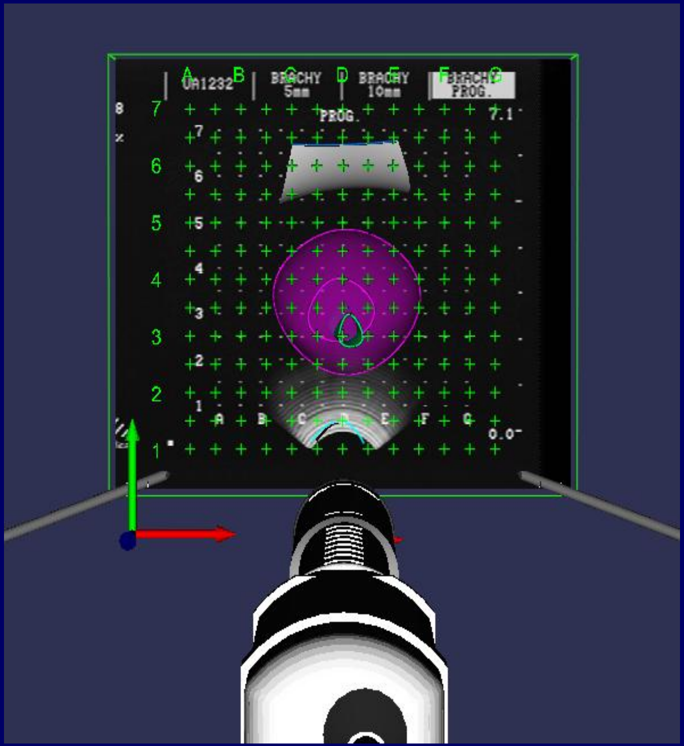

Overall Calibration I – before   Overall Calibration II – after

Jefferson™
Kimmel Cancer Center
NCI-designated

Calibration Results

Probe driver

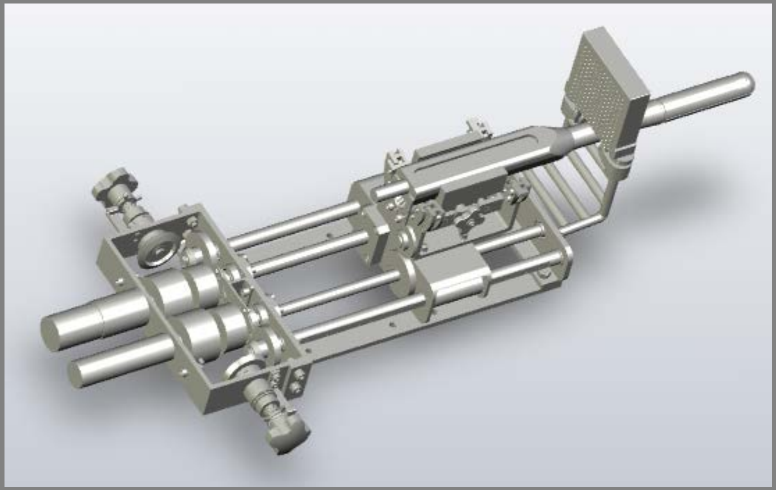

Accuracy: translation - 0.05mm
rotation - 0.1deg

	Measured value
Range	± 90 deg
Accuracy	0.1
Repeatability	± 0.03 deg

Table 1: US rotation performance

	Measured value
Parallelism	Axes Z and X
Accuracy (Z)	0.15 mm
Range (Z)	228.6 mm
Repeatability	0.03 mm
Accuracy (X)	0.05 mm
Range (X)	228.6 mm
Repeatability	0.03 mm

Table 2: US translation performance - parallelism

Jefferson™ Kimmel Cancer Center
NCI-designated

Calibration Results

Needling mechanism

	Measured value
Parallelism	Axe Y
Accuracy (Z)	0.15 mm
Range (Z)	101.6 mm
Repeatability (Z)	0.03 mm

Table 1 Gantry vertical movement

	Measured value
Parallelism	Axes Z and X
Accuracy (Z)	0.15 mm
Range (Z)	279.4 mm
Repeatability	0.03 mm
Accuracy (X)	0.18 mm
Range (X)	279.4 mm
Repeatability	0.03 mm

Table 2: Gantry lateral movement performance

	Measured value
Accuracy	0.03 mm
Speed	± 0.01 rev/s

Table 3: Cannula rotation

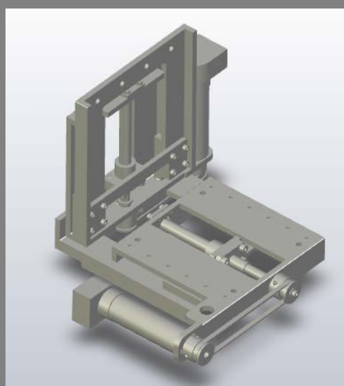

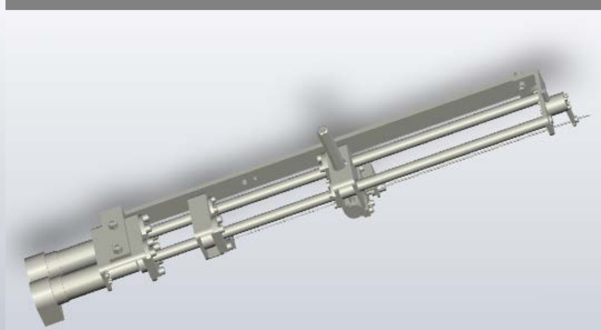

	Measured value
Parallelism	Axes Z and X
Accuracy (Z)	0.15 mm
Range (Z)	279.4 mm
Repeatability	0.03 mm
Accuracy (X)	0.18 mm
Range (X)	279.4 mm
Repeatability	0.03 mm

movement performance

- ***Translation movements*** precision ***stylet and cannula*** are in the range of ***0.03-0.08mm***
- ***Lateral and vertical*** precision for ***gantry*** is 0.03mm

The ***fiducial error*** for ***images*** is less than ***0.1mm*** in **x** and **y** image coordinates.

Jefferson Kimmel Cancer Center NCI-designated

Calibration Test - Seed Deposition

Assessment of the deposited seeds revealed that the accuracy (relative error) of seed placement is

0.15mm (SD=0.15mm) in x,
0.13mm (SD=0.11mm) in y
0.11mm (SD=0.11mm) in z

The 3D (Euclidean) rms error is 0.227 mm.

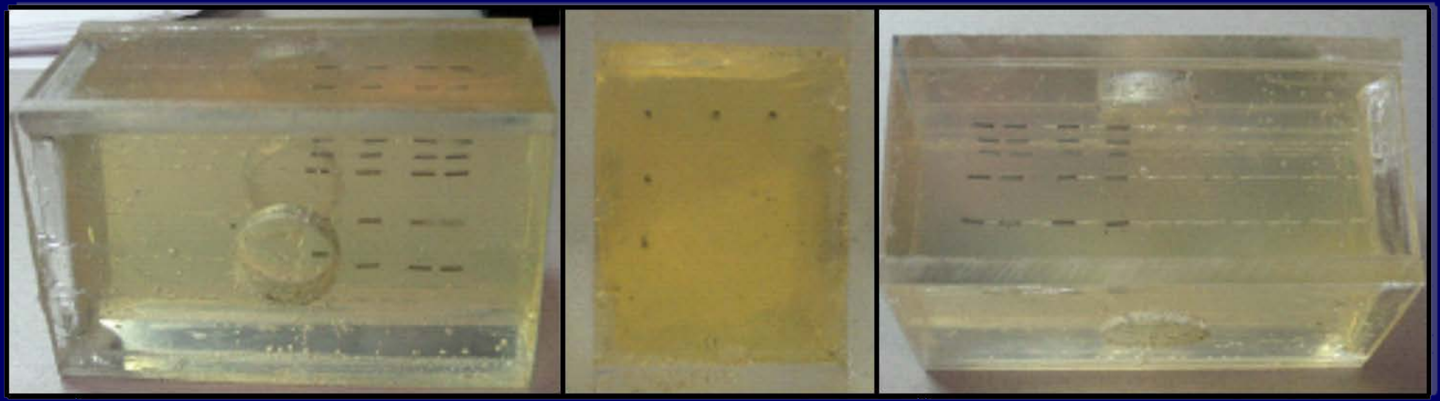

Seeds deposited into PVC phantom
(lateral, frontal and top view)

Jefferson™ Kimmel Cancer Center NCI-designated

EUCLIDIAN Operation

Homing Procedure

Seed Delivery

Jefferson™
Kimmel Cancer Center
NCI-designated

Some pertinent features of EUCLIDIAN

- All the hardware and software are designed and developed in house
- Fully automated ultrasound-based IGBT system; however, at any time the physician can takeover the control using a teach/user-pendent
- 9dof positioning module – 3dof cart and 6dof platform motorized vertical lift (y), electro-magnetic locks on x, y and z axes, 3dof rotation has mechanical locking arrangement
- Motorized 7dof surgery module
- No physical template required
- 3 force sensors – to detect pubic arch interference (PAI), to confirm seed delivery, to detect needle deviation and bending, and potentially to sense tumor foci
- Can cover 62mm x 67mm surgical area; 10^0 angulation
- PID controller and sensor data acquisition algorithm
- Dosimetric planning, 3D visualization, needle tracking, seed detection in software
- Needle and seed passages are sterilizeable, other parts are easy to clean and decontamination
- Provision for quick manual takeover (if required)
- Preliminary results reveal seed delivery accuracy of 0.23mm

Jefferson™ Kimmel Cancer Center NCI-designated

Multi-Channel Robotic System

MRDI (Multichannel Robot-assisted Delivery and Intervention)

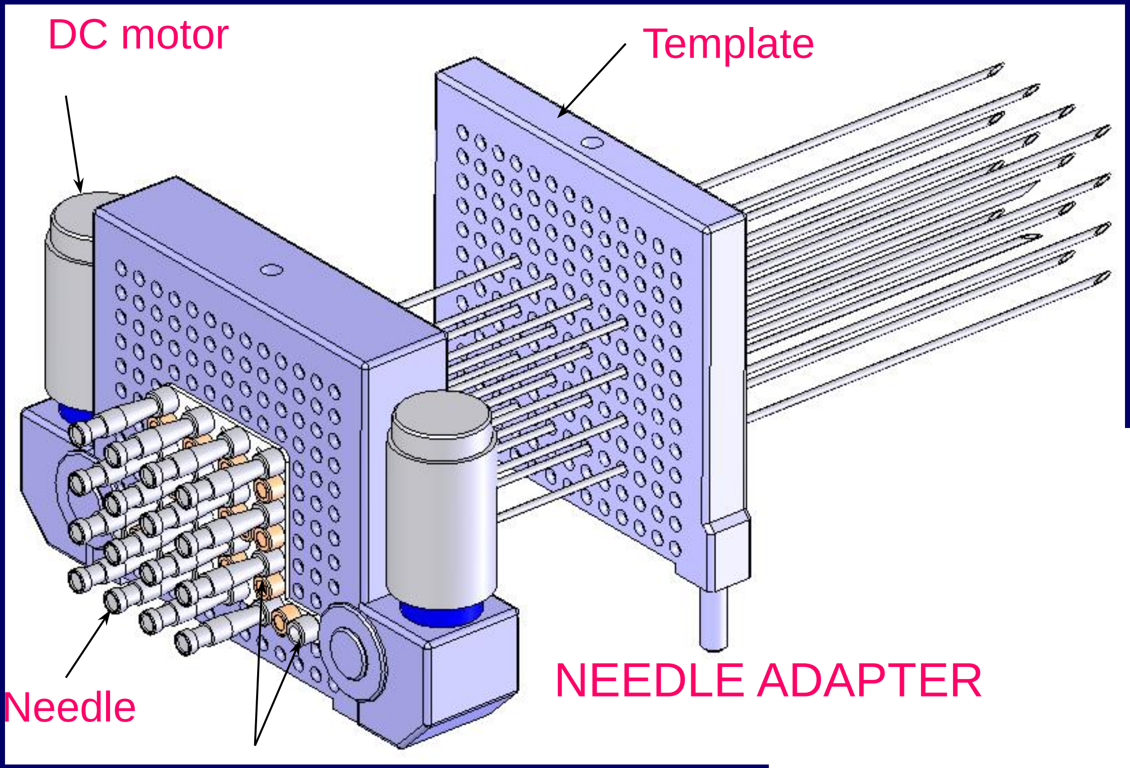

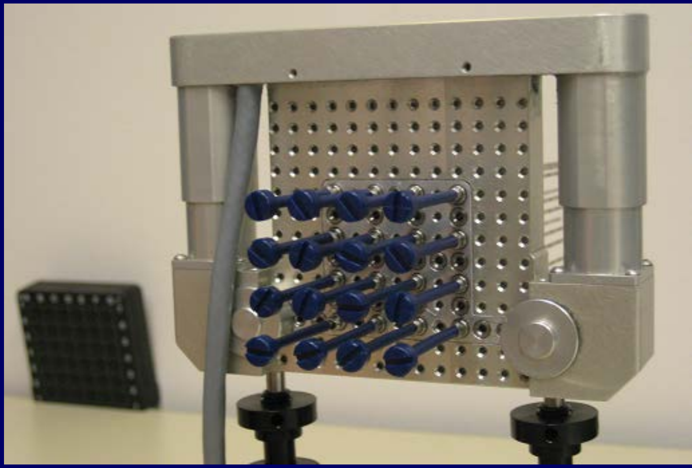

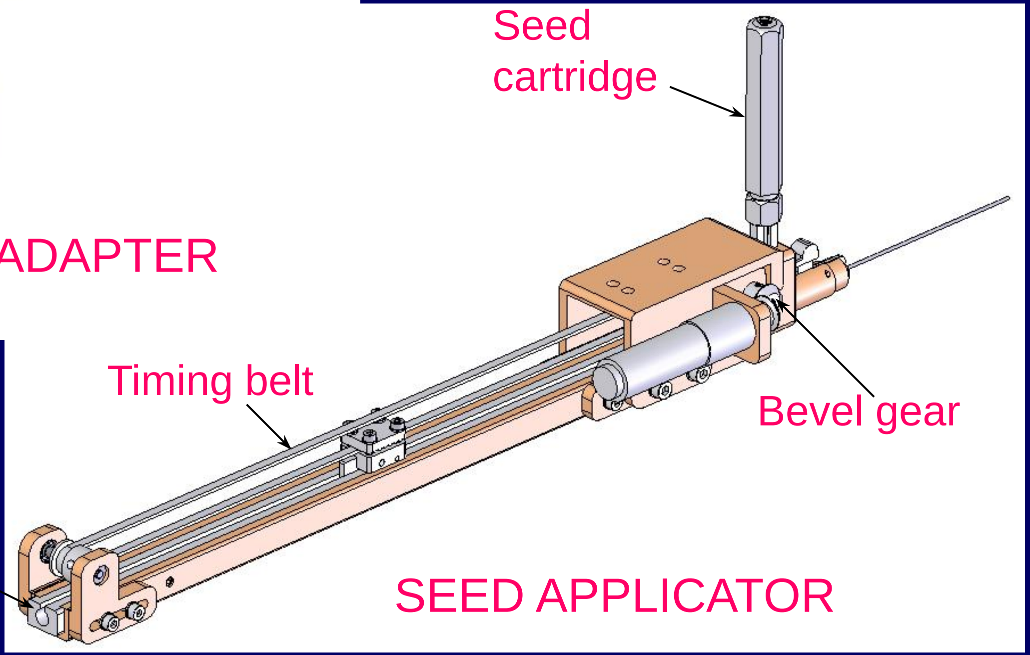

Jefferson™
Kimmel Cancer Center
NCI-designated

MRDI (Multichannel Robot-assisted Delivery and Intervention)

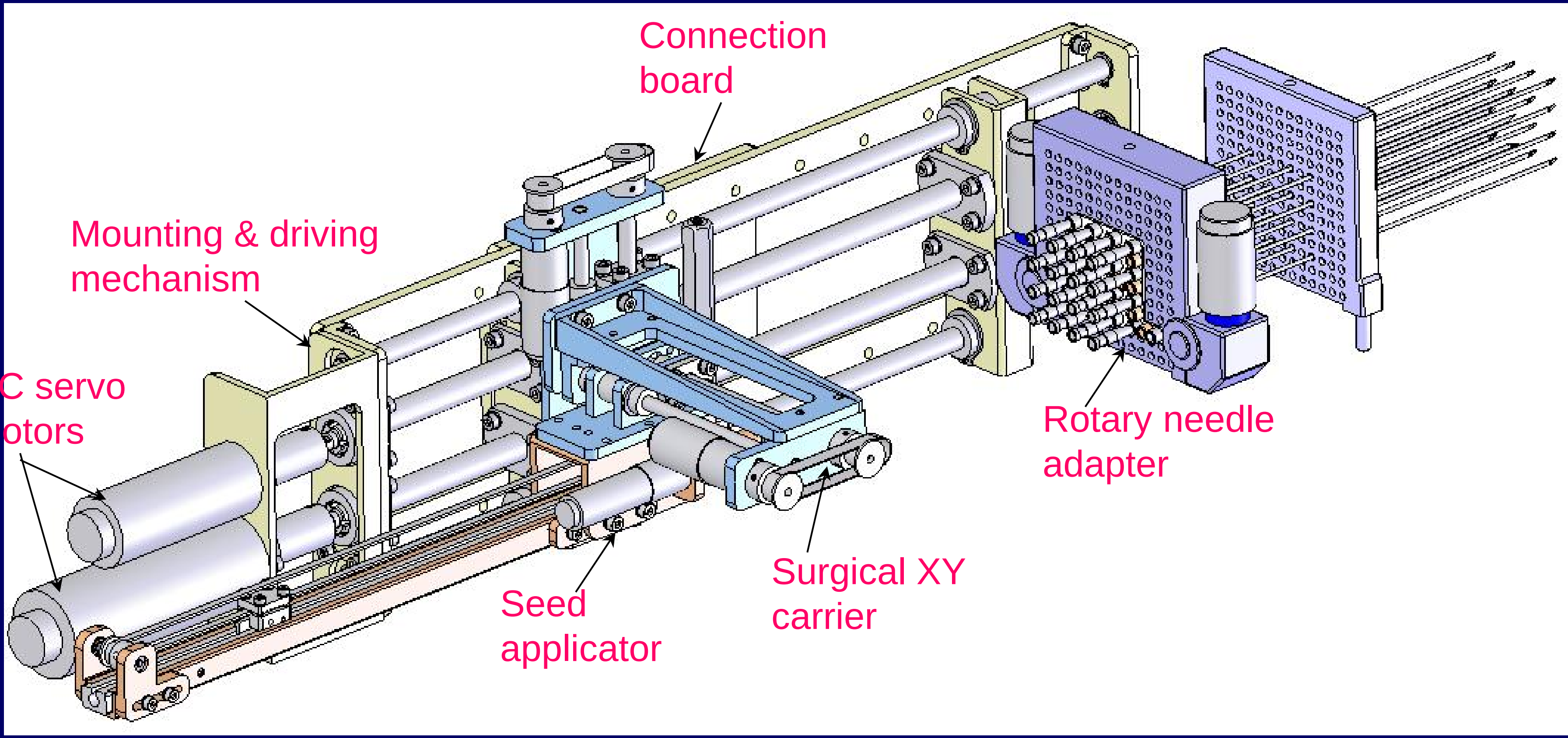

Jefferson Kimmel Cancer Center NCI-designated

MRDI (Multichannel Robot-assisted Delivery and Intervention)

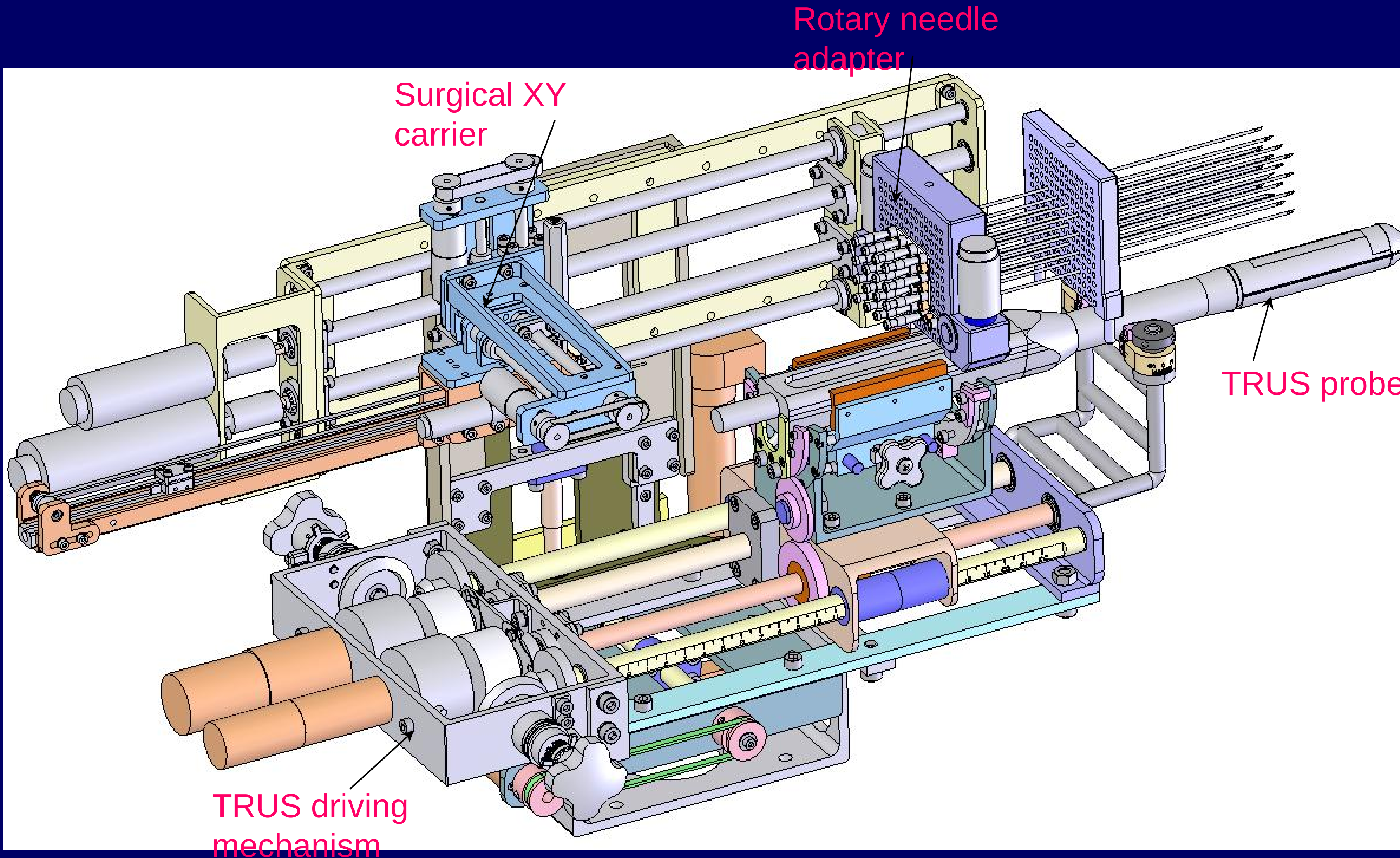

Jefferson™
Kimmel Cancer Center
NCI-designated

Tumor Sensing Study

OBJECTIVE

- To develop a real-time tissue sensing strategy by analyzing needle insertion forces combined with patient-specific criteria
  - Detect tumor foci “JIT” for targeted therapy
  - Maximize use of data that can be gathered during needle interventions under robotic assistance (e.g. during prostate brachytherapy)

HYPOTHESIS

- Tissue mechanical heterogeneities of tumor can be distinguished from those of normal variants (glandular, fibromuscular tissues) by accurate force-torque measurements during needle incursion

Jefferson™
Kimmel Cancer Center
NCI-designated

EVIDENCE SUPPORTING THE HYPOTHESIS

- Variations in stiffness between tumor and normal tissue [1], as well as between patients [2]
- Basis of tissue elastography imaging
  - Diseased tissues: changes in tissue composition, consistency, elasticity and stiffness
- DRE, BSE …
- Necrotic regions – potentially requiring selective, localized dose escalation

1. V. Jalkanen, B.M. Andersson, A. Bergh, B. Ljungberg, and O.A Lindahl., “Prostate tissue stiffness as measured with a resonance sensor system: a study on silicone and human prostate tissue in vitro”, Medical & Biological Engineering & Computing, 44 (7), 593-603 (2006).
2. V. Jalkanen, “Resonance Sensor Technology for Detection of Prostate Cancer”, Department of Applied Physics and Electronics, Umeå University, Umeå, Sweden (2006)

PATIENT-SPECIFIC FACTORS

- Age
- Ethnicity
- BMI
- Prostate volume
- Prostate density
- Gleason score
- PSA
- Clinical stage

Jefferson™
Kimmel Cancer Center
NCI-designated

METHOD: Patient-Specific Factors Modeling

- Regression model: Baseline mean force in normal tissue

$$F_b = \sum_{i=0}^{\mathbf{N}} \beta_i X_i^{n_i}$$

N = statistically significant terms

- Tumor detection model: threshold force in tumor

$$F_t = F_b + \Delta$$

Discriminator: sensitivity vs. specificity,

i.e. ROC analysis

- Optimize diagnostic power
  - Objective: Max $\mathrm{F}(\beta), \beta \in \Phi = \{\beta_{il} \le \beta_i \le \beta_{ih}, i = 0,1,2\}$
    - F_1 : area under curve (AUC) of ROC.
    - Sequential Quadratic Programming method

Jefferson™ Kimmel Cancer Center

NCI-designated

MATERIAL AND METHODS

- 23 patients who underwent radical prostatectomy enrolled in IRB-approved clinical study with informed consent
- Prostatectomy sample was brought to the research lab within 10 min of complete resection
- The prostate was placed into a pre-prepared PVC phantom
- Two stabilization needles were used to mimic the effect during brachytherapy procedure

Jefferson™ Kimmel Cancer Center NCI-designated

MATERIAL AND METHODS (cont.)

- 18-gauge diamond tip brachytherapy needles (Mick Radio-Nuclear Instruments, Inc., NY)
- 6DOF robotic system equipped with 6DOF Force-Torque sensor (Nano17®, ATI Industrial Automation, NC)
- Insertion speed 10 mm/s; apex to base
- Needle progression into the prostate and 3D deformation were recorded in 2 orthogonal planes simultaneously under ultrasound (GE LOGIQ-9, model 2404587, Milwaukee, WI; Acuson model 128xP, Mountain View, CA)

Jefferson™ Kimmel Cancer Center NCI-designated

Real-time Prostate Cancer Detection (needle insertion force)

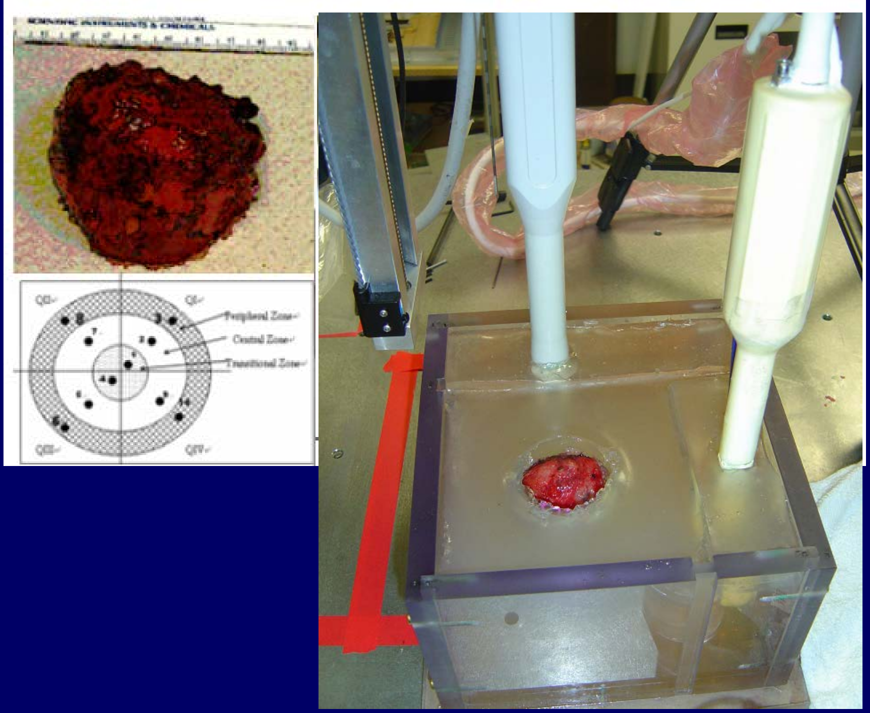

Needle insertion force experiment with Human Prostate (n=23)

Histopathology

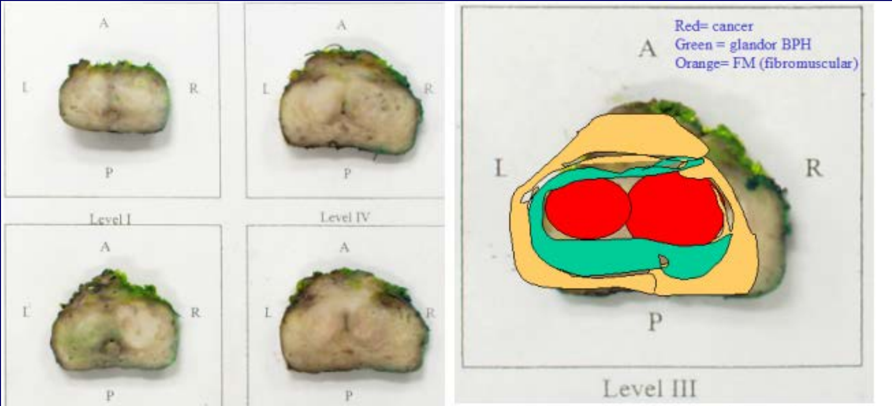

	Level III(midial)
1	BPH+FM(8:2)
2	G+FM(5:5)
3	G+FM(7:3))
4	CA+FM(8:2)
5	CA+FM(2:8)
6	FM(10)
7	CA (10)
8	G+FM(5:5)
9	BPH+G+FM(3:2:5)
10	FM(10)

G: Gland
FM: Fibromuscular
CA: Cancer
BPH: Benign Prostatic Hyperplasia

Jefferson™
Kimmel Cancer Center
NCI-designated

MATERIAL AND METHODS (cont.)

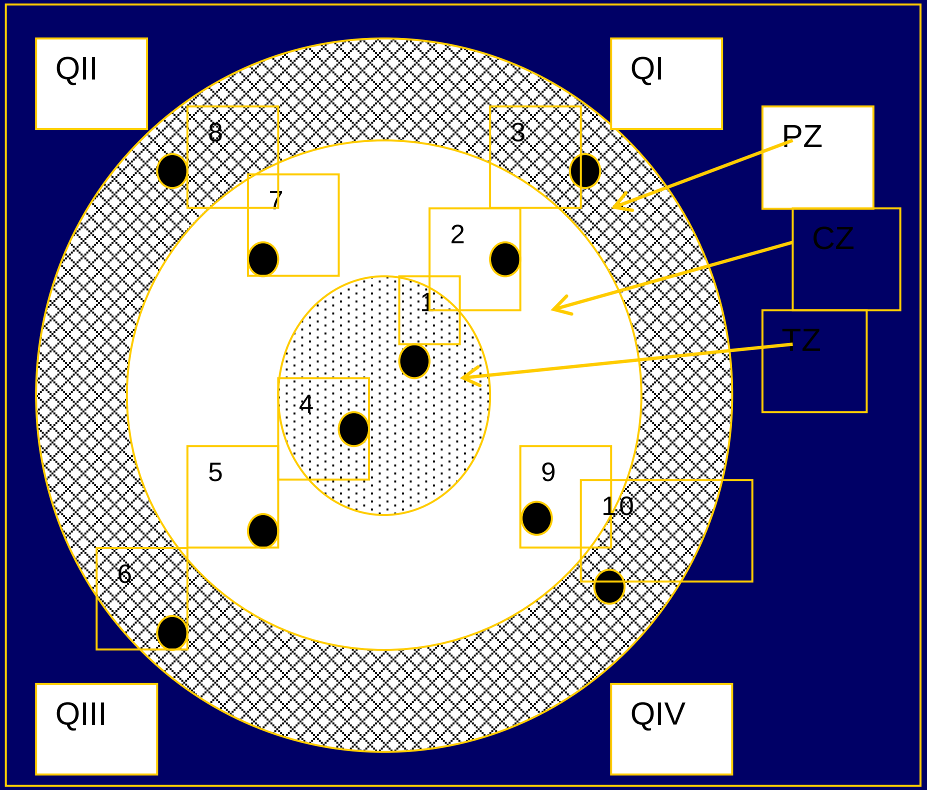

- 10 locations in three zones (peripheral, central and transitional) of the prostate
- Pathological analysis:
  - 4 mm sections through the prostate
  - Needle tracks identified
  - Histology reported at pre-selected levels from apex to base

Jefferson™ Kimmel Cancer Center NCI-designated

Patient	case#5		Level I (Apex)	Level III (midial)	Level V (medial)	Level IX (base)
xyz	abcd	1	G(V, minute CA)+FM(5:5)	BPH+FM(8:2)	G+FM(4:6)	SV+G+FM(1:4:5)
56Y		2	G+FM (5:5)	G+FM(5:5)	G+FM(5:5)	G+FM(6:4)
43 gms		3	dilated G +FM (7:3)	G+FM(7:3))	G+FM(3:7)	G(dilated)+FM (5:5)
4.4 x 5 x 2.9 (cm)*		4	CA+G+FM(3:2:5)	CA+FM(8:2)	G+FM(2:8)	G+FM(pact) (4:6)
CA: 3+3=6/10		5	CA+BPH+FM (4:3:3)	CA+FM(2:8)	G+FM(2:8)	G+FM(pact) (4:6)
11 sections		6	G+FM(4:6)	FM(10)	G+FM(2:8)	G+FM (4:6)
		7	CA+FM (5:5)	CA (10)	CA+G+FM(1:2:7)	SV+G+FM(1:4:5)
		8	G+FM(4:6)	G+FM(5:5)	G+FM(4:6)	G(dilated with focal PIN) +FM(6:4)
		9	CA+G+FM(4:2;4)	BPH+G+FM(3:2:5)	G+FM(3:7)	BPH+G+FM(pact) (2:3:5)
		10	CA+G+FM(2:4:4)	FM(10)	G+FM(2:8)	G+FM(4:6)

Key:

SV=seminal vesicle; G=Gland; FM=fibromuscular tissue of prostate;

CA=adenocarcinoma of prostate; G(V)=Glands near Verumountanum.

Jefferson™ Kimmel Cancer Center NCI-designated

MATERIAL AND METHODS (cont.)

- Pathology data used as ground truth
- Data from ~half of the study patients were used to optimize the model
- Data from the remaining patients were used to test/validate the model
  - ROC analysis: Area under the curve (AUC) used as measure of diagnostic power
- Selection of patients for modeling: factorial design

RESULTS

Needle Insertion Force Profiles

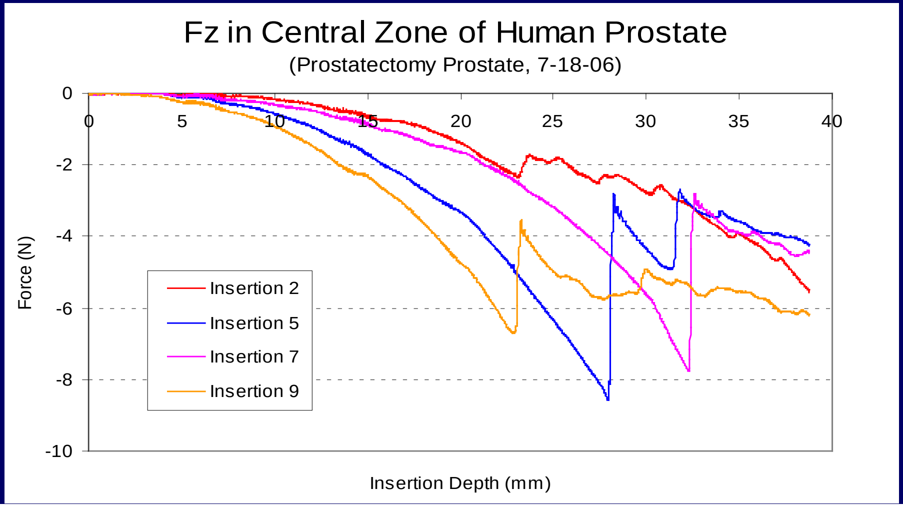

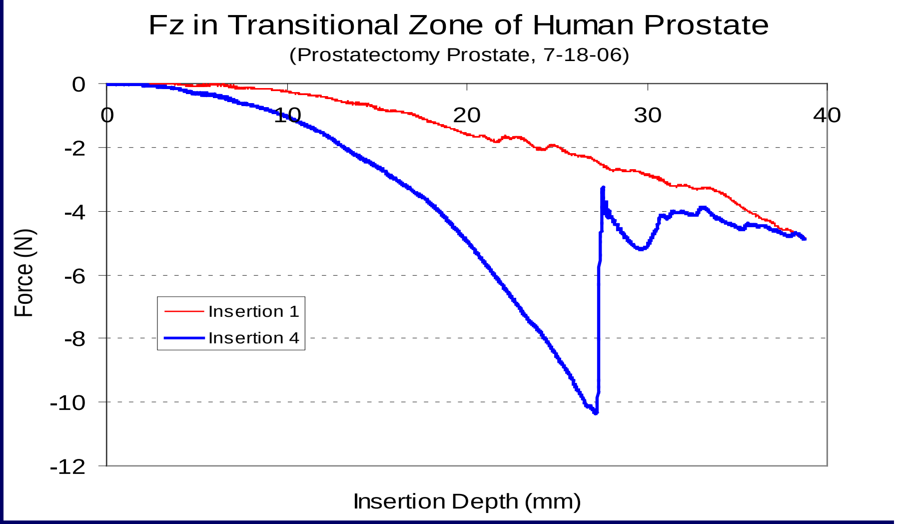

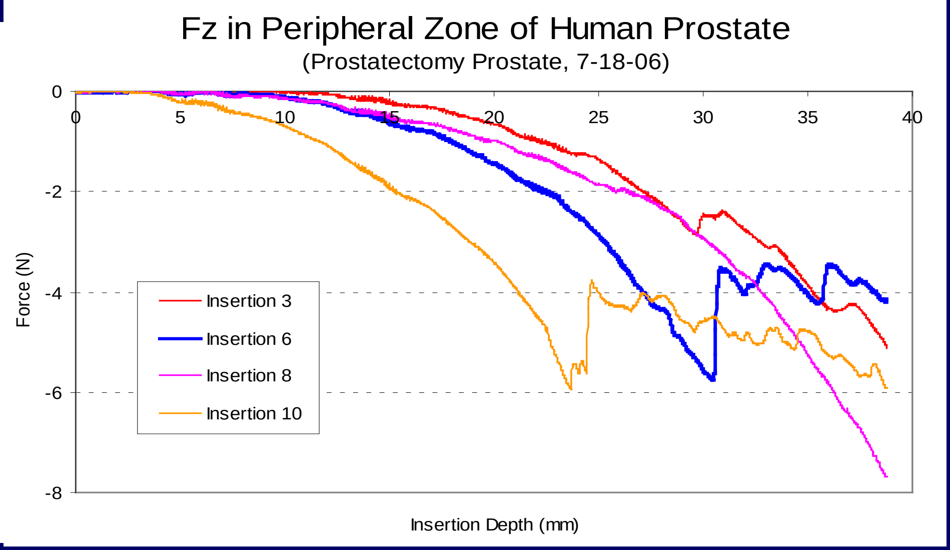

Jefferson™ Kimmel Cancer Center
NCI-designated

RESULTS: Force Analysis

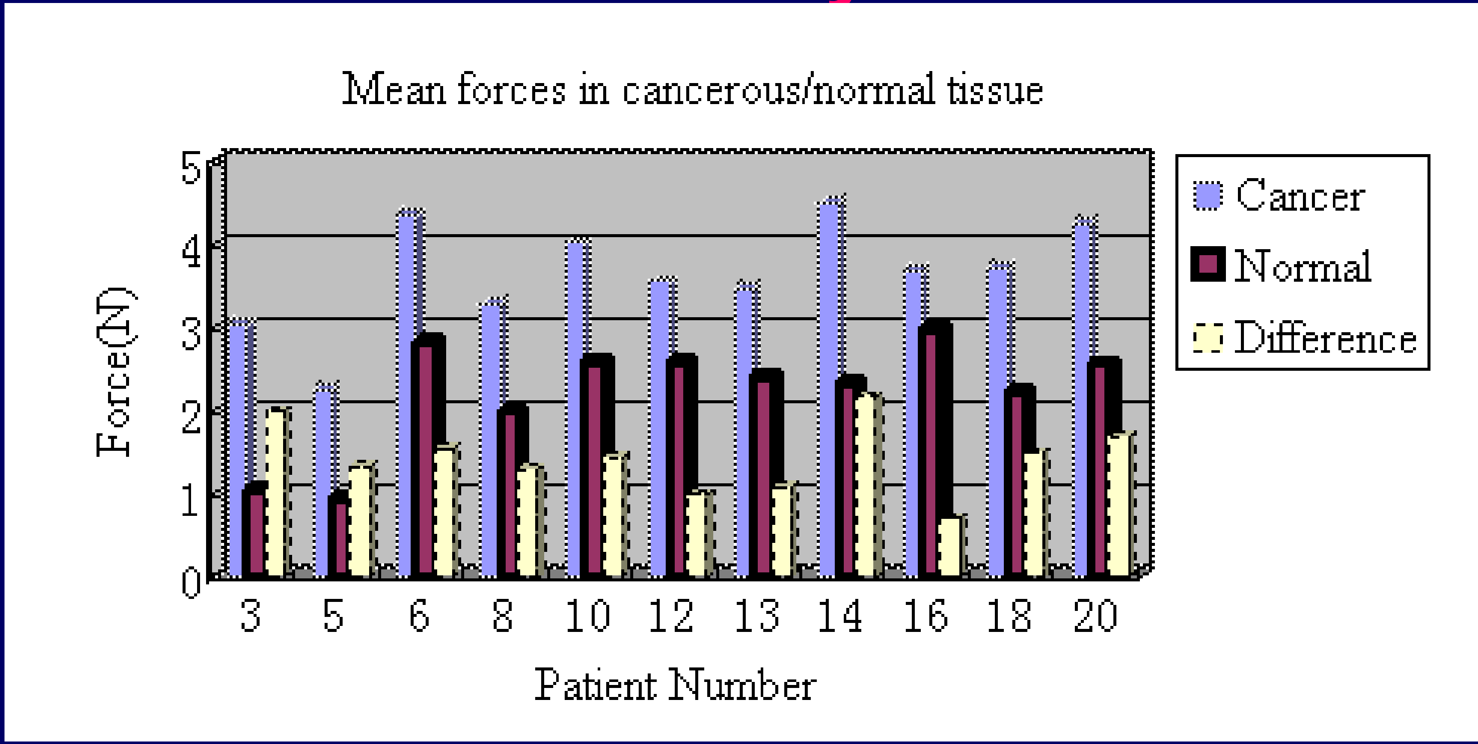

- Needle insertion force: cutting force + visco-elastic friction force
- Variation of the forces : indicator of tissue composition variability
- **$F_c > F_n$: 0.7N ~ 2.2N**

Jefferson™ Kimmel Cancer Center NCI-designated

RESULTS: Patient-specific Factors

- **Patient-specific factors**

  Start with all terms in constructing the model:

  patient age, ethnicity, BMI, clinical stage of cancer, Gleason score, prostate volume, prostate density and PSA
- **Backward stepwise regression**
  - p value: stepwise elimination of least significant terms in model
  - Multicolinearity: Variance inflation factors (VIF)
  - Autocorrelation of model residuals: Durbin-Watson number
- **Significant factors:** prostate density and PSA
  - Higher density and higher PSA value tend to predict larger insertion forces

Jefferson™ Kimmel Cancer Center NCI-designated

RESULTS: Model Validation

- Model tuning: 10 patients
  - (x1:density, x2:PSA)
  - max(AUC)=0.80

$$F_b = \text{-}0.06\text{-}0.06x_1\text{-}0.175x_2$$

- Model validation: 11 patients

  - **AUC=0.90**

  - classifier 1.7: sensitivity 100%, specificity 76%
  - classifier 1.9: sensitivity 86%, specificity 79%

Jefferson™ Kimmel Cancer Center NCI-designated

International Collaboration

Centre for Advanced Mechanisms and Robotics

School of Mechanical Engineering

Tianjin University

Division of Medical Physics, Department of Radiation Oncology

Thomas Jefferson University

2013

(1) MRI-guided surgical robot

a. Mechanism Design
b. Control System Design
c. Machinability Research
d. Reliability Analysis

(2) Ultrasound-guided surgical robot

a. Introduction on robot
b. Treatment Planning Software (TPS) Design

(3) Needle-tissue interaction

a. Tissue-equivalent material preparation
b. Needle-tissue interaction forces investigation

Jefferson™ Kimmel Cancer Center NCI-designated

(1) MRI-guided surgical robot

a. Mechanism Design: The first generation of the robot

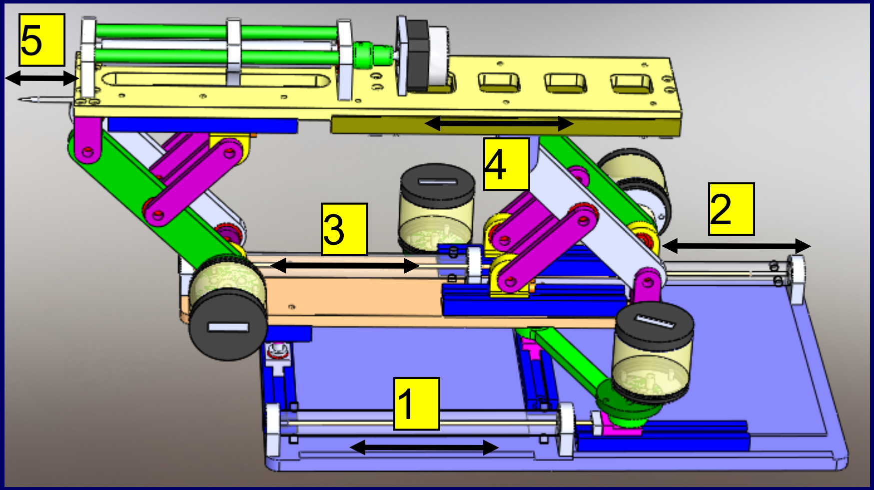

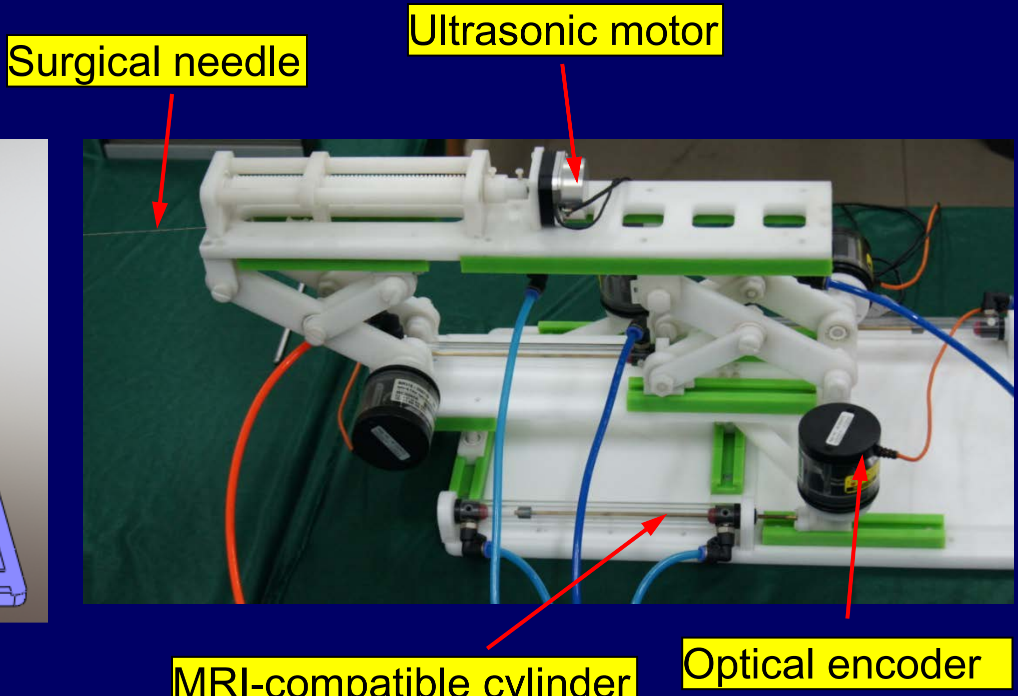

Fig.1 Virtual prototype of the surgical robot

Fig.2 Physical prototype of the surgical robot

Jefferson™ Kimmel Cancer Center NCI-designated

(1) MRI-guided surgical robot

a. Mechanism Design: The second generation of the robot

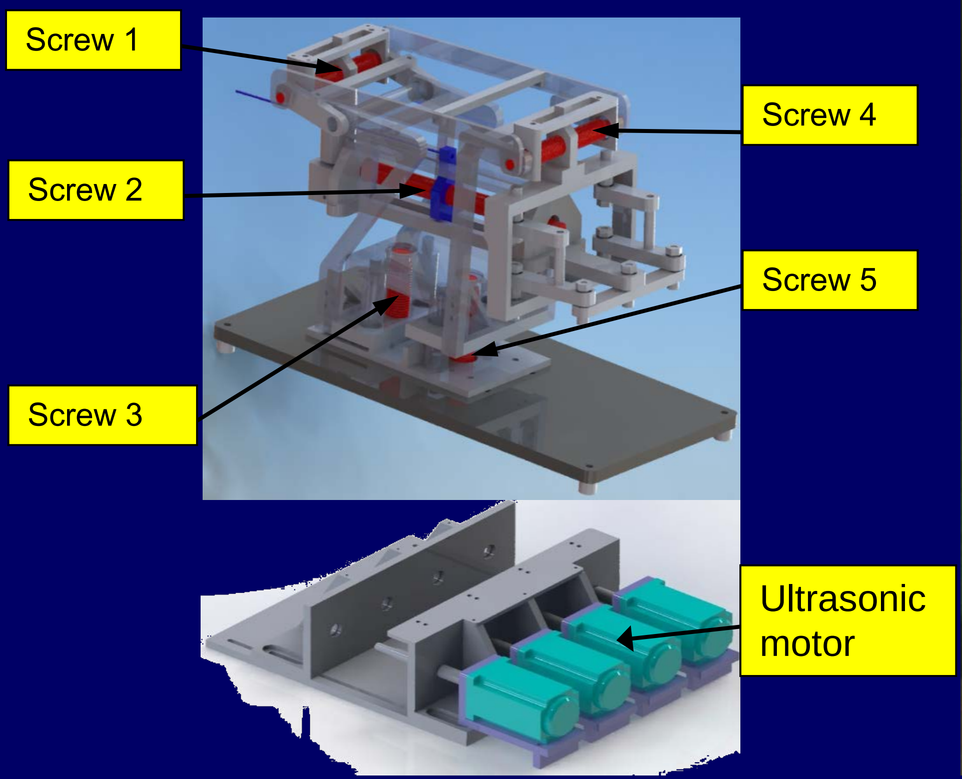

Fig.3 Virtual prototype of the surgical robot

Fig.4 Physical prototype of the surgical robot

Jefferson™ Kimmel Cancer Center NCI-designated

(1) MRI-guided surgical robot

a. Mechanism Design：The third generation of the robot

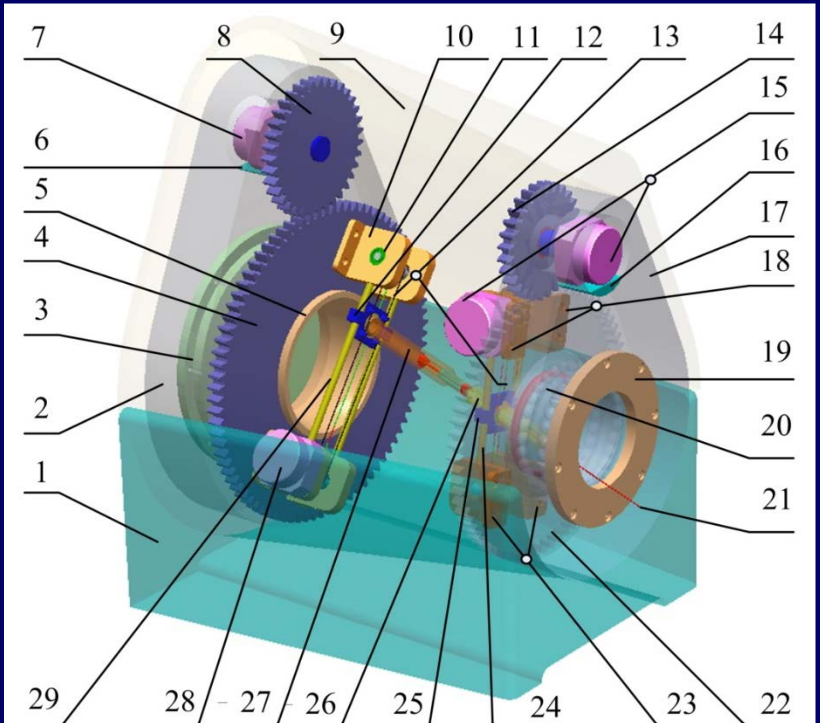

1-base, 2,17-bracket, 3,19-bearing end plate, 4,22-gearwheel, 5-gear shaft, 6,16-motor base, 7,15,28-ultrasonic motor, 8,14-pinion, 9-cover, 10,18,23-bearing pedestal, 11,20-bearing, 12, 25-slider, 13-transmission wire, 21-puncture needle(end effector), 24,29-guiding bar, 26, 27-needle guards

Fig.5. Virtual prototype of the third generation of the surgical robot

Jefferson™ Kimmel Cancer Center NCI-designated

(1) MRI-guided surgical robot

b. Control System Design

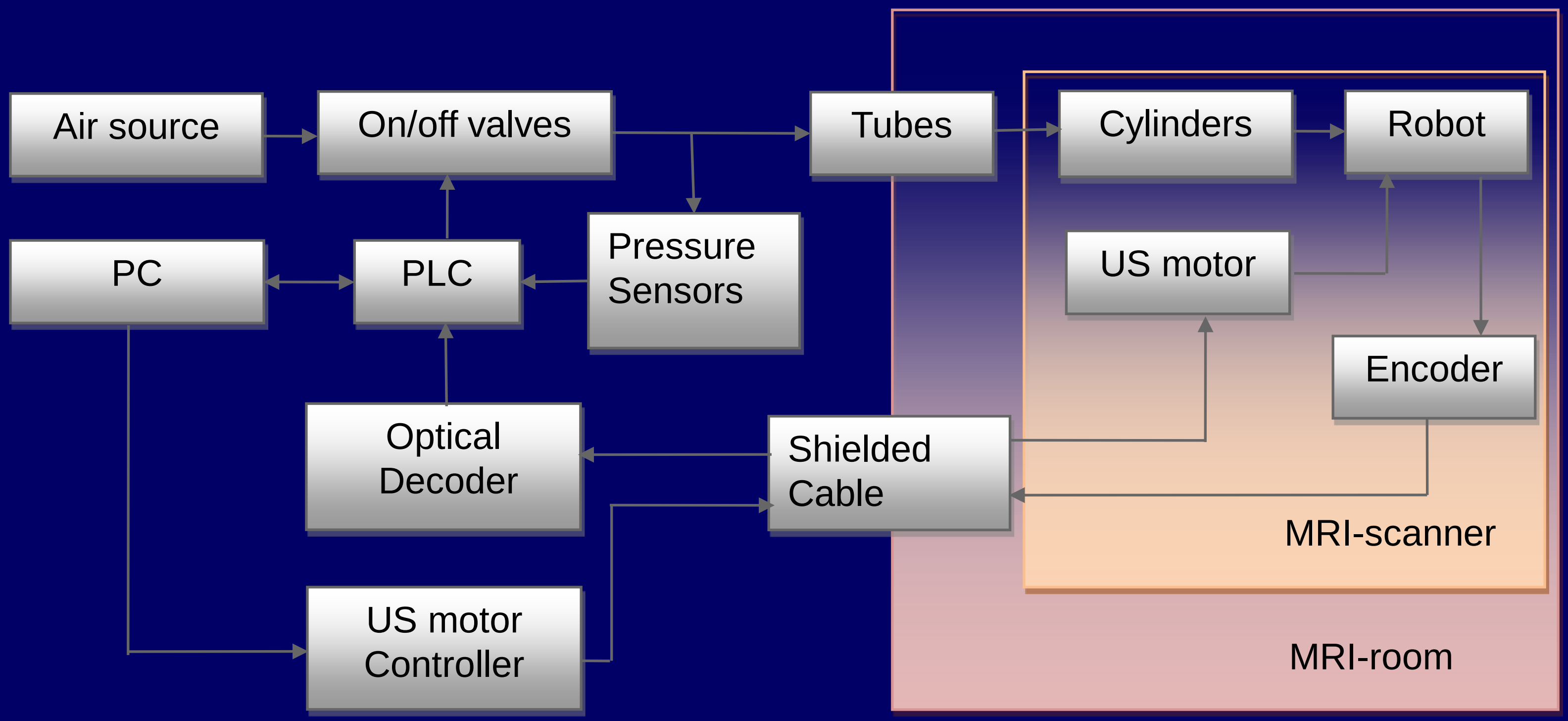

Fig.6. Flow diagram the control system

(1) MRI-guided surgical robot

b. Control System Design

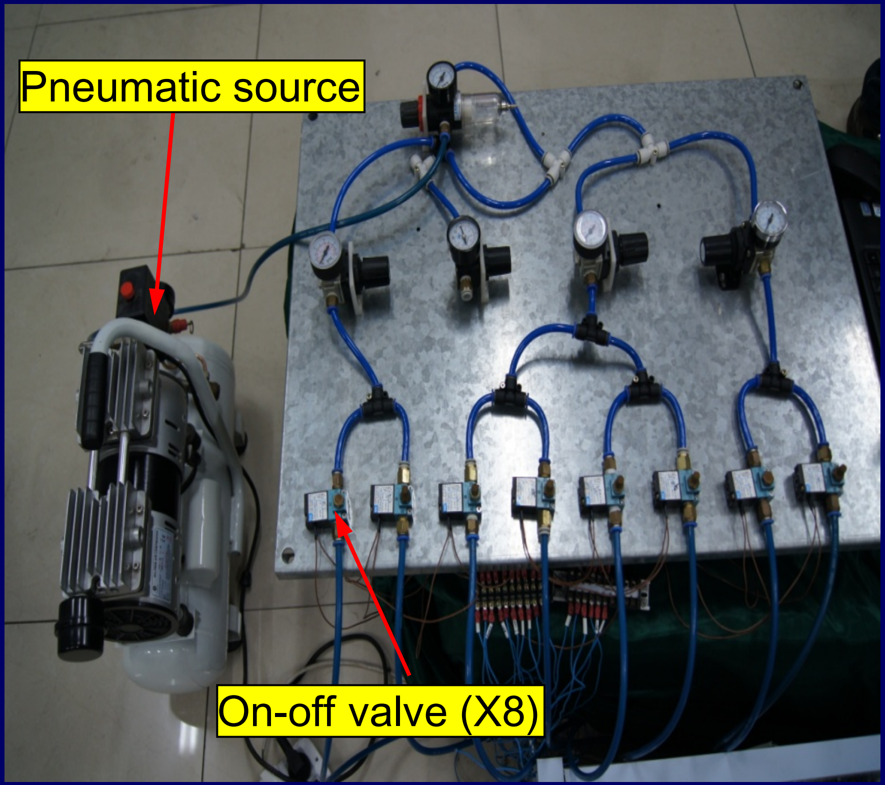

Fig.7. Pneumatic system

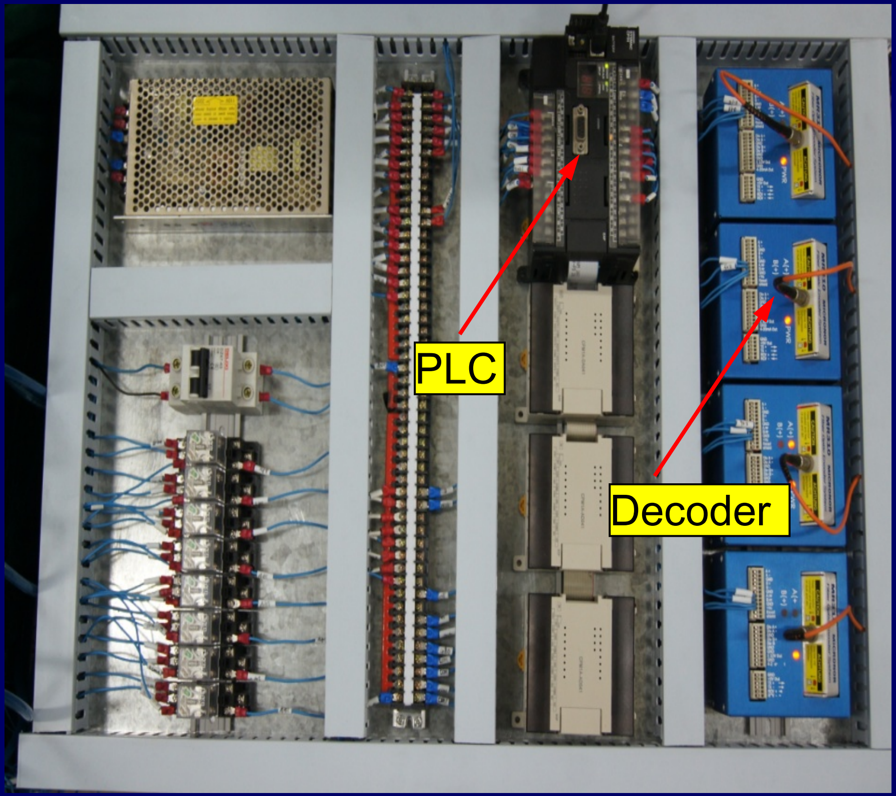

Fig.8. Electrical system

Jefferson™ Kimmel Cancer Center NCI-designated

(1) MRI-guided surgical robot

b. Control System Design

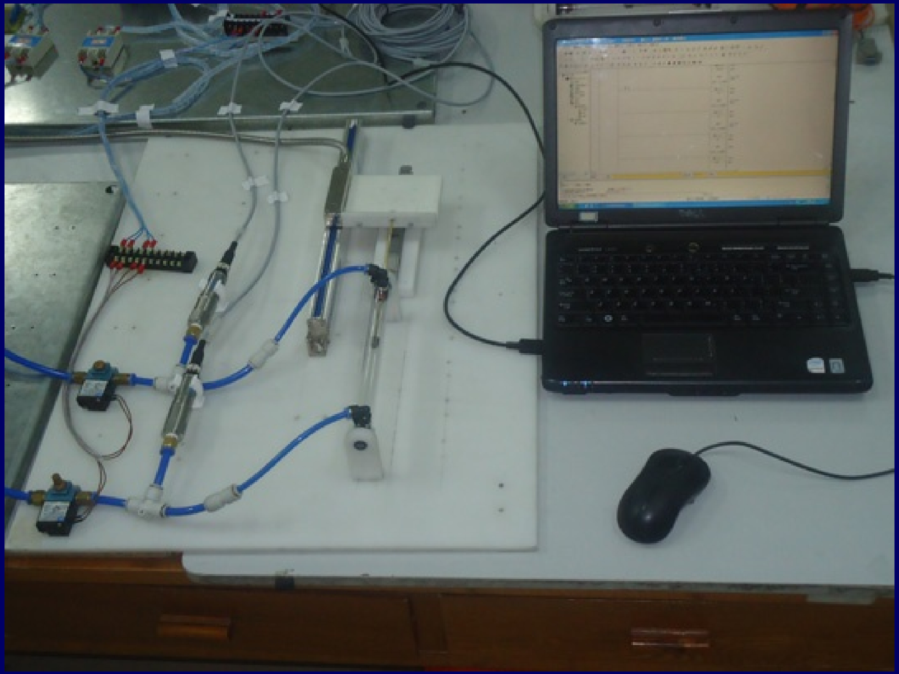

Fig.9. Experimental setup on different length tubes.

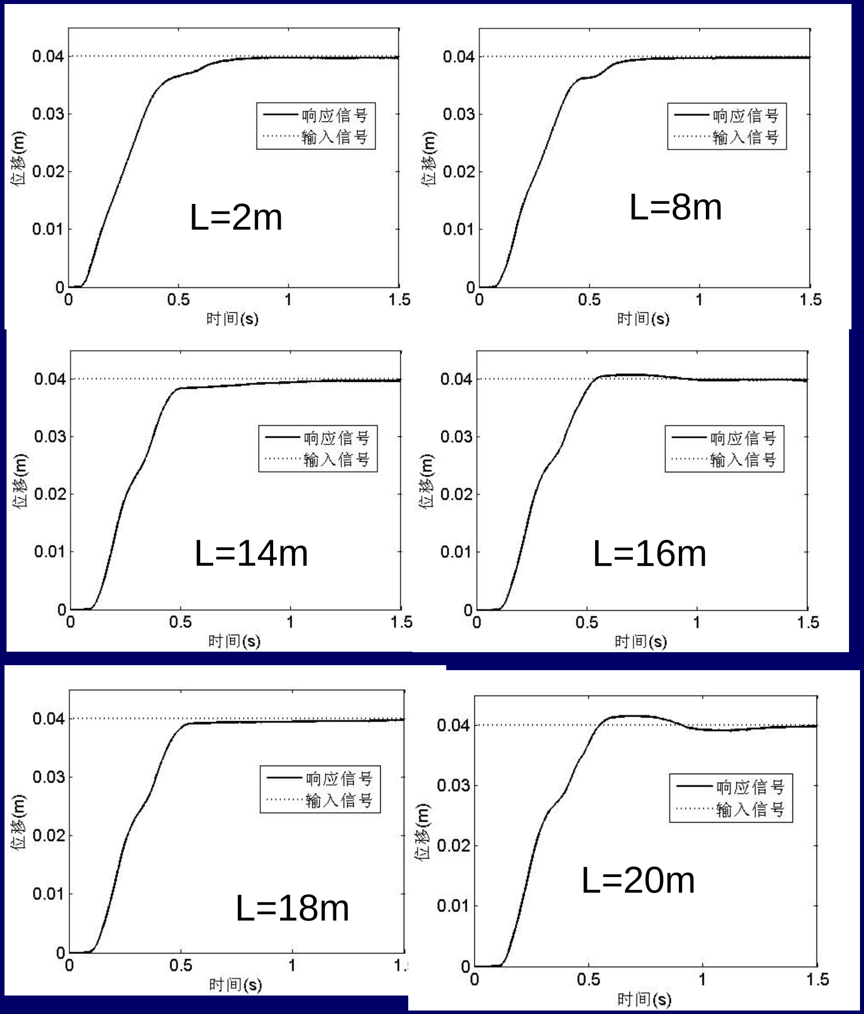

Fig.10. Experimental results

Jefferson Kimmel Cancer Center
NCI-designated

(1) MRI-guided surgical robot

c. Machinability Research

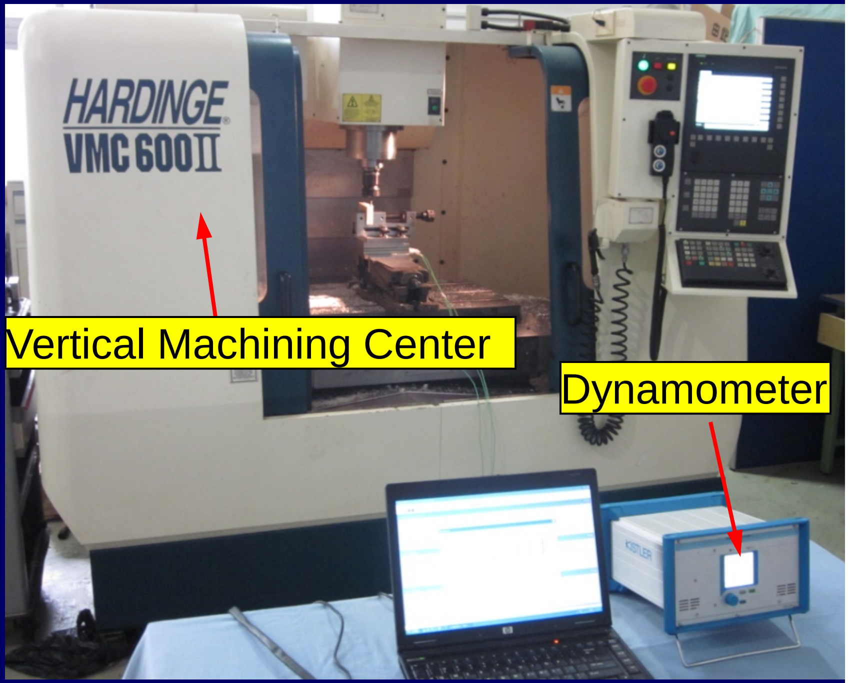

(a) Experimental setup

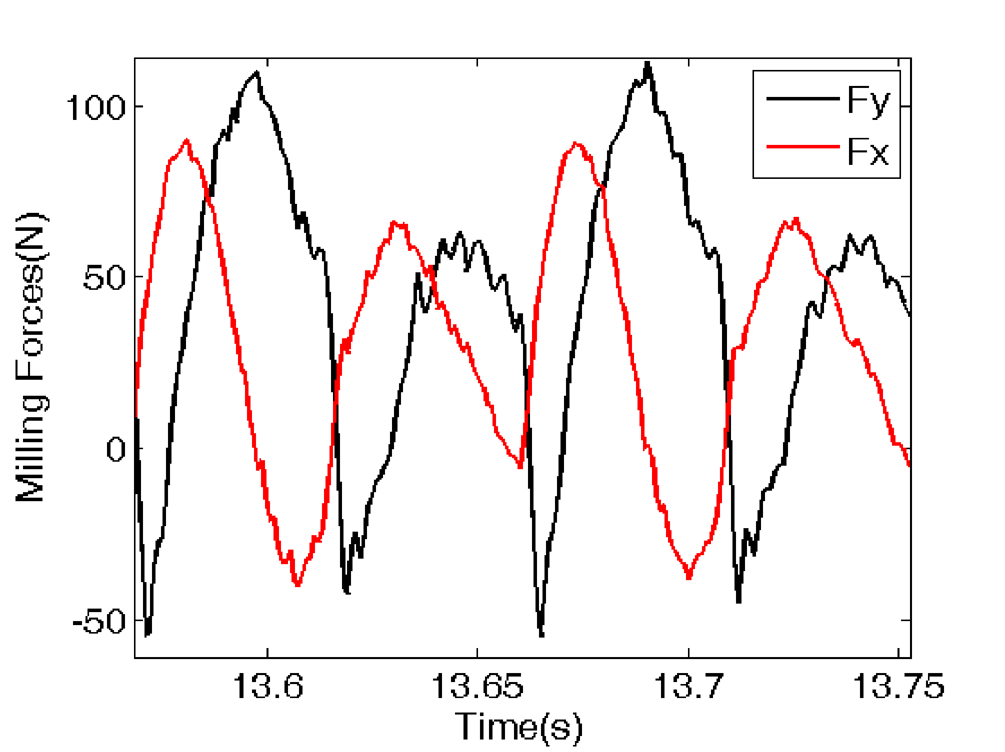

(b) Experimental results

Fig.11. Milling force experiment

Jefferson
Kimmel Cancer Center
NCI-designated

(1) MRI-guided surgical robot

c. Machinability Research

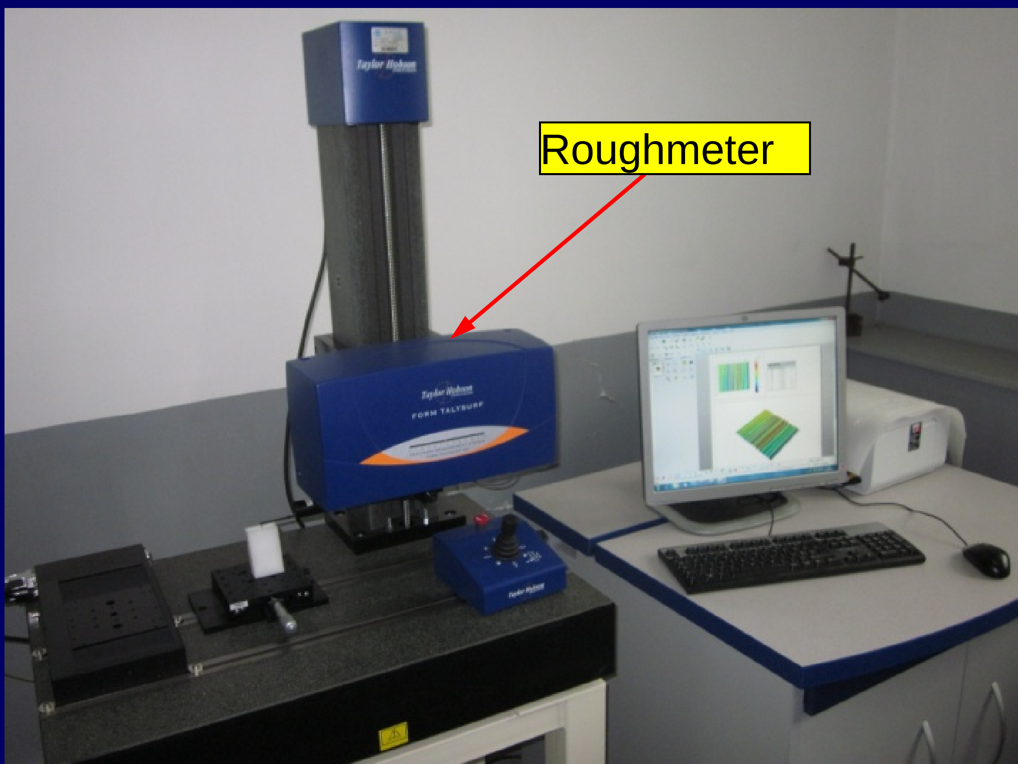

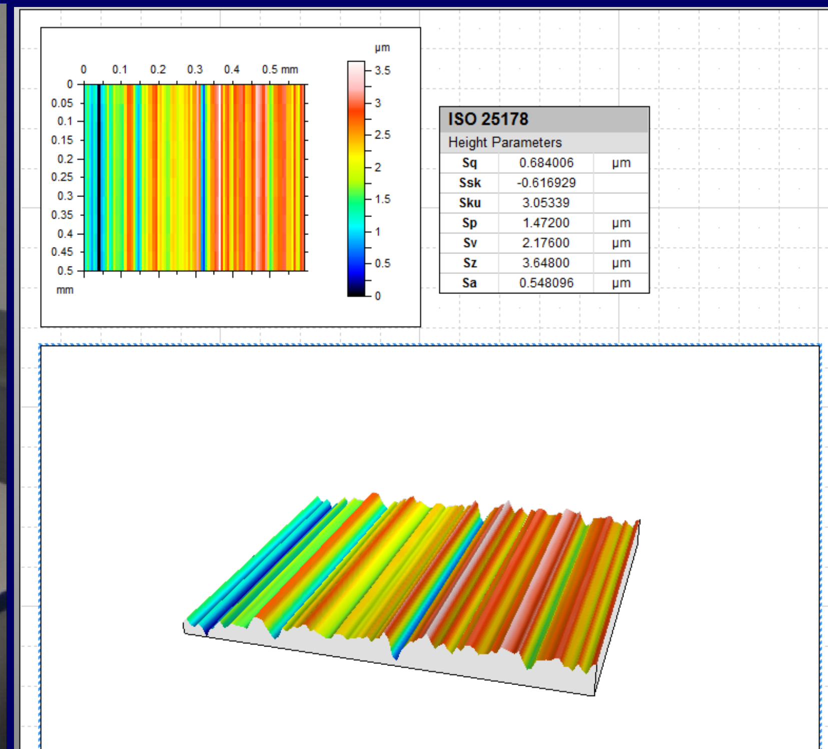

(a) Experimental setup

(b) Experimental results

Fig.12. surface roughness experiment

Jefferson™ Kimmel Cancer Center NCI-designated

(1) MRI-guided surgical robot

d. Reliability Analysis

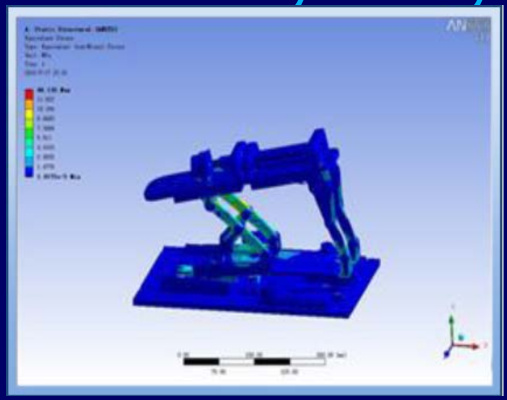

Fig.13. FEM analysis of the surgical robot

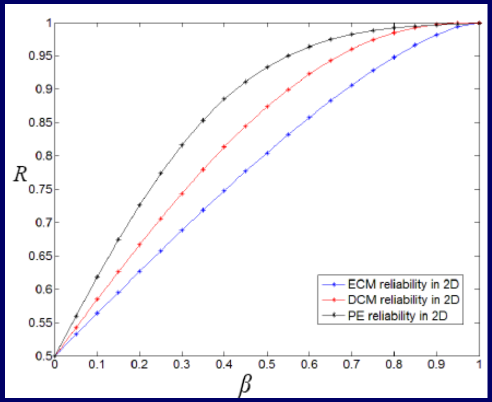

Fig.14. Relation curves between reliability and reliability index ^{2} in 2D

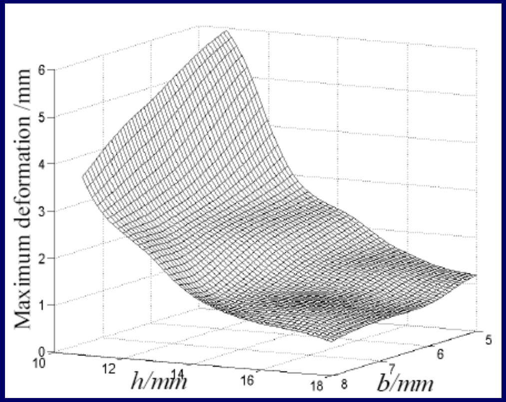

Fig.15. Response surface of maximum deformation

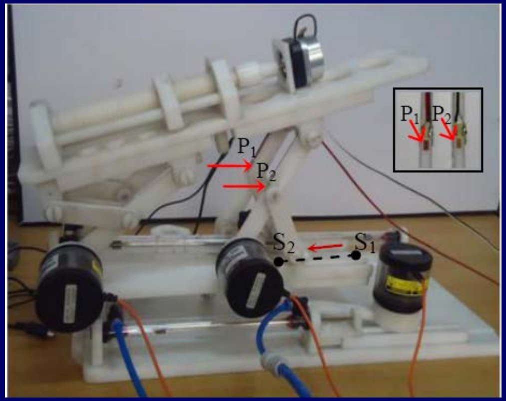

Fig.16. Sample robot based on optimization

Jefferson™
Kimmel Cancer Center
NCI-designated

(2) Ultrasound-guided surgical robot

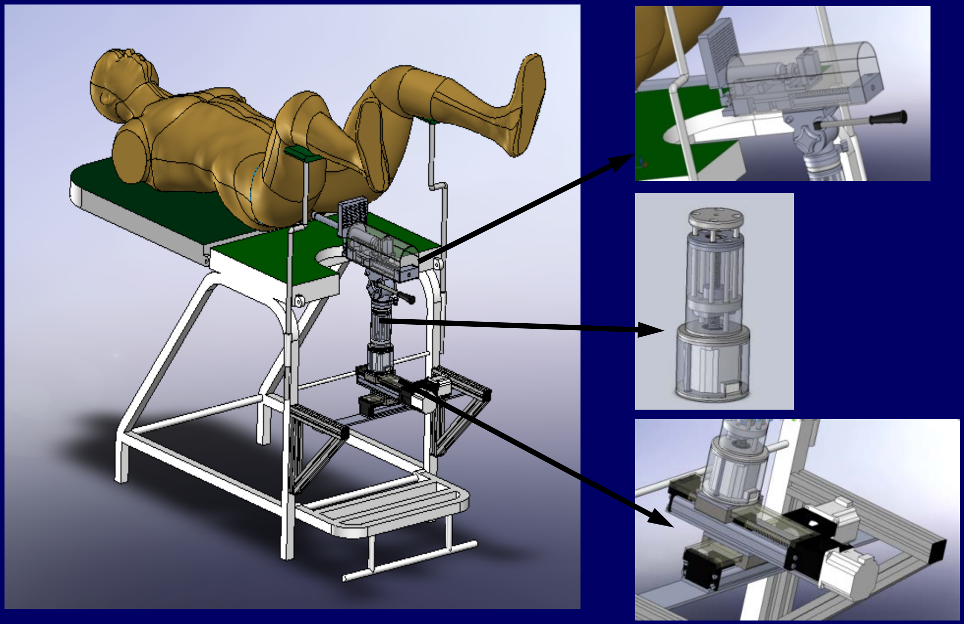

Fig.17. Ultrasound-guided surgical robot

Jefferson™
Kimmel Cancer Center
NCI-designated

(3) Needle-tissue interaction

a. Tissue-equivalent material preparation

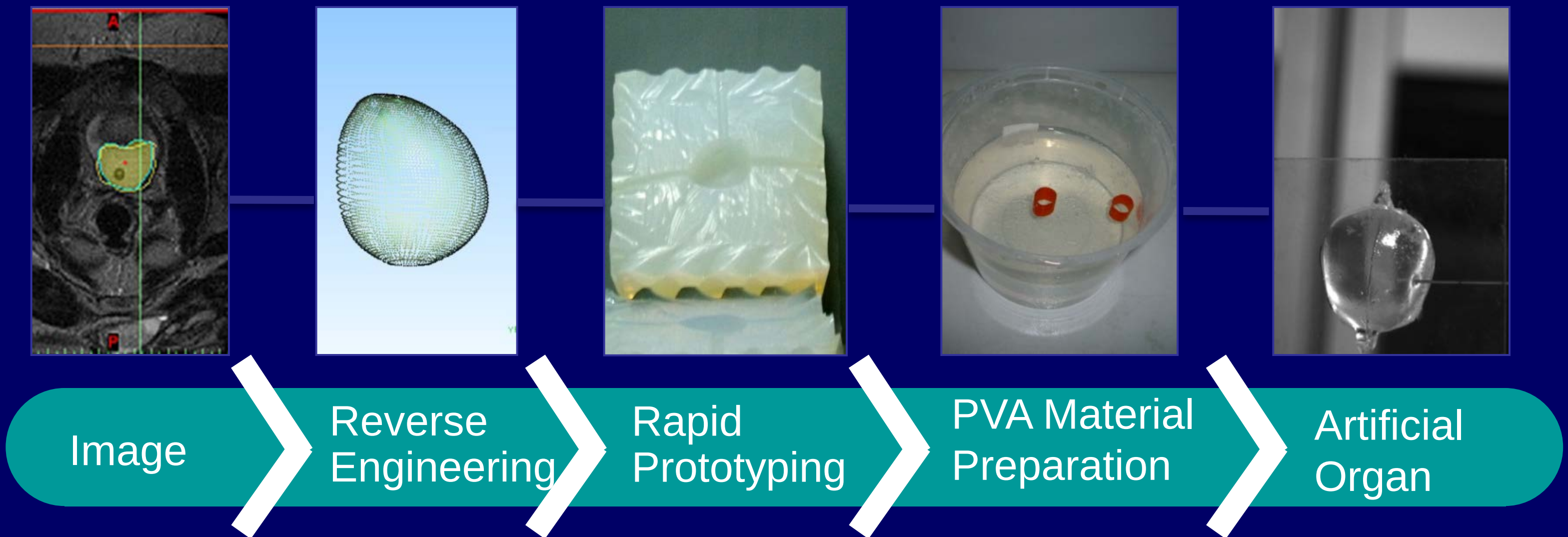

Uniaxial tensile test setup

Scanning Electron Microscope

Jefferson™ Kimmel Cancer Center NCI-designated

Fig. 18. The preparation process of the artificial organ

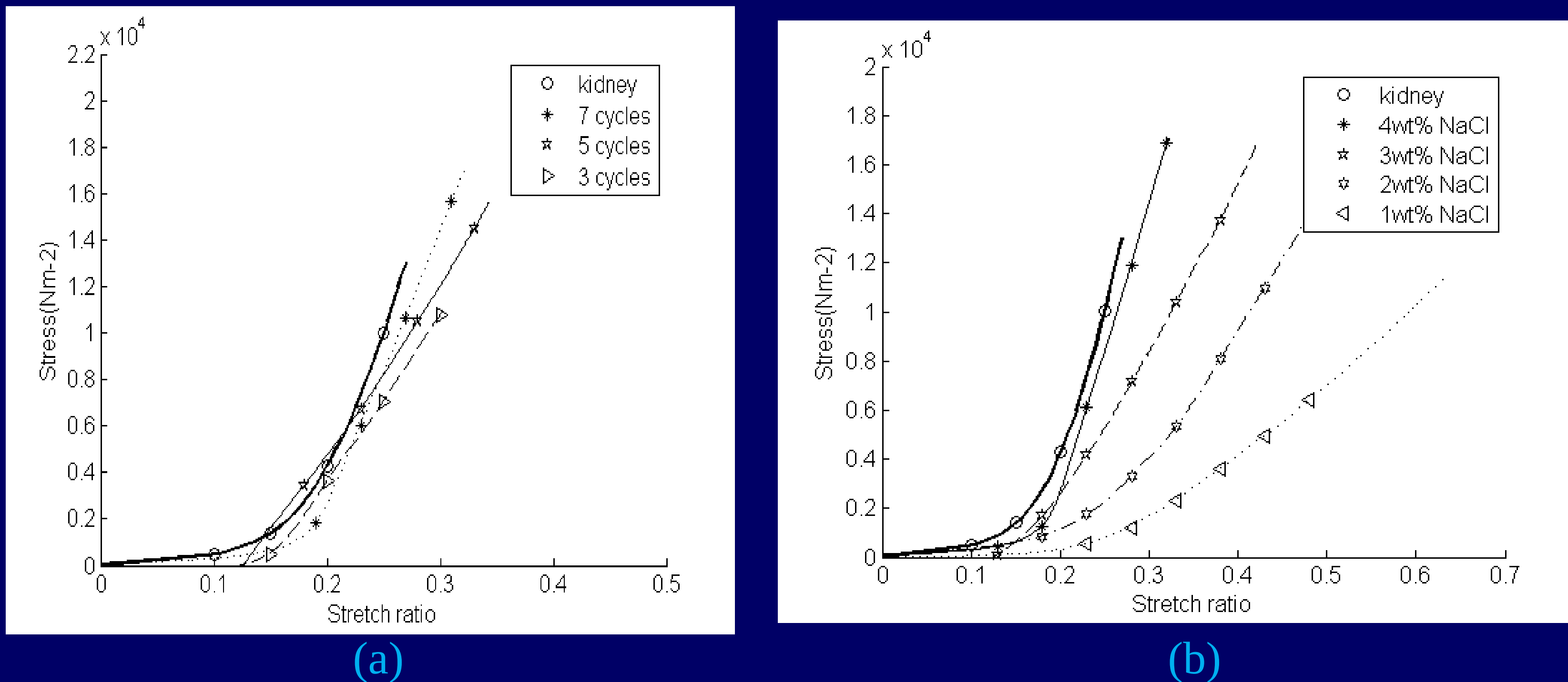

Fig. 19. The stress-strain diagram used to compare biomechanical properties of PVA materials and porcine kidney tissue

a. Tissue-equivalent material preparation

- Morphology characterization

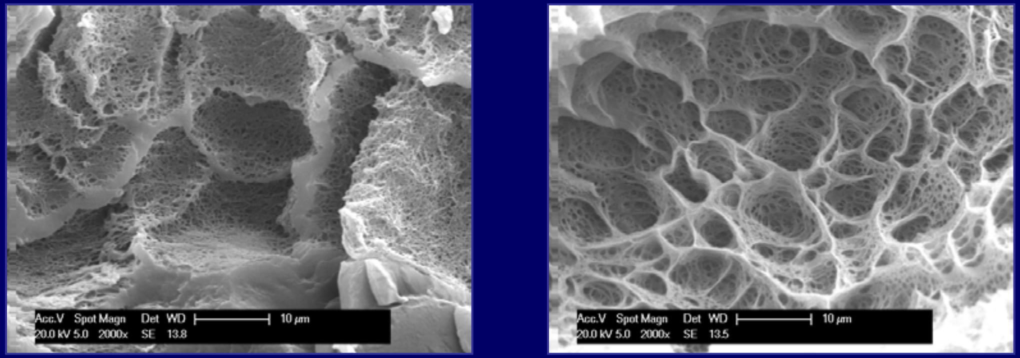

Fig. 20. The SEM images of different NaCl concentrations

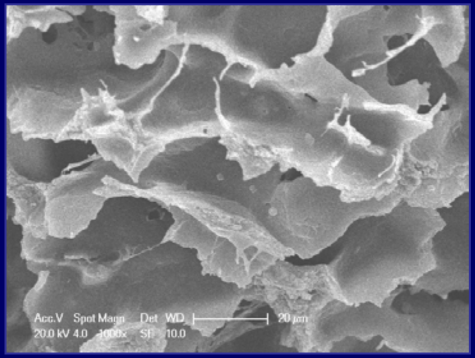

Fig. 22.The SEM images of porcine liver

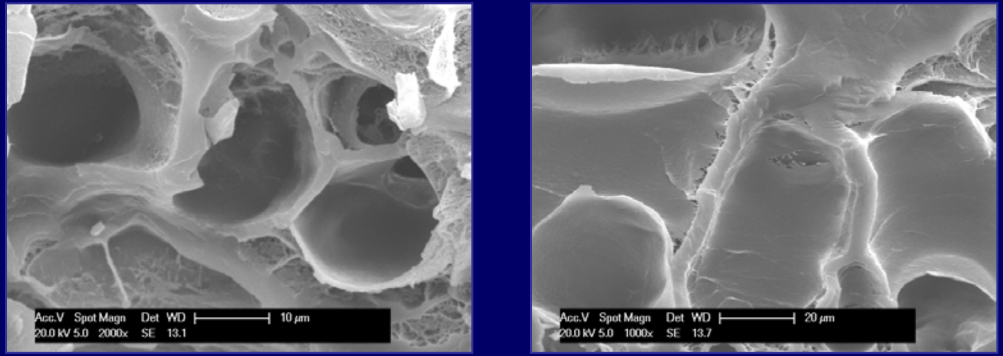

Fig. 21. The SEM images of different cross-linking cycles

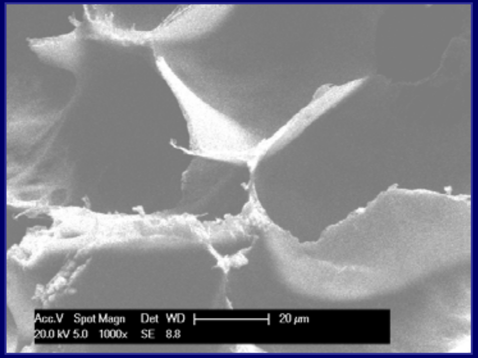

Fig. 23.The SEM images of porcine kidney

Jefferson™ Kimmel Cancer Center NCI-designated

(3) Needle-tissue interaction

b. Needle-tissue interaction forces investigation

- Force modeling for needle insertion

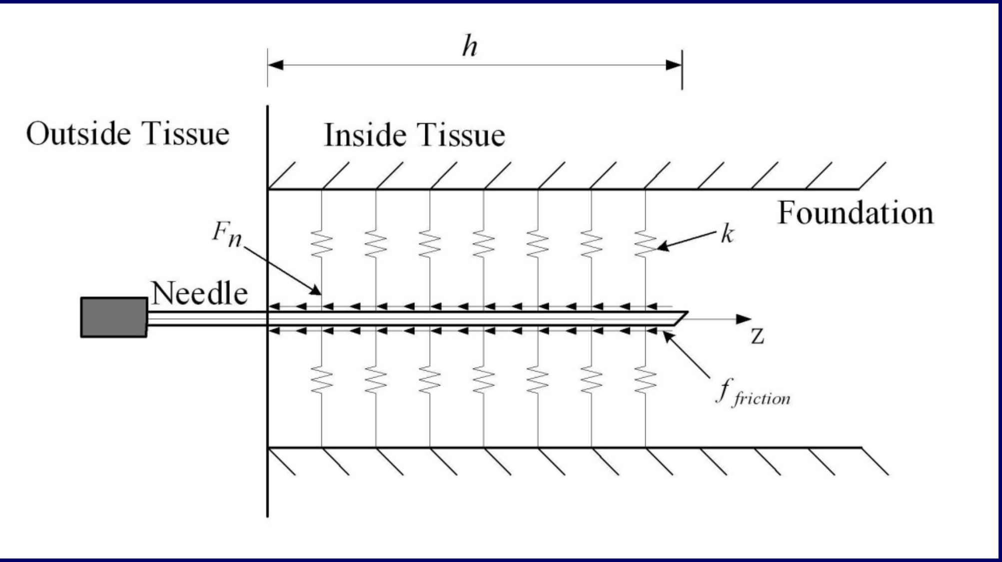

Fig.24. Modified Winkler's foundation model

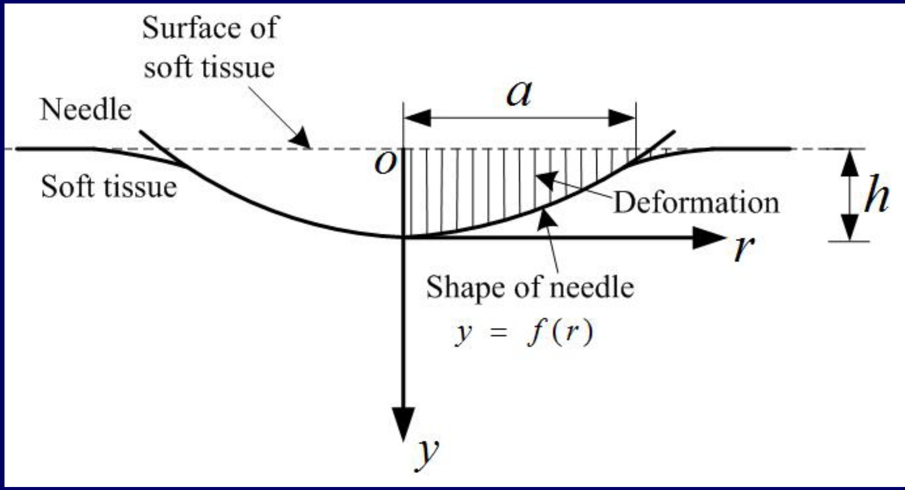

Fig.25. The sketch of the contact model

(3) Needle-tissue interaction

b. Needle-tissue interaction forces investigation

- ➢ Experimental setup

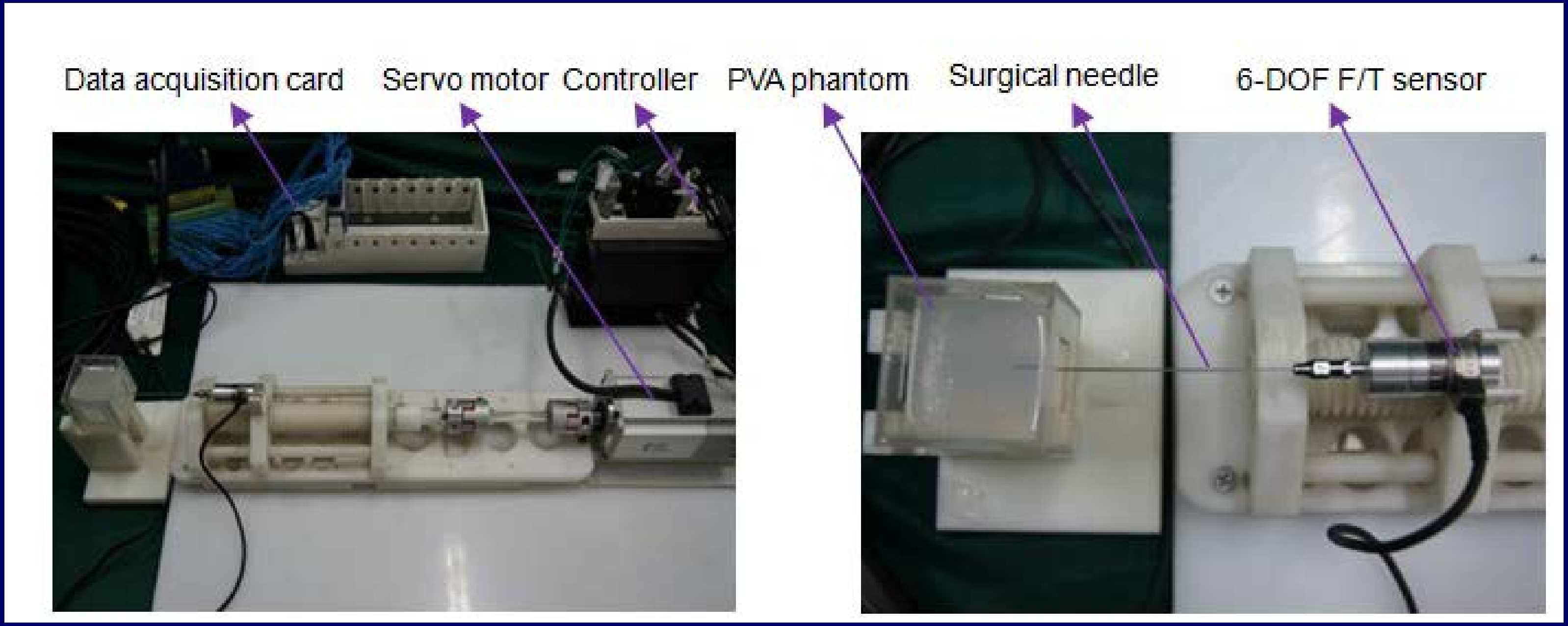

(a) 1 DOF experimental setup for needle insertion

(b) 6 DOF F/T sensor and the PVA phantom

Fig.26 Experimental setup for needle-tissue interaction forces

Jefferson™ Kimmel Cancer Center NCI-designated

(3) Needle-tissue interaction

b. Needle-tissue interaction forces investigation

- Experiment results

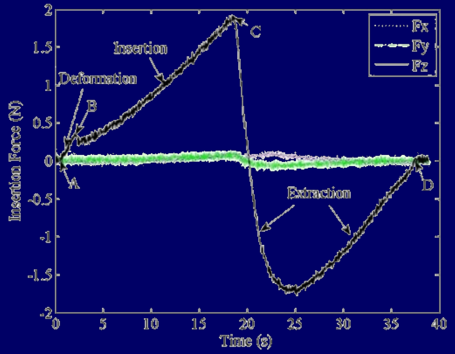

Fig.27 . Forces versus time curve for needle insertion

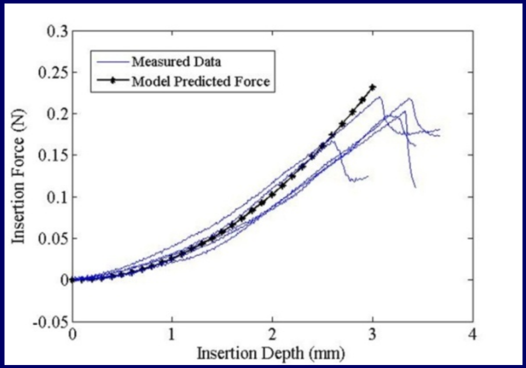

Fig.28 . The stiffness force phantom puncture of the capsule

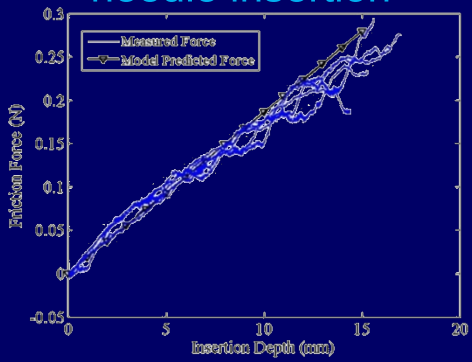

Fig.29. The friction model predicted force and the measured force

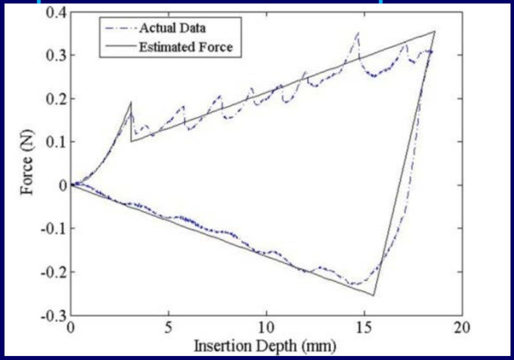

Fig.30. The needle insertion force model is compared to interaction force on PVA phantom.

Jefferson™ Kimmel Cancer Center
NCI-designated

(3) Needle-tissue interaction

b. Needle-tissue interaction forces investigation

- Trajectory planning

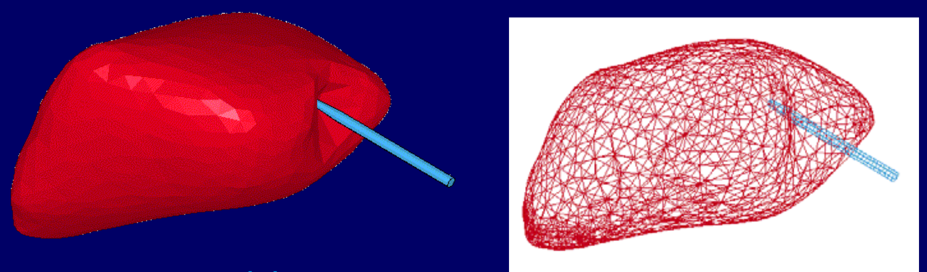

(a) (b)

Fig.31. The dynamic FEA model of prostate

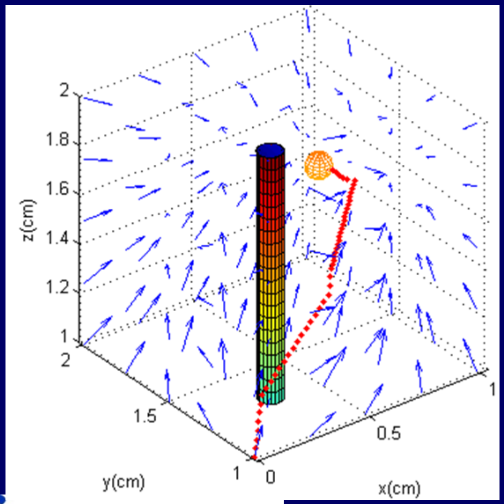

Fig.32. Trajectory planning result without considering deformation with a sphere target and cylinder obstacle.

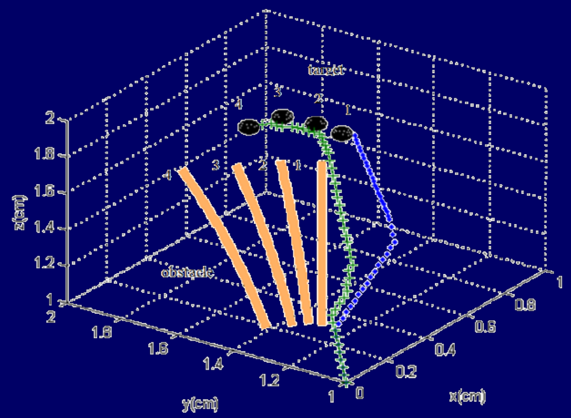

Fig.33. Trajectory planning result considering deformation

Jefferson™ Kimmel Cancer Center NCI-designated

Curved and Smart (Active) Needles

Thomas Jefferson University

Temple University

Case Western Reserve University

Jefferson™
Kimmel Cancer Center
NCI-designated

Needle Steering Techniques

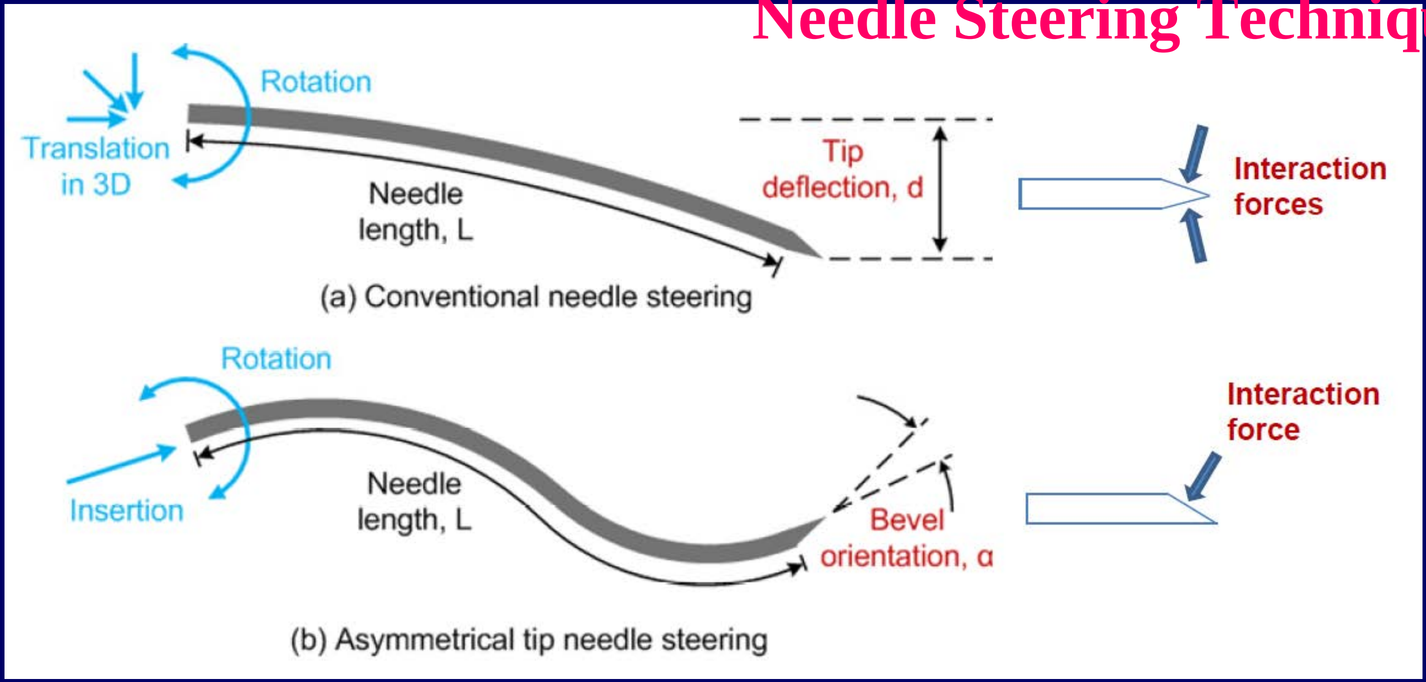

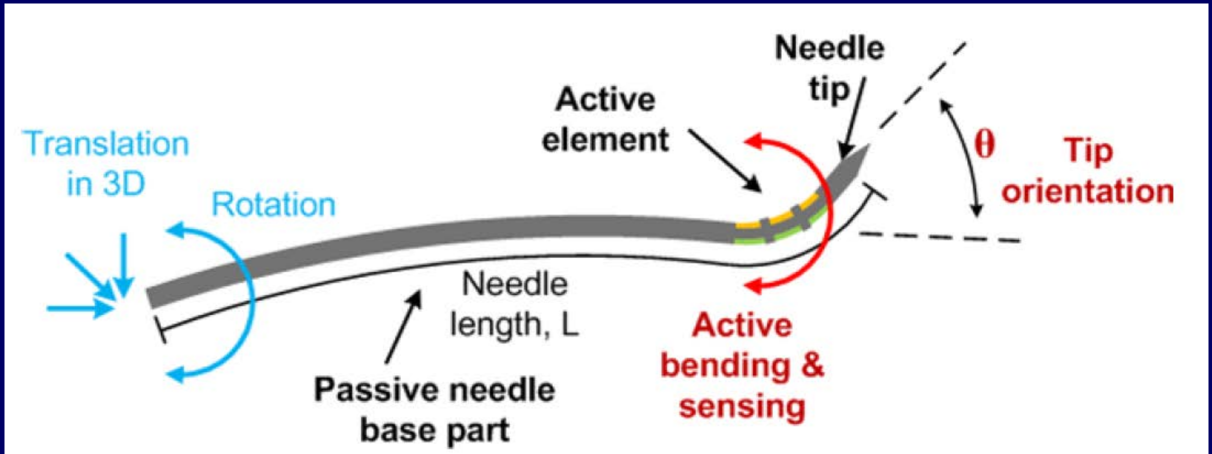

(c) Smart (active) needle steering

Ryu, PhD Thesis, 2012

Jefferson Kimmel Cancer Center NCI-designated

Rectilinear and Curvilinear Techniques for Prostate Brachytherapy

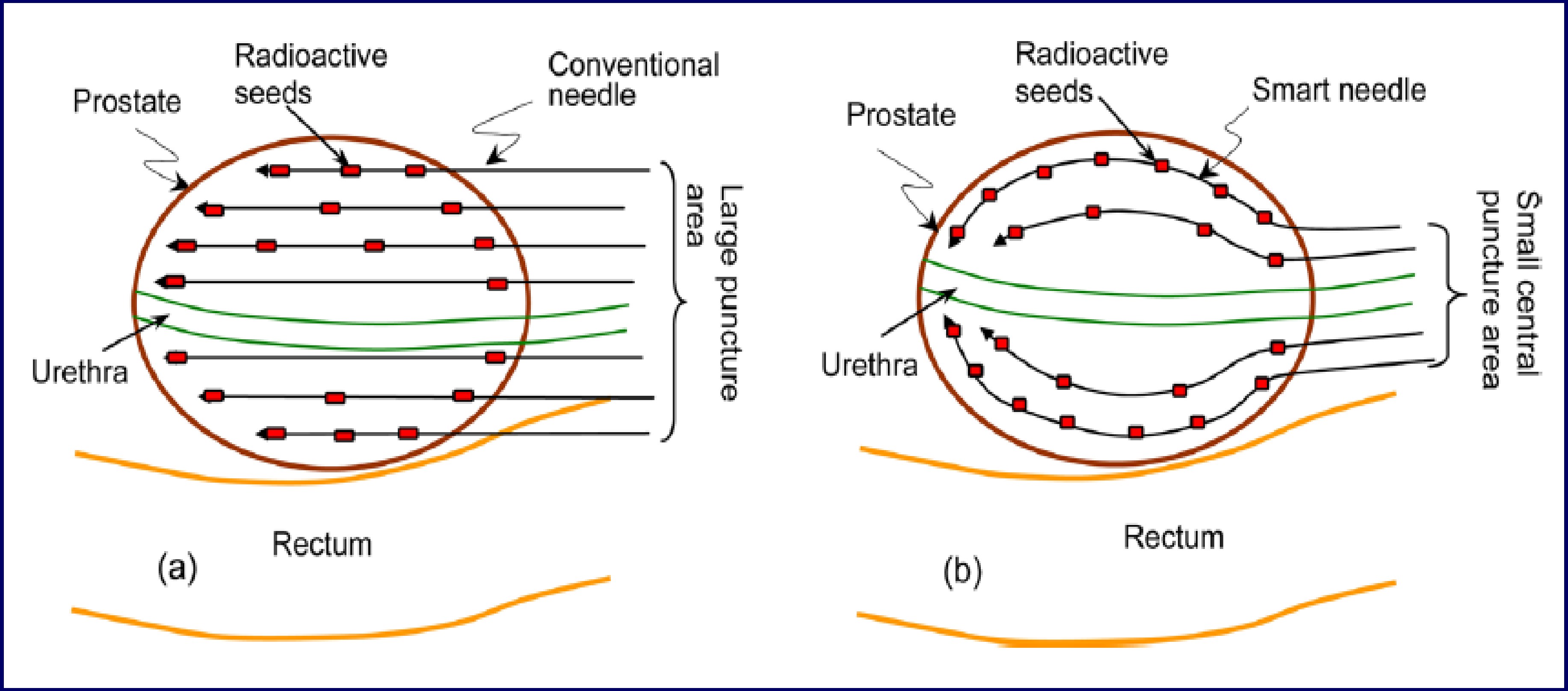

(a) Conventional rectilinear approach.

(b) Curvilinear conformal smart needle insertion.

Podder et al., MedPhys 2012

Jefferson™ Kimmel Cancer Center NCI-designated

Dose Distribution in Rectilinear Technique

A Representative Case

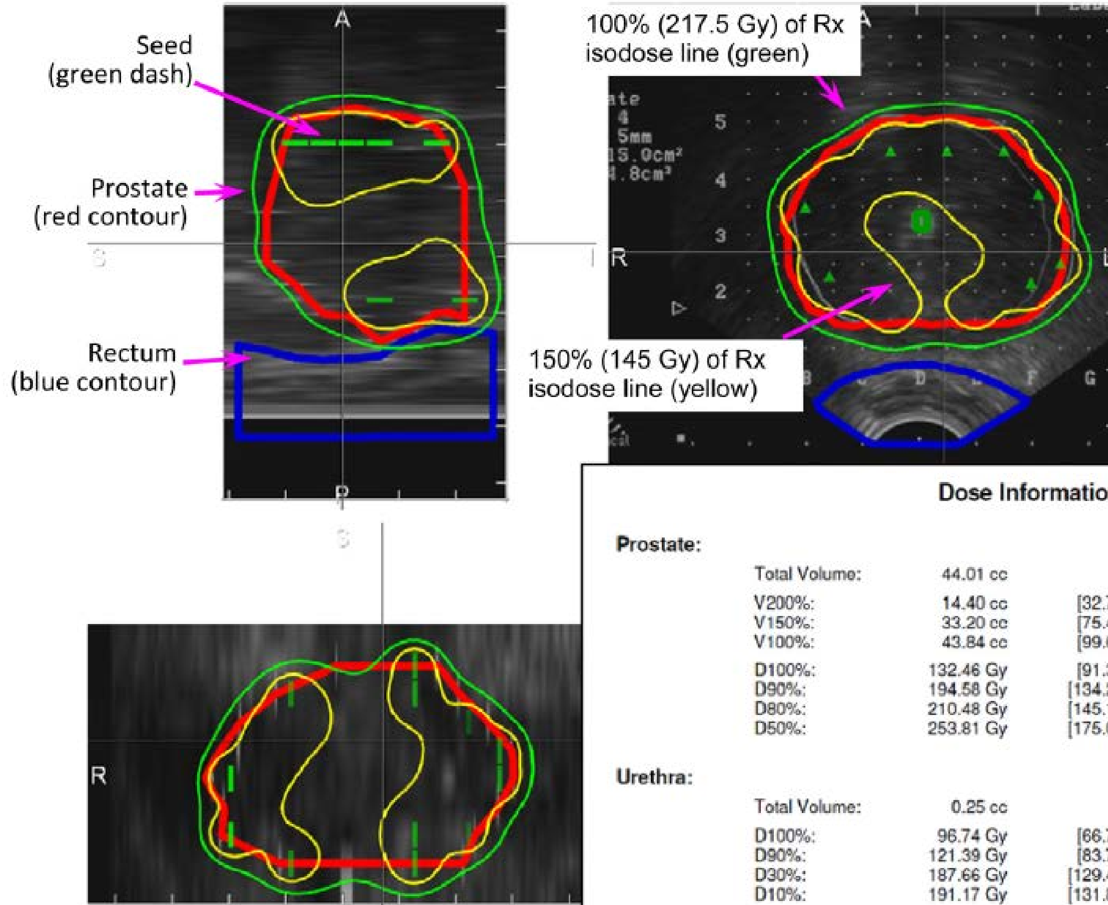

(a) Rectilinear implantation
(22 needles, 68 seeds, 41.68 U, 1cc = 1cm^3)

Dose Information

Prostate:			
	Total Volume:	44.01 cc	
	V200%:	14.40 cc	[32.72%]
	V150%:	33.20 cc	[75.44%]
	V100%:	43.84 cc	[99.61%]
	D100%:	132.46 Gy	[91.35%]
	D90%:	194.58 Gy	[134.20%]
	D80%:	210.48 Gy	[145.16%]
	D50%:	253.81 Gy	[175.04%]
Urethra:			
	Total Volume:	0.25 cc	
	D100%:	96.74 Gy	[66.72%]
	D90%:	121.39 Gy	[83.72%]
	D30%:	187.66 Gy	[129.42%]
	D10%:	191.17 Gy	[131.84%]
Rectum:			
	Total Volume:	19.43 cc	
	V100%:	0.40 cc	[2.04%]
	D30%:	65.56 Gy	[45.22%]
	D5%:	119.07 Gy	[82.12%]

Dose Distribution in Curvilinear Technique

A Representative Case

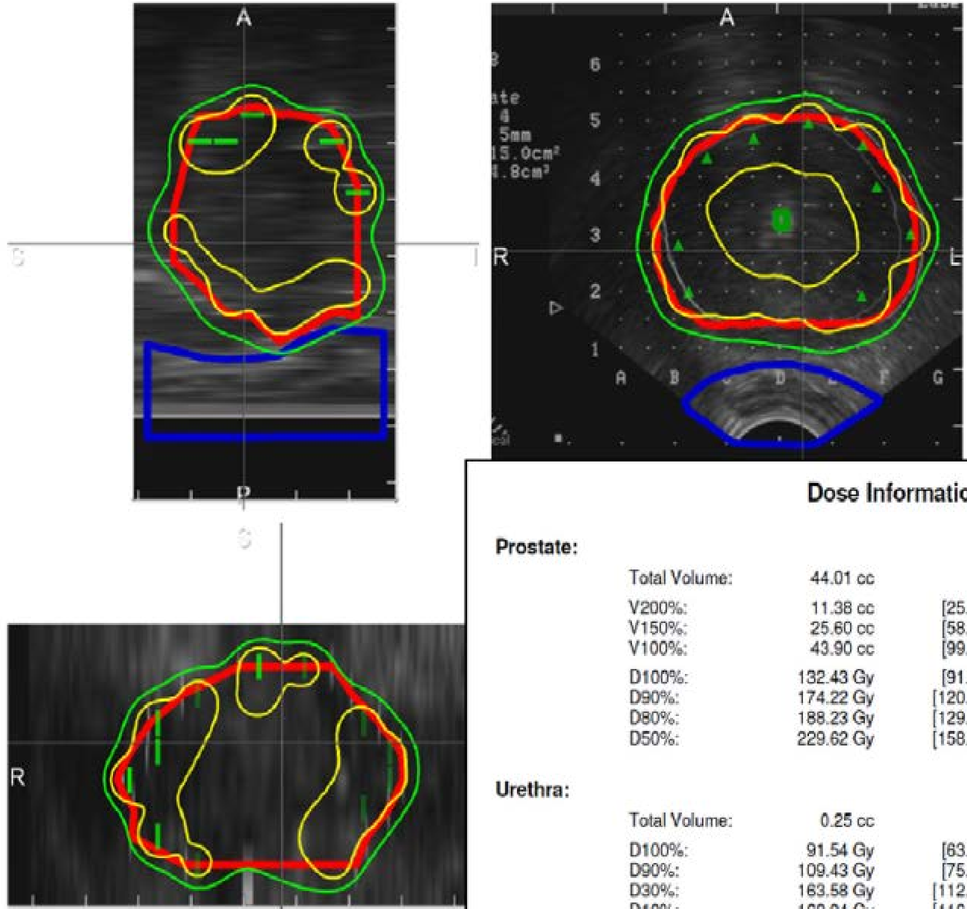

(b) Curvilinear implantation
(14 needles, 63 seeds, 38.43 U, 1cc = 1cm^3)

Dose Information

Prostate:			
	Total Volume:	44.01 cc	
	V200%:	11.38 cc	[25.85%]
	V150%:	25.60 cc	[58.16%]
	V100%:	43.90 cc	[99.76%]
	D100%:	132.43 Gy	[91.33%]
	D90%:	174.22 Gy	[120.15%]
	D80%:	188.23 Gy	[129.81%]
	D50%:	229.62 Gy	[158.36%]
Urethra:			
	Total Volume:	0.25 cc	
	D100%:	91.54 Gy	[63.13%]
	D90%:	109.43 Gy	[75.47%]
	D30%:	163.58 Gy	[112.81%]
	D10%:	168.94 Gy	[116.51%]
Rectum:			
	Total Volume:	19.43 cc	
	V100%:	0.08 cc	[0.42%]
	D30%:	61.29 Gy	[42.27%]
	D5%:	106.37 Gy	[73.36%]

Jefferson™ Kimmel Cancer Center
NCI-designated

DVH for Rectilinear vs. Curvilinear Techniques

A Representative Case

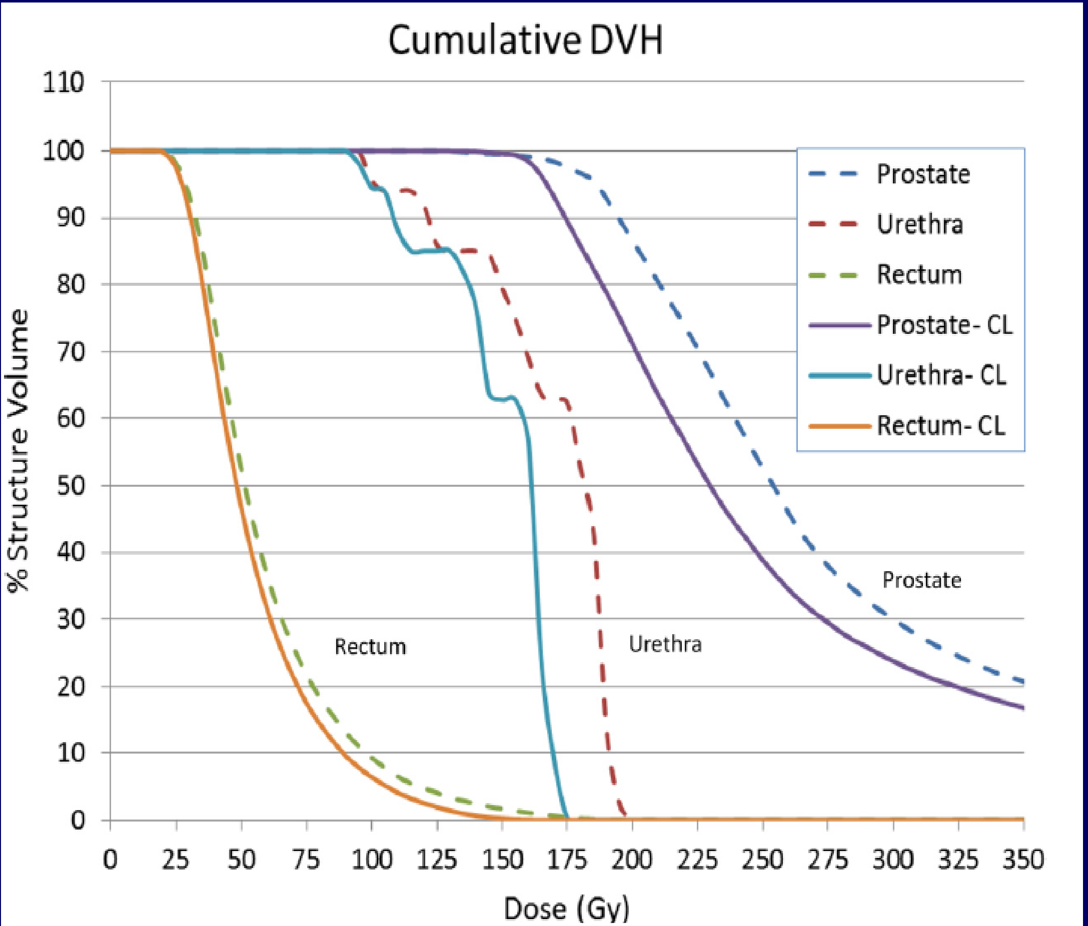

- Conventional **rectilinear** implantation (**dotted** lines)
- Proposed **curvilinear** implantation (**solid** lines)

Jefferson™
Kimmel Cancer Center
NCI-designated

Rectilinear and Curvilinear Techniques for Prostate Brachytherapy

TABLE I. Comparison of proposed curvilinear approach and conventional rectilinear approach.

20 patient PSI cases

Parameter ($n = 20$)	Rectilinear method Average ± SD (range)	Curvilinear method Average ± SD (range)	Difference	p-value (two-tailed)
Total needle	19.2 ± 2.6 (14–23)	13.2 ± 1.4 (10–15)	−6.0 (−30.5%)	< 0.001
Total seed	62.5 ± 11.2 (43–85)	55.1 ± 10.4 (38–74)	−7.4 (−11.8%)	< 0.49
Total activity (mCi)	38.3 ± 6.3 (28.3–47.3)	33.8 ± 4.9 (25.3–40.3)	−4.5 (−11.8%)	< 0.37
Prostate (average = 41.3 cm^3, range = 26.6–53.2 cm^3):				
D_{90} (Gy)	198.7 ± 9.9 (182.9–215.2)	183.3 ± 6.8 (176.3–194.5)	−15.4 (−7.8%)	< 0.04
V_{100} (cm^3)	99.98 ± 0.06 (99.8–100)	99.97 ± 0.06 (99.83–100)	−0.01 (−0.01%)	< 0.85
V_{150} (cm^3)	80.9 ± 6.8 (68.5–89.8)	65.7 ± 5.3 (57.8–75.9)	−15.2 (−18.8%)	< 0.01
V_{200} (cm^3)	43.7 ± 6.0 (32.7–53.4)	28.9 ± 3.3 (26.0–35.5)	−14.8 (−33.9%)	< 0.001
Urethra:				
D_{10} (Gy)	209.9 ± 12.2 (186.2–228.7)	189.2 ± 8.1 (178.3–208.8)	−20.7 (−9.9%)	< 0.02
D_{30} (Gy)	205.1 ± 10.4 (184.3–219.9)	184.3 ± 7.4 (172.5–200.2)	−20.8 (−10.1%)	< 0.01
Rectum:				
D_5 (Gy)	160.2 ± 15.9 (137.9–196.8)	130.5 ± 12.3 (111.0–151.1)	−29.7 (−18.5%)	< 0.03
V_{100} (cm^3)	0.93 ± 0.51 (0.19–2.0)	0.21 ± 0.17 (0.03–0.61)	−0.72 (−77.8%)	< 0.001

Jefferson™ Kimmel Cancer Center NCI-designated

Curvilinear vs. Rectilinear Approach for PSI

- Small puncture area
- Accurate needle placement
- Improved dose distribution
- Better sparing of OARs
- Less needles, seeds
- Expected less traumas
- Expected reduction of toxicities

Jefferson™ Kimmel Cancer Center
NCI-designated

Curved Needles for Surgical Procedures

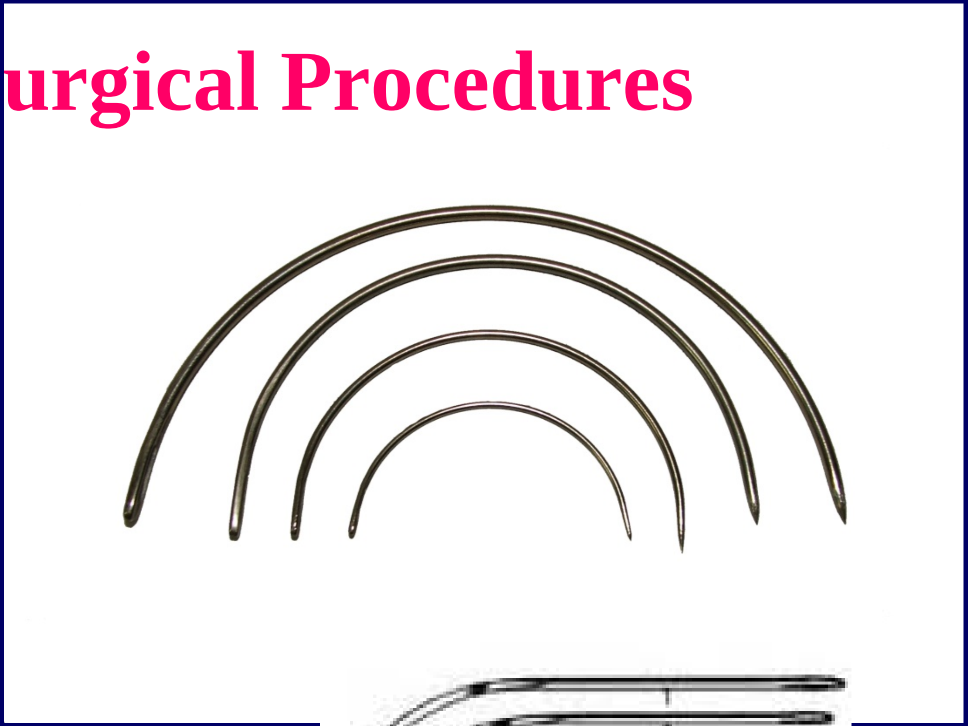

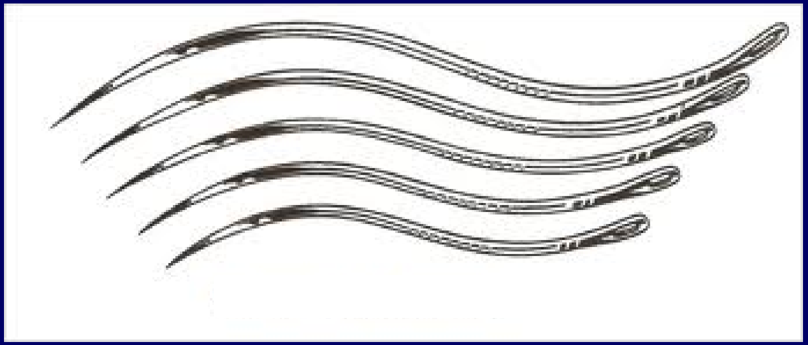

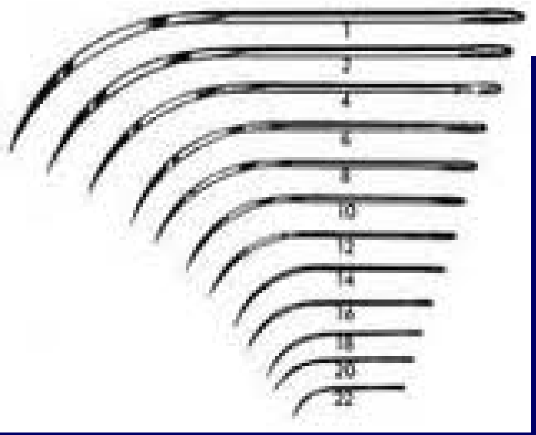

Jefferson™
Kimmel Cancer Center
NCI-designated

Smart (active) needle

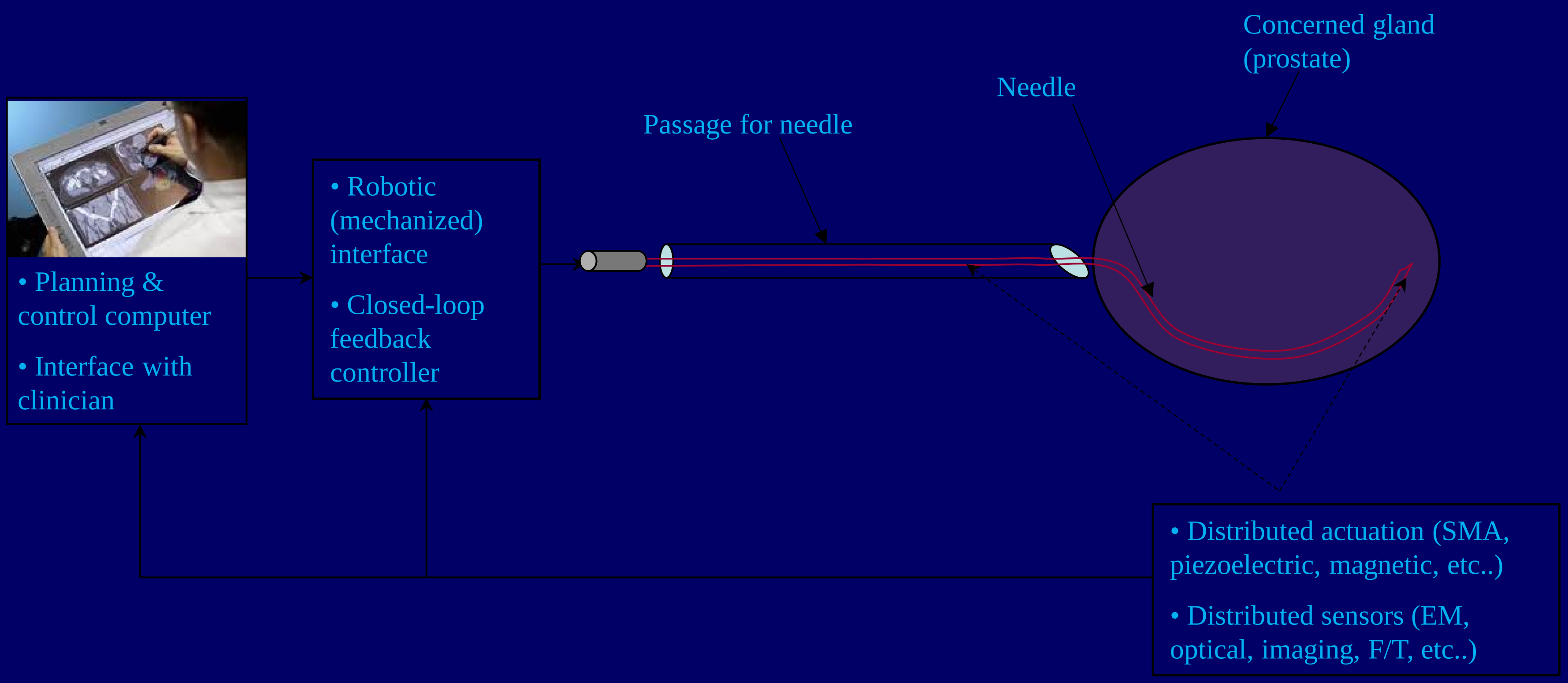

Curved Needle vs. Smart (active) Needle

Curved needle:

o Fixed geometrical configuration

- rigid body
- less conformity
- challenging for insertion in organ
- actuation from proximal end only
- limited sensory feedback

Smart (active) needle:

o Variable controlled configuration

- flexible configuration
- distributed actuation
- good geometric conformity
- distributed sensory system (EM, imaging, F/T, optical, etc.)
- distributed actuation and control

Jefferson™
Kimmel Cancer Center
NCI-designated

Modeling and Control of Pre-curved Needle Continuum

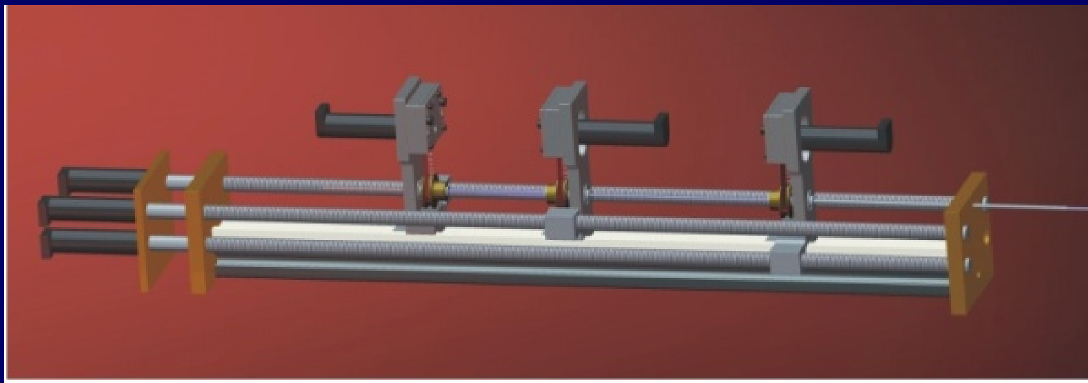

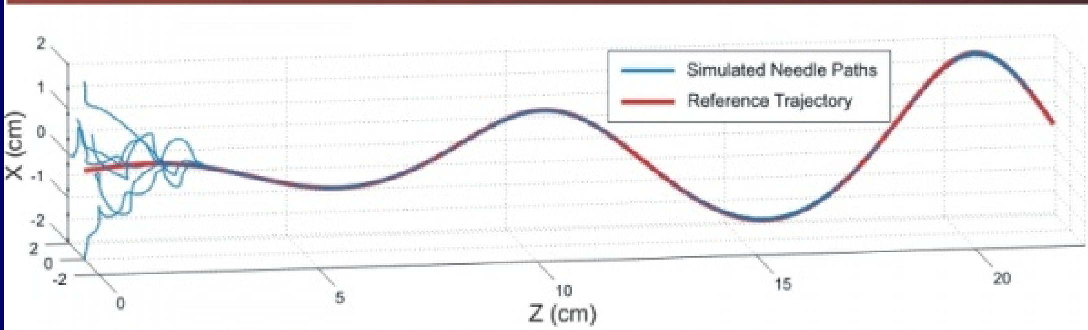

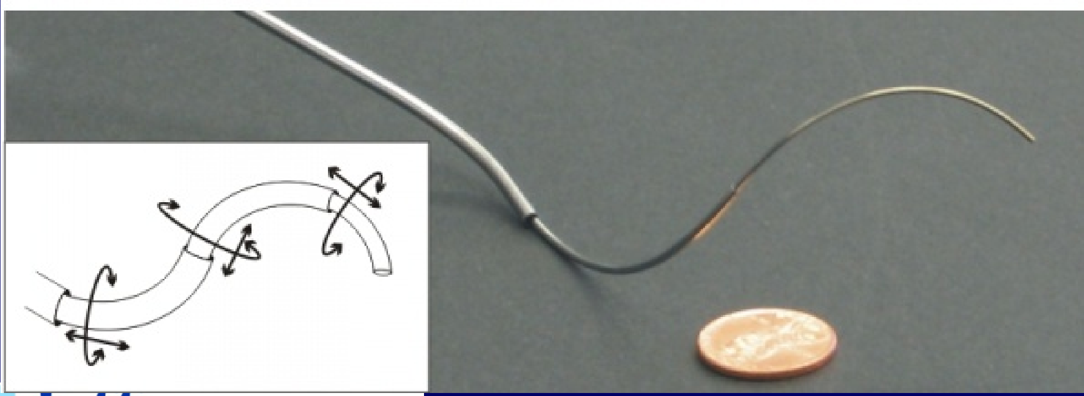

The figures (from top to bottom) show-

(1) a CAD drawing of a new active cannula or steerable needle actuation unit,

(2) a simulation showing that controller can stabilize bevel-steered needles to a 3D reference trajectory from various initial poses,

(3) an active cannula prototype with inset line drawing indicating DOF.

Webster et al., MICCAI 2008

Jefferson™
Kimmel Cancer Center
NCI-designated

Steerable Needle (bevel-tip)

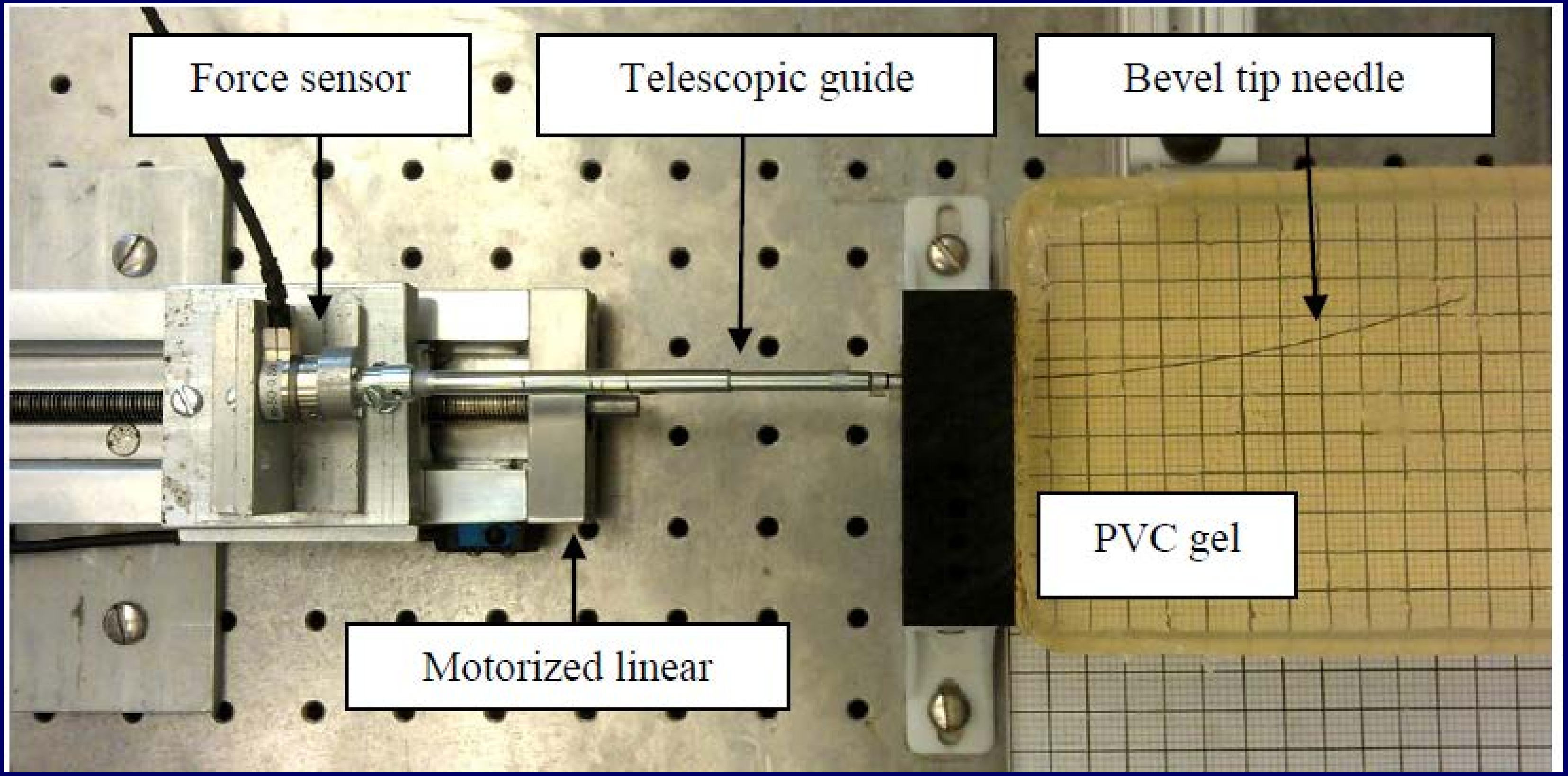

Image-Guided Flexible Needle Steering by Robotic Arm

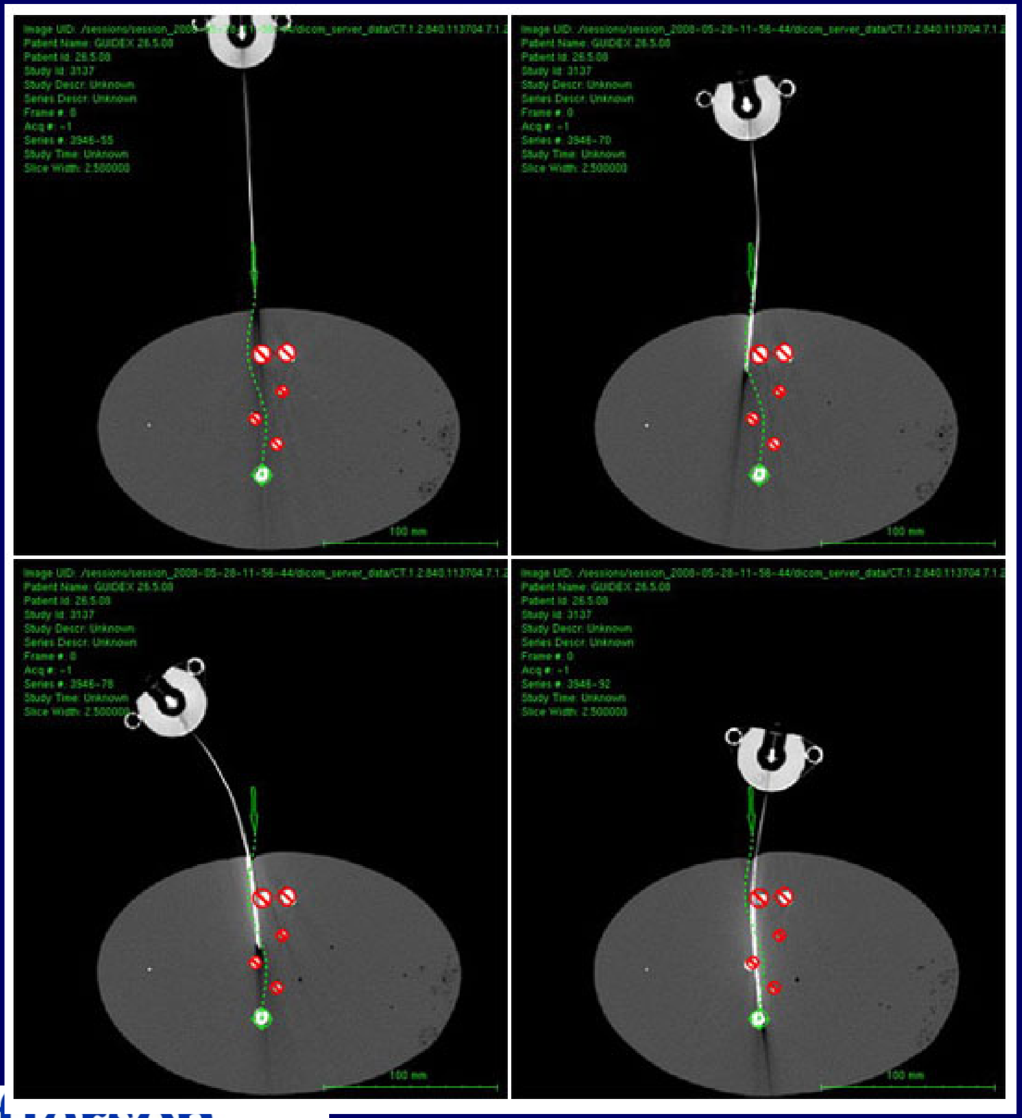

This example illustrates trajectory planning and realization of curved trajectory by a robot. The whole movement is done in the same CT slice and the needle is kept in plane.

Glozman et al., MICCAI 2008

Jefferson™ Kimmel Cancer Center
NCI-designated

Motion Planning for Steerable Medical Needles

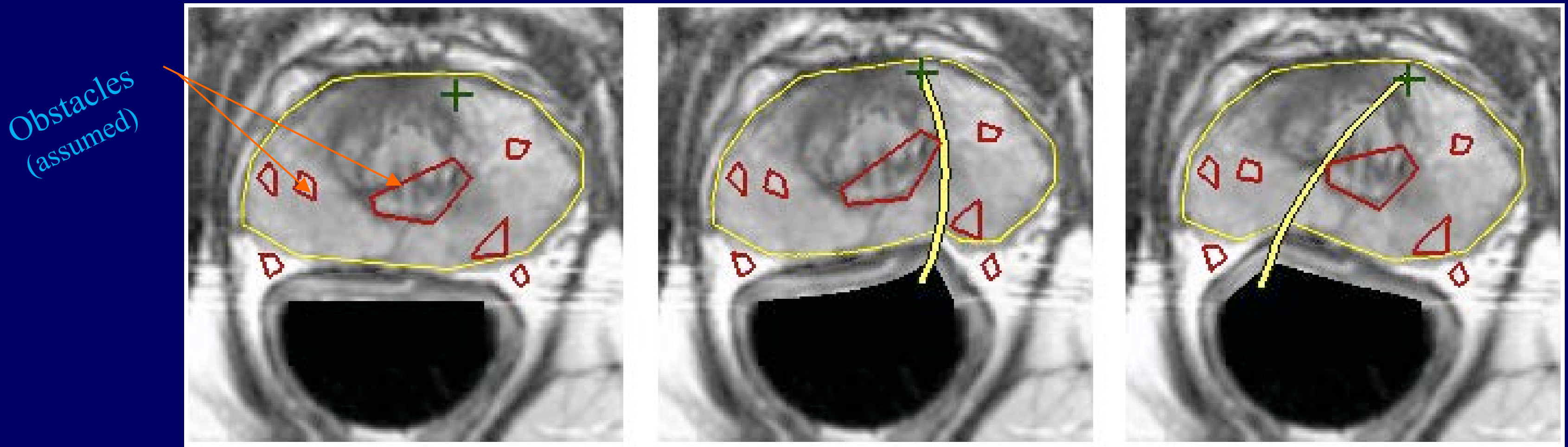

(a) Human Prostate, Tumor Target, and Obstacles

(b) Bevel-left Needle Trajectory Plan

(c) Bevel-right Needle Trajectory Plan

In this example based on an MR image of the prostate, a biopsy needle attached to a rigid rectal probe (black half-circle) is inserted into the prostate (outlined in yellow) using simulation. Obstacles (red polygons) and the target (green cross) are overlaid on the image (a). The target is not accessible from the rigid probe by a straight line path without intersecting obstacles. However, bevel-tip needles bend as they are inserted into soft tissue. The planner computes a locally optimal bevel-left needle insertion plan that reaches the target, avoids obstacles, and minimizes insertion distance (b). Using different initial conditions, the planner generates a plan for a bevel-right needle (c). Due to tissue deformation, the needle paths do not have constant curvature.

Alterovitz et al., MICCAI 2008

Jefferson™ Kimmel Cancer Center
NCI-designated

Needle (flexible) Steering via Duty-cycled Spinning

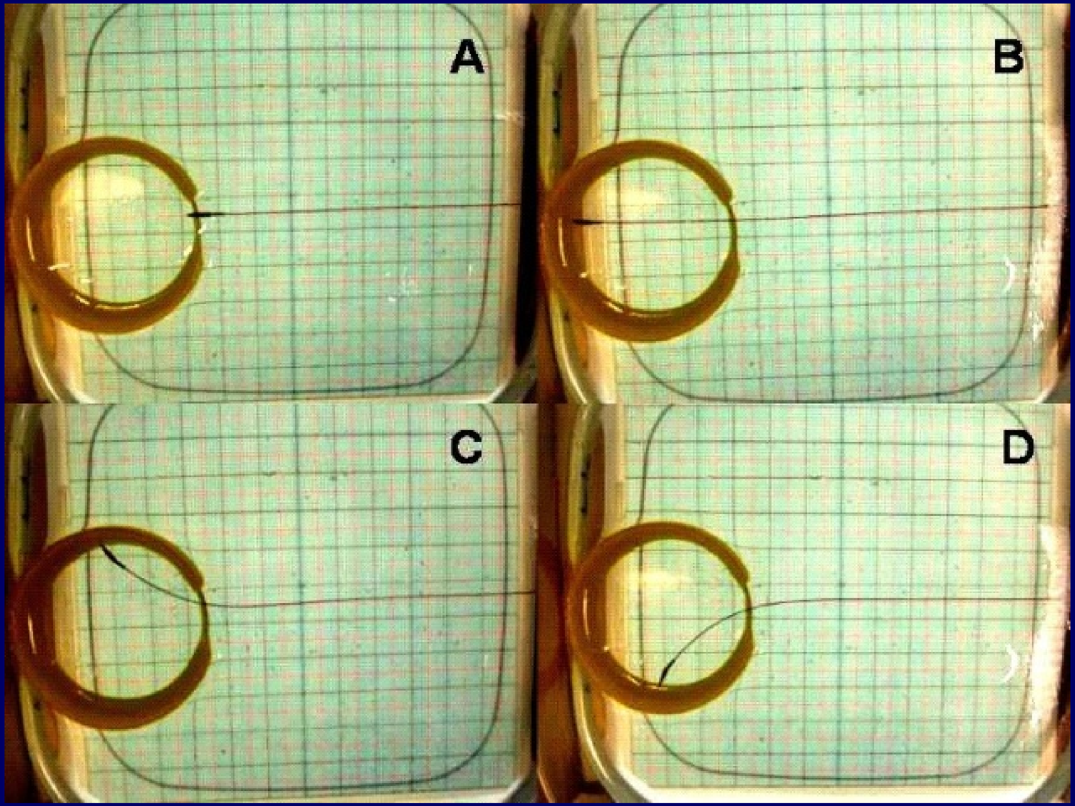

Simulation in a gelatin sample of multi-point "coverage" of a lesion zone using duty-cycled spinning of a bevel-tip needle. The needle is steered to the edge of a treatment zone (A). The needle is then advanced straight forward to the boundary (B). Then the needle returns to the entry point (A), and is advanced to other points in the treatment zone (C, then D), each time returning to the same starting point (as in A). The black gridlines are 1 cm apart.

Jefferson™ Kimmel Cancer Center NCI-designated

Riviere et al., MICCAI 2008, IEEE EMBS 2012

Modeling and Planning of Needle Insertions in Deformable Tissue

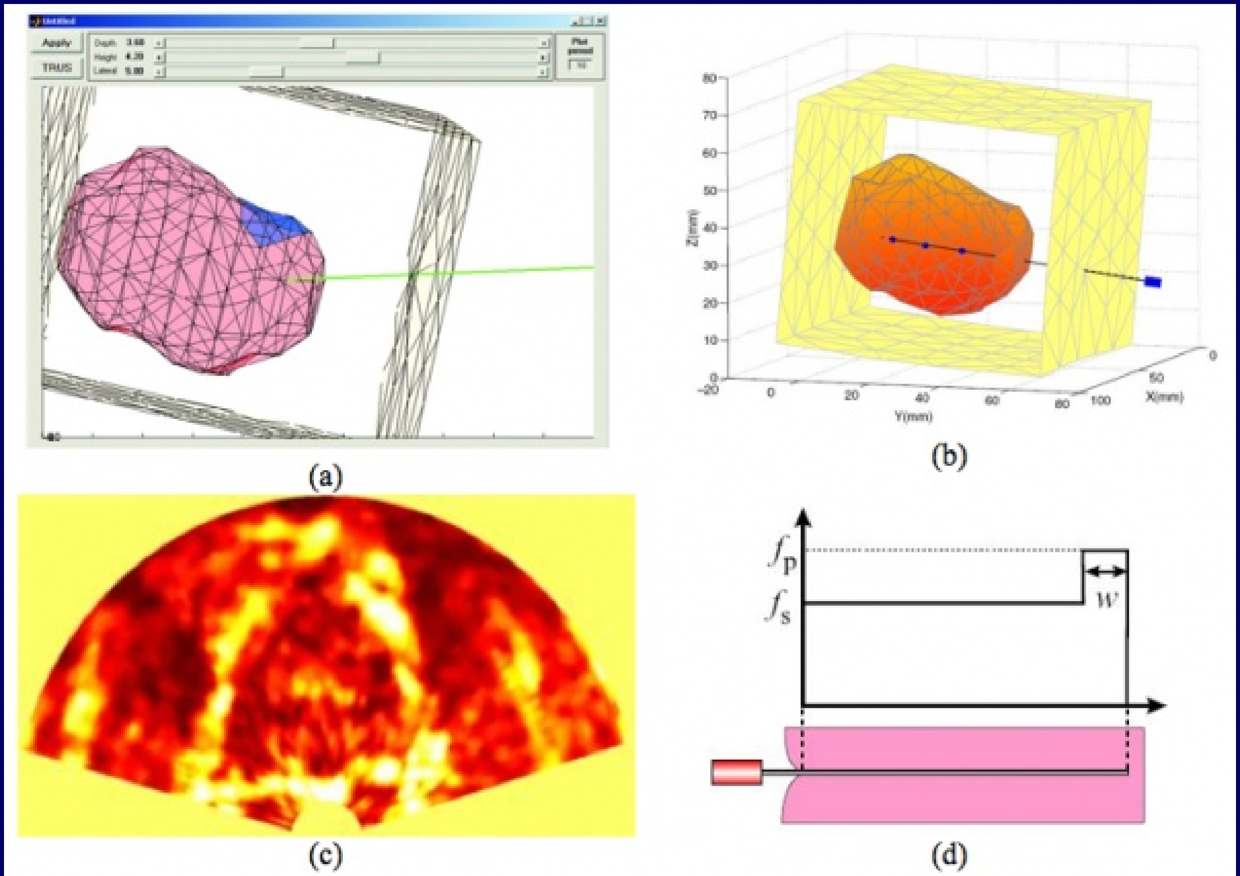

(a) (b) (c) (d)

(a) shows the needle insertion simulator with a simplified mesh of the prostate and the surrounding tissue.

(b) shows the needle inserted with optimal initial insertion parameters. In this situation the needle passed through the targets in the presence of the tissue deformation.

(c) Vibro-elastographic image of the prostate in the transverse view.

(d) the three-parameter force distribution along the needle shaft.

Salcudean et al., MICCAI 2008

Optically Actuated MR-compatible Active Needle

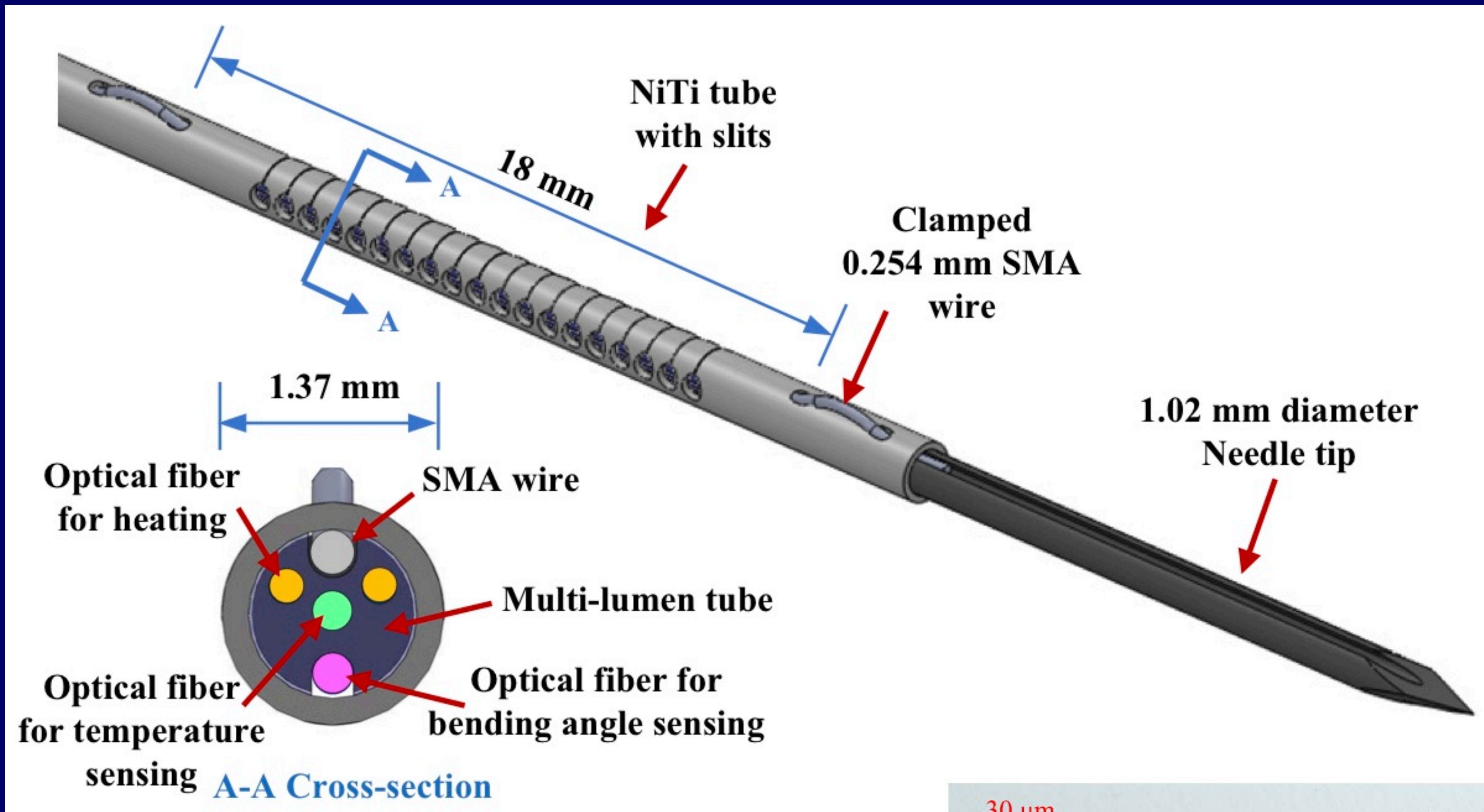

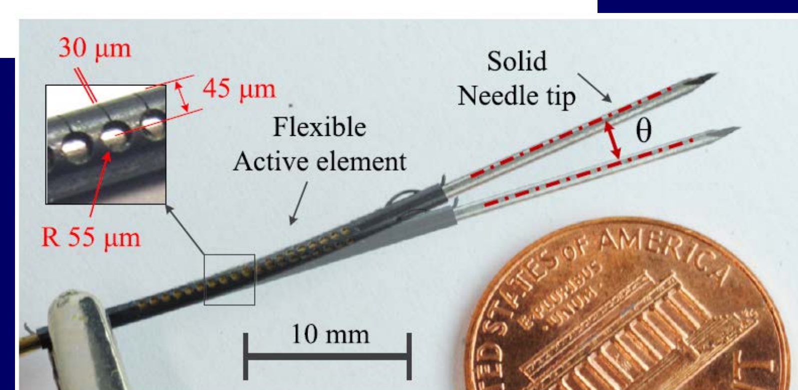

Ryu, IEEE IROS, 2011

Jefferson Kimmel Cancer Center NCI-designated

Optically Actuated MR-compatible Active Needle

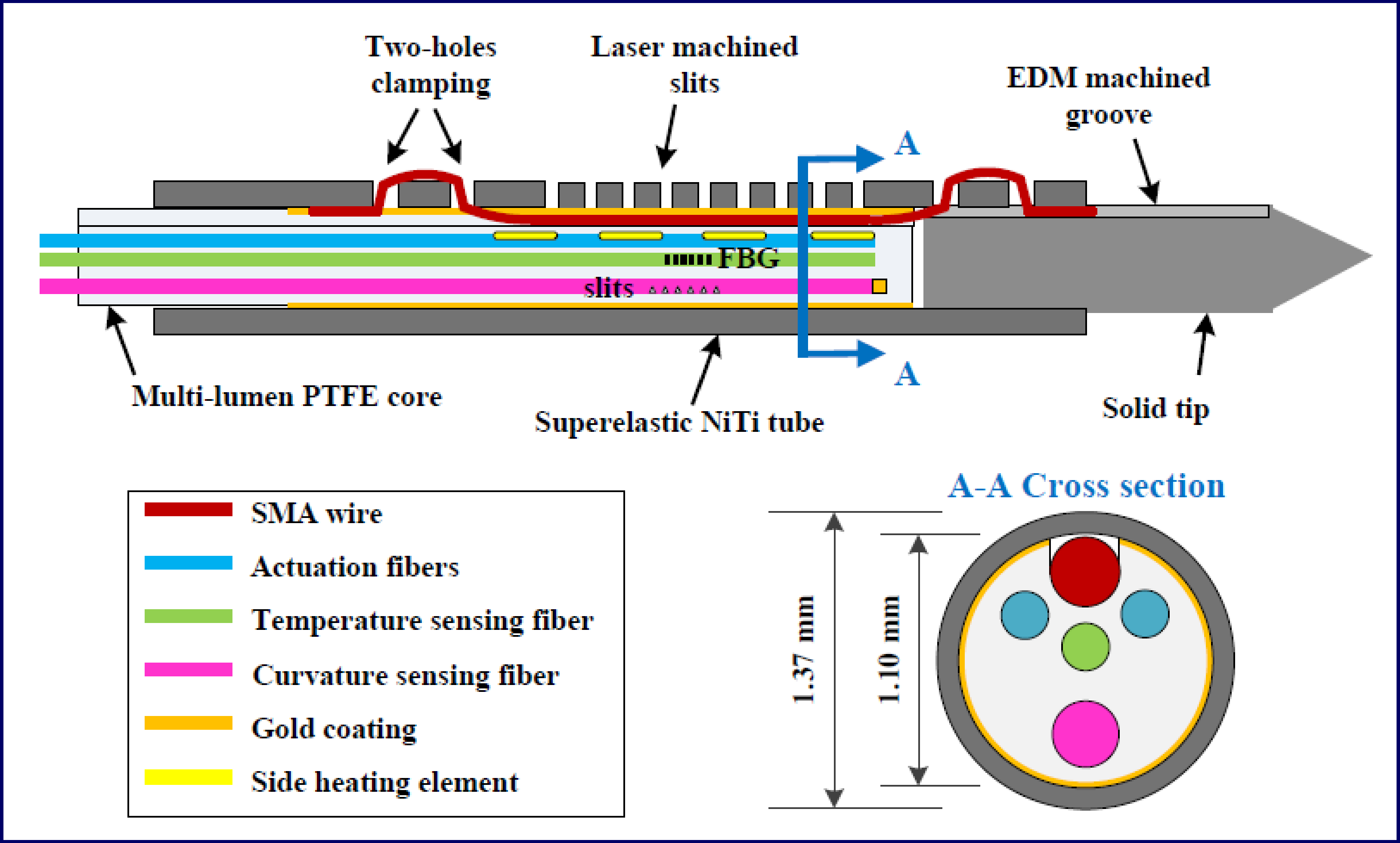

Ryu, PhD Thesis, 2012

Jefferson™ Kimmel Cancer Center NCI-designated

Optically Actuated MR-compatible Active Needle

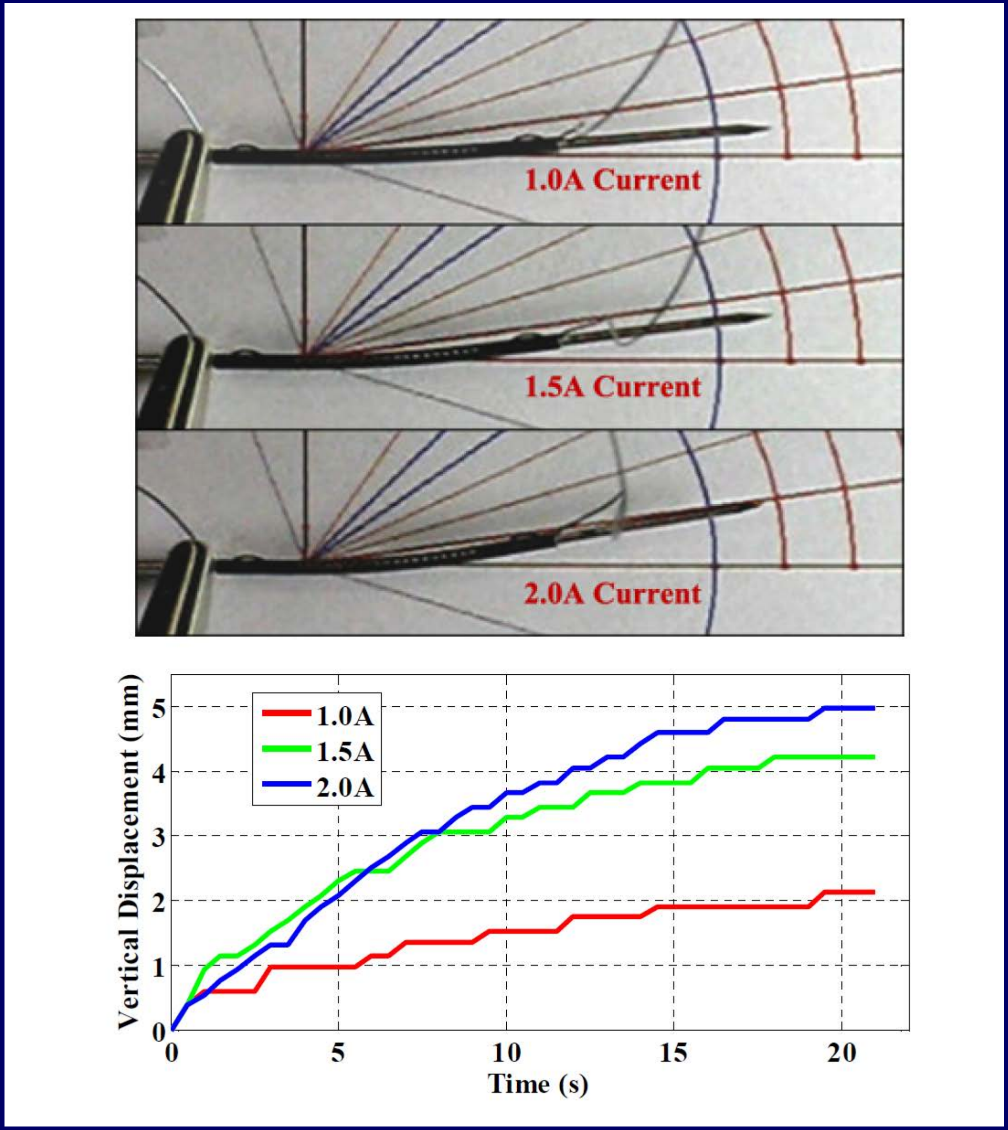

Ryu, IEEE IROS, 2011

Vertical deflection of the active needle tip with Joule heating.

Jefferson™ Kimmel Cancer Center NCI-designated

Optically Actuated MR-compatible Active Needle

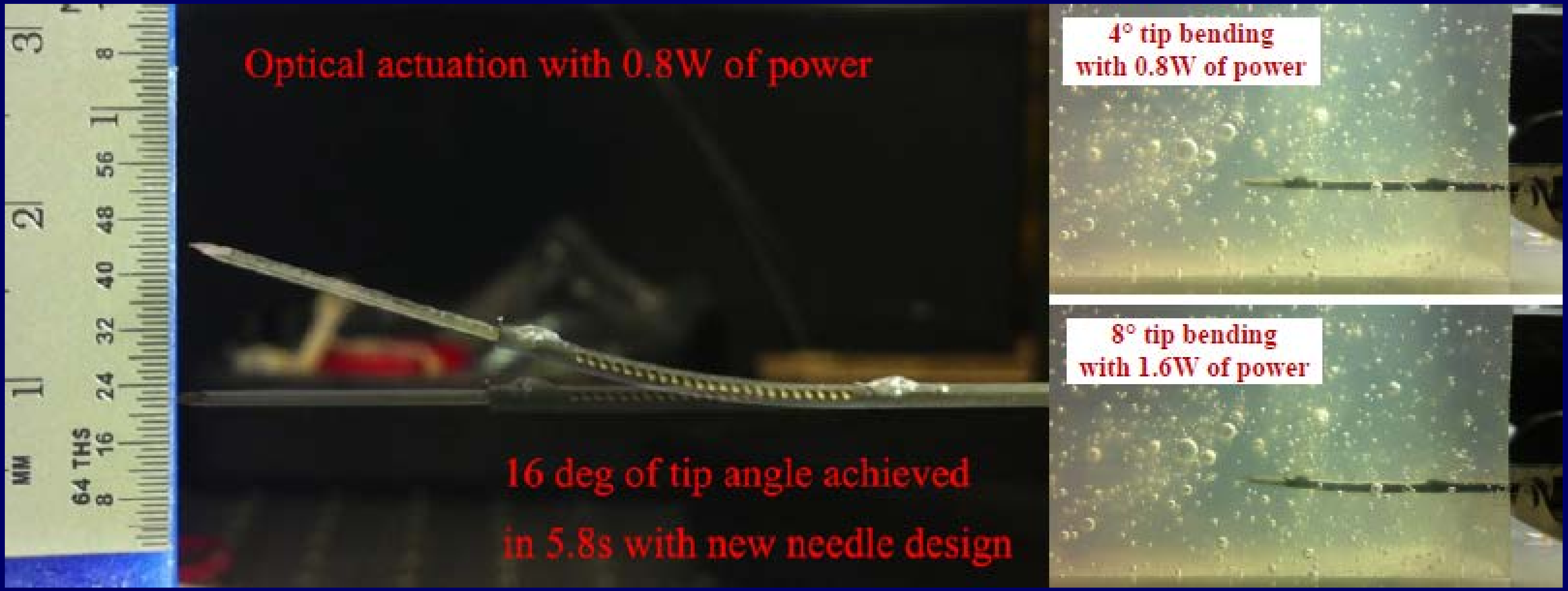

Optical activation of the new needle prototype and mechanical phantom tests: (left) as expected, two times faster bending achieved (right) bending capability in tissue phantom slightly increased but limited by heat loss and tissue reaction force

Ryu, PhD Thesis, 2012

Jefferson™ Kimmel Cancer Center NCI-designated

SMA-actuated Smart (active) Needle Design

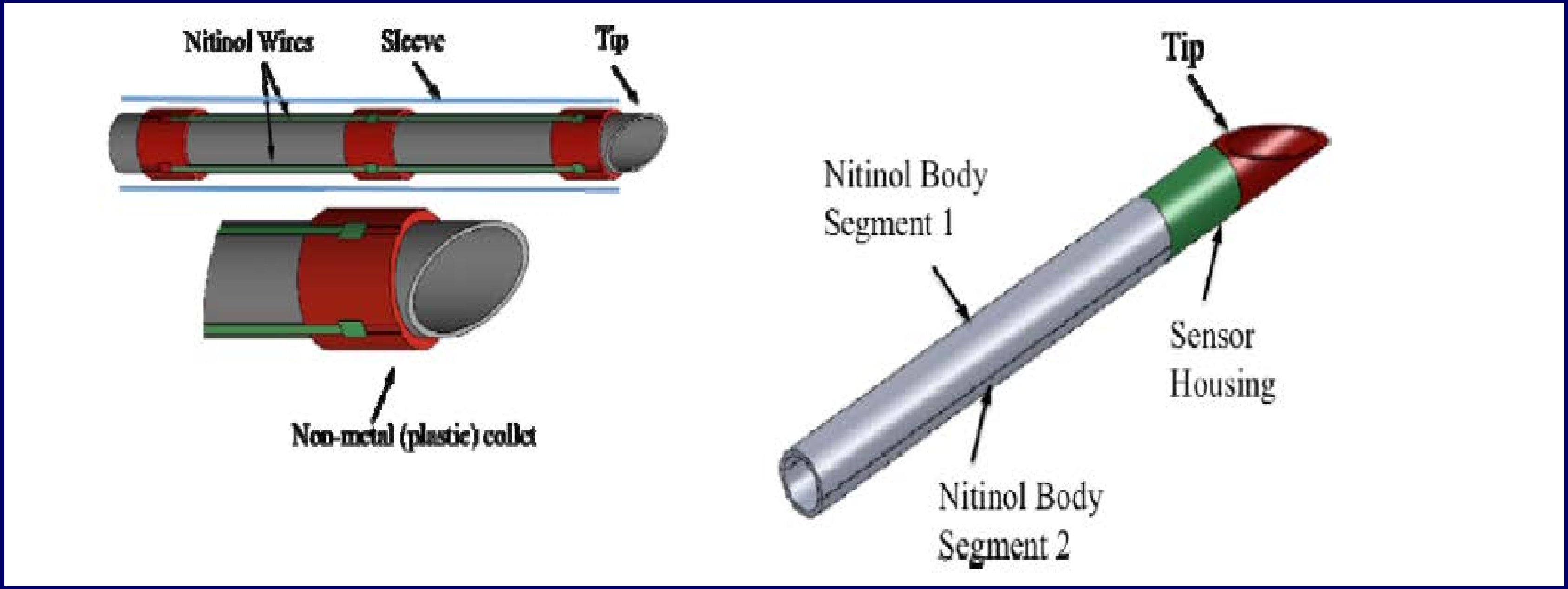

Two types of needle design and actuation techniques: Longitudinal body segment design (left) and lateral body segment design (right).

Podder et al., MedPhys 2012

Jefferson Kimmel Cancer Center NCI-designated

SMA-actuated Smart (active) Needle Control

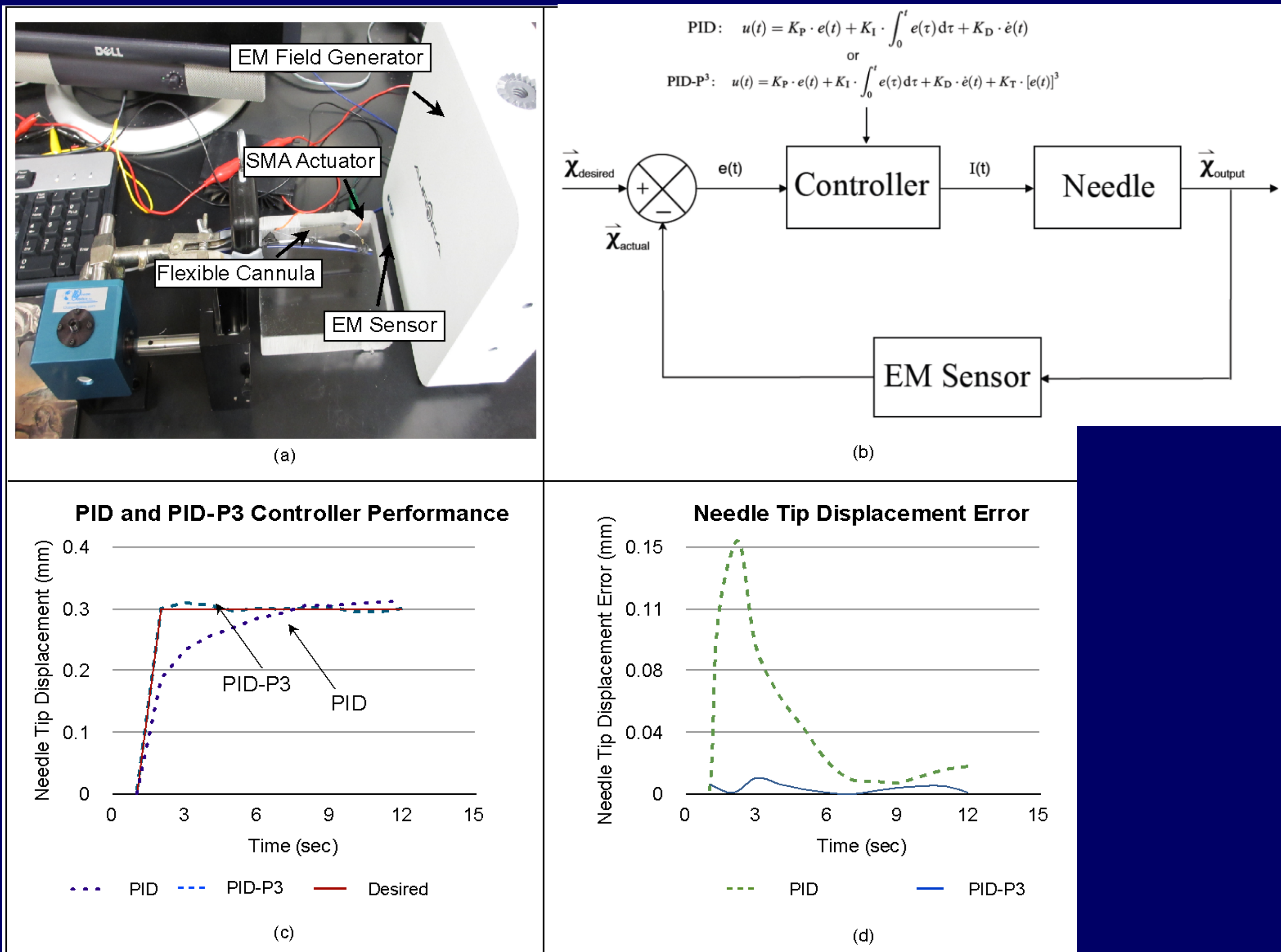

(a) Experimental setup, (b) control block diagram, (c) control performance, (d) errors.

Jefferson™
Kimmel Cancer Center
NCI-designated

SUMMARY

- IGBT robotic platforms are in active development and testing in preclinical settings.
  - About 15 robotic systems developed in 5 countries.
- Accuracy in needle placement and seed delivery as assessed in phantoms are promising.
  - The 3D seed placement error is at sub-millimeter level (EUCLIDIAN).
- Clinical study is the next step.
  - Where applicable, FDA Investigational Device Exemption (IDE) has been obtained (EUCLIDIAN).
- AAPM Working Group on Robotic Brachytherapy was formed in 2008
  - AAPM TG192 formed in 2009, to produce report in <1 yr

Jefferson™ Kimmel Cancer Center NCI-designated

SUMMARY (cont.)

- The feasibility of cancer discrimination in real time along interstitial needle tracks is demonstrated.
  - ROC analysis: validation set achieved AUC = 0.90
  - The proposed technique may be implemented in robotic brachytherapy with online force sensing and real-time planning to achieve targeted dose painting.
- Investigation in tissue-mimicking phantom materials, needle-tissue interaction models, flexible needle control and “smart” (active) needle prototypes further broadens the landscape of interstitial interventions such as implantation therapy and targeted biopsy/tissue resection under robotic assistance.

Thank you!

Work supported by:

NCI BRP Grant
R01 CA91763
"Robotic-Assisted Platform for Intratumoral Delivery"

DoD CDMRP PCRP Idea Development Grant
PC050733
"Multi-channel Robotic System for Concurrent Delivery and Immobilization of Interstitial Therapeutic Agents"

and

DoD CDMRP PCRP Synergistic Grant
W81XWH-11-1-0397
"Development of a Smart Needling Device for Image-Guided Percutaneous Intervention and Delivery of Therapeutic Agents in Prostate"

Jefferson™ Kimmel Cancer Center
NCI-designated

Tarun Podder, PhD
Wan Sing Ng, PhD
Deborah Rubens, MD
John Strang, MD
Edward Messing, MD
Lydia Liao, MD, PhD, MPH
Yongde Zhang, PhD
Yida Hu, PhD
Ivan Buzurovic, MS
Lei Fu, MS, ME
Kaiguo Yan, PhD
Jason Sherman, MS
Adam Dicker, MD, PhD
Shan Jiang, PhD
Parsaoran Hutapea, PhD